X-602-76-135
PREPRINT

LOW-ENERGY ELECTRON SCATTERING FROM CO II. Ab-initio STUDY USING THE FRAME-TRANSFORMATION THEORY

N. CHANDRA

JUNE 1976

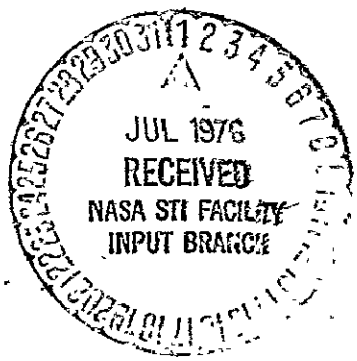

GSFC
GODDARD SPACE FLIGHT CENTER
GREENBELT, MARYLAND

For information concerning availability
of this document contact:

Technical Information Division, Code 250
Goddard Space Flight Center
Greenbelt, Maryland 20771

(Telephone 301-982-4488)

LOW-ENERGY ELECTRON SCATTERING FROM CO

II. Ab-initio STUDY USING THE FRAME-TRANSFORMATION THEORY

N. Chandra*†
Theoretical Studies Group
National Aeronautics and Space Administration
Goddard Space Flight Center
Greenbelt, Maryland 20771, U.S.A.

*National Academy of Sciences - National Research Council Resident Research Associate.

† Present Address: Department of Physics and Astronomy, Louisiana State University, Baton Rouge, Louisiana 70122, U.S.A.

LOW-ENERGY ELECTRON SCATTERING FROM CO

II. Ab-initio STUDY USING THE FRAME-TRANSFORMATION THEORY

N. Chandra

ABSTRACT

The Wigner-Eisenbud R-matrix method has been combined with the frame-transformation theory to study electron scattering from molecular systems. The R-matrix, calculated at the boundary point of the molecular core-radius—which defines the inner-region—in a molecule fixed-frame of reference in the fixed-nuclei approximation, has been transformed to the space-frame in order to continue the solution of the scattering equations in the outer-region where rotational motion of the nuclei is taken into account. This procedure has been applied to a model calculation of thermal-energy electron scattering from CO. The dependence of the rotational transition cross-sections on the core-radius has been studied. This test case demonstrates, for the first time, the usefulness of frame-transformation theory to study the scattering of electrons from polar molecules in general and CO in particular by more ab-initio methods. A general methodology has been developed for adapting the single-center pseudo-potential method to the proposed amalgamation of the R-matrix and the frame-transformation theories in order to perform a fundamental calculation of the interior problem. A comprehensive study of e^--CO scattering is carried out

on the basis of this methodology. The calculated momentum transfer cross-section is in very good agreement with the experimental measurements for thermal energy electron scattering from carbon monoxide. The rotational excitation and de-excitation, and total scattering and momentum transfer cross-sections computed from this method also reproduce the 1.75 eV $^2\Pi$ resonance; while those obtained from an extension of the model calculation mentioned above fail to do so. In particular, we find that for rotationally inelastic scattering in the resonance region the cross-sections for (0→4) and (1→3) transitions are the largest among those which start from the ground and first rotational states of CO molecule respectively. The angular distributions for various electron impact rotational transitions in carbon monoxide have also been computed.

CONTENTS

ILLUSTRATIONS

ILLUSTRATIONS(continued)

TABLES(continued)

INTRODUCTION

The absence of a center of symmetry in heteronuclear diatomic molecules, which also gives rise to a non-vanishing permanent dipole moment, makes it more difficult, physically as well as numerically, to study electron scattering from polar molecular targets compared to that from homonuclear systems. We have shown in a recent communication[1] (hereafter referred to as I) that for electron scattering in a frame of reference attached to the molecule (i.e., the molecular-frame or the body-frame of reference) the single-center expansions of the bound and continuum molecular orbitals converge very well even for complex targets, albeit at a slow rate for low symmetry systems.

For heteronuclear molecules this problem of slow convergence is compounded by the fact that because of the presence of a long-range r^{-2} electron-dipole interaction potential the phase shift for higher angular momenta behaves[1] as $\ell^{-1/2}$ for electron scattering from a fixed polar molecule in body-frame of reference. As a result, the total scattering cross-section, averaged over all molecular orientations, diverges logarithmically[1] in the fixed-nuclei approximation[2]. (However, as proved in I, the momentum transfer cross-section is finite even in this approximation.) The fact that the time-averaged field of a

rotating dipole is zero makes it necessary that in order to obtain finite total cross-section the rotational motion of the nuclei should be included in the equations for scattering of an electron from a polar molecule.

Amongst the existing theoretical formulations of electron-molecule collisions, the use of the fundamental theory of Arthurs and Dalgarno[3] for scattering of a structureless particle from a rigid rotor makes a natural choice to study the electron-polar molecule scattering. This space (lab)-frame formulation of the collision problem retains the rotational kinetic energy terms in the total Hamiltonian of the (electron + molecule)-system.

There have been several attempts to apply this theory to electron scattering from various polar molecular targets.[4] Almost all of these studies are, however, phenomenological in nature based upon some ad-hoc semi-emperical potentials where no account has been taken to represent the highly anisotropic short-range terms and the exchange effects of the electron-molecule interaction in the scattering equations.

In the formalism of Arthurs and Dalgarno[3] the total wave function of the (electron + molecule)-system is expanded in the basis set designated collectively by the quantum number j for nuclear rotation, ℓ for orbital angular momentum of the incident electron (and also v if the nuclear vibration is taken into account). This expansion, in principle, should yield accurate cross-sections for electron impact (vibration-) rotation transitions in a diatomic molecule. However, in practice it has been found that even for such simple system as H_2, where the

short-range terms are not so non-central and strong, it is extremely difficult to carry out the expansion in (v)jℓ basis channels to complete convergence limit.[2, 5] Therefore, the application of this theory to electron scattering from more complex systems with an emphasis to represent the nuclear singularities and the exchange effects in the scattering equations as accurately as possible and in a non-phenomenological way will become almost impossible numerically.

Although the expansion of the total wave function in ℓ, which forms the only basis channel for electron scattering in a body-frame of reference in fixed-nuclei approximation, does converge very well, but the fact that the total cross-section for scattering from polar molecules in this approximation is not finite[1] also excludes the possibility of using the adiabatic-nuclei theory[2] to calculate vibration-rotation excitation cross-sections for elèctron-heteronuclear molecule collisions.

The natural question which one should ask now is that is it physically valid to perform the Born-Oppenheimer separation of the electronic and nuclear motions at some stage in the electron-molecule collision process? The well-known answer to this question lies in the fact that whether in any part of the whole scattering region the duration of collision is smaller than the time period for vibration and/or rotation of the nuclei. When the electron is far away from the molecular core, where the nuclear singularities are not so effective and the short-range and exchange terms have almost vanished, the slow motion of the

electron compared to the vibration-rotation will certainly cause the Born-Oppenheimer approximation to break down. In this outer region, therefore, one will have to include the nuclear kinetic energy terms in the scattering equations.

The validity of the Born-Oppenheimer approximation in the inner-molecule core region is, however, a much more involved question. A naive reasoning based upon the observation that an increase in the incident electron's velocity due to strong attractive short-range forces will cause the electron to move faster in this region than the vibrating-rotating nuclei will lead to the conclusion that the separation of the electronic and nuclear motions will always be valid in the inner-region. However, as recently discovered by Chandra and Temkin[6] in their study of vibrational excitation in e^--N_2 scattering and previously discussed by Herzenberg[7] for other molecular systems, a trapping of the incident electron in the non-central molecular field—which is a combination of the centrifugal barrier, permanent moments, and the induced dipole polarizability—may always enhance the transition time such that before the incident electron becomes free again the molecular nuclei are able to change their configuration. Under these circumstances one can certainly not neglect the effects of the nuclear motion relative to that of the incident electron. Therefore the validity of the Born-Oppenheimer approximation in the molecular core-region is not always a pre-determined fact.

When the separation of the motions of the incident electron and the nuclei in the molecular core-region is a viable approximation one can always neglect the nuclear vibration-rotation in the inner part of the configuration space. These two different physical situations—where one uses a fixed-nuclei approximation in the inner-region and consider the nuclear rotation in the outer-region in a space-fixed frame of reference—have been combined by an orthogonal transformation operator at the common boundary point by Chang and Fano[8] in their frame-transformation (f.-t.) theory of electron-molecule scattering.

If the Born-Oppenheimer approximation is valid for electron collision with certain polar molecules in the core-region then the f.-t. theory will provide a natural frame-work for studying electron scattering from such target systems. A fixed-nuclei treatment in the inner-region will make very convenient the inclusion of nuclear singularities and the exchange effects in the scattering equations. At the same time the introduction of the nuclear rotation in the scattering equations in the outer-region will cause all the scattering cross-sections to be finite which are otherwise undefined in fixed- and adiabatic-nuclei approximations. The convergence problem in the basis set $(j\ell)$ in a lab-frame in the outer-region is not expected to be so severe now as the strong non-central short-range interaction potential terms are almost negligible and it is only the long-range terms which will have to be considered.

Among the diatomic heteronuclear molecules, carbon monoxide is a case of particular interest. Apart from being important from a space and environmental

point of view, high-energy CO lasers play a significant role in scientific applications. The electron swarm data for CO molecule have yielded scattering cross-sections over a considerable range of energy.[9] Moreover, the time period for the rotational motion of carbon monoxide is larger than the duration of collision of an electron with this molecule. Being iso-electronic to N_2, it has a closed-shell ground electronic state configuration. We have reported in I that the single-center pseudo-potential method, originally introduced by Burke and Chandra[10] in their fixed-nuclei study of $e^- - N_2$ scattering and recently proved to be extremely successful[6] in electron impact vibrational excitation of nitrogen molecule, works very well even for electron scattering from CO.

In view of these considerations and in continuation to our efforts of studying the electron-molecule collisions from first principles using ab-initio methods,[1,2,6,10,11] we have, therefore, employed the f.-t. theory to study rotationally elastic and inelastic e^- - CO scattering. Earlier Chandra and Gianturco[12] gave a brief description of the methodology of applying the f.-t. theory to study electron-molecule scattering in general and e^--CO scattering in particular. (Note that the results of this letter with regard to CO are no longer valid because of an error discovered later and discussed in detail in I.) Short reports on the progress of the present work have been given elsewhere.[13]

In Section II we shall review the essential elements of the f.-t. theory and give the relevant formulae. Chang and Fano[8] have suggested that the wave-functions and their derivatives, obtained by solving the fixed-nuclei scattering

equations in the inner-region, should be transformed separately to a space-fixed frame of reference to continue the solution of the scattering equations in the outer-region. In our methodology of implementing the f.-t. theory we calculate the Wigner[14] $\underline{R}$-matrix at the boundary point by using the solutions and the derivatives of the fixed-nuclei equations in the inner-region. This $\underline{R}$-matrix is then transformed to the lab-frame by applying the orthogonal transformation given by Chang and Fano.[8] The computation of a body-frame $\underline{R}$-matrix, its transformation to a space-fixed frame of reference, and then the subsequent matching to the solutions of the outer-region equations for calculating the $\underline{S}$-matrix has been discussed in Section III.

To our knowledge the present work shall constitute the very first application of the f.-t. theory for studying the electron-molecule collisions. (Henry and Chang[15] and Chang[16] had tried to apply this theory to e^--H_2 scattering. In their studies they have made an approximation by neglecting the solutions of the scattering equations in the outer-region in the lab-frame. In a recent communication[17] Chandra has shown that under this approximation the f.-t. and the adiabatic-nuclei theories are equivalent. Therefore, the e^--H_2 calculation of Henry and Chang[15] and also that of Chang[16] essentially reduces to an application of the adiabatic-nuclei theory.) In order to carry out a complete f.-t. treatment the numerical implementation of the procedure, briefly pointed out in the preceding paragraph, becomes a complex and arduous task. We, therefore, thought it to be extremely important to test this theory and develop a feeling about its

physics and the confidence in our numerical procedure by applying it first to a previously undertaken semi-empirical calculation based upon some simple potential.

In the first part of Section IV we describe in detail our test study of the application of the f.-t. theory to a model calculation of thermal energy electron scattering from CO done by Crawford and Dalgarno[18] and compare our new results with those of their rotational close-coupling calculations. In the second part of this section we discuss how the single-center pseudo-potential method can be adapted to our methodology, the effect of different choices of the boundary point—defining the inner-molecular core region—where a transformation is performed from a molecule- to a space-fixed frame of reference, and the convergence of the $(j\ell)$ basis set in the outer-region. The final differential and integrated cross-sections for electron impact rotational transitions in a CO molecule together with the total scattering and momentum transfer cross-sections are also presented in Section IV. In the concluding Section V we shall briefly discuss, on the basis of our present experience, the usefulness of the f.-t. theory in studying the electron-molecule collision in general and the electron-polar molecule scattering in particular.

II. THEORY

A. Electron Scattering in a Space-Fixed Frame of Reference

The total Hamiltonian of the (electron + molecule)-system can be written as (in a.u.)

$$-\frac{1}{2}\nabla^2_{\vec{r}} + H_e(\vec{r}_1,\ldots\vec{r}_N;\vec{R}) + H_{rot}(\hat{R}) + V(\vec{r}_1,\ldots\vec{r}_N,\vec{r};\vec{R}). \qquad (2.1)$$

The Schrodinger equation

$$H_e(\vec{r}_1,\ldots\vec{r}_N;\vec{R})\ \Phi_n(\vec{r}_1,\ldots\vec{r}_N;\vec{R}) = \epsilon_n(R)\ \Phi_n(\vec{r}_1,\ldots\vec{r}_N;\vec{R}) \qquad (2.2)$$

describes the n^{th} state of the motion of N electrons of the target molecule,

$$H_{rot}(\hat{R})\ Y_{jm_j}(\hat{R}) = Bj(j+1)\ Y_{jm_j}(\hat{R}) \qquad (2.3)$$

is the eigenvalue equation for the rotation of the nuclei when the molecule is in its $^1\Sigma$ electronic state, and in Eq. (2.1) we do not consider the vibrational motion of the nuclei. In Eq. (2.3) the rotational constant $B = (2I)^{-1}$, where I is the moment of inertia of the molecule. The electron-molecule interaction energy is given by

$$V(\vec{r}\,'_1,\ldots\vec{r}\,'_N,\vec{r}\,';\vec{R}) = \sum_{i=1}^{N}\frac{1}{|\vec{r}\,'-\vec{r}\,'_i|} - \left(\frac{Z_A}{|\vec{r}\,'-\vec{R}_A|} + \frac{Z_B}{|\vec{r}\,'-\vec{R}_B|}\right) \qquad (2.4)$$

where Z_A and Z_B are the atomic charges of the two nuclei A and B separated by distances $|\vec{R}_A|$ and $|\vec{R}_B|$ from the center of mass of the molecule.

In our discussion primed co-ordinates will always be referred to the body-frame of reference which is rotating with the molecule and whose polar axis is defined along the line joining the two nuclei with center of mass of the molecule as its origin. The space-fixed frame of reference or the so called lab-frame will be denoted by unprimed coordinates. The polar axis of this frame is along

the direction of incidence. We follow Rose's convention[19] and define three Euler angles α, β, and γ in order to rotate a space co-ordinate system into coincidence with the molecule-fixed frame. For a linear molecule angle γ can have any arbitrary value (we set it to be equal to zero) and β and α are the polar angles[19] Θ and Φ of the internuclear axis with respect to the lab frame. Therefore, $\vec{R} = (R,\Theta,\Phi)$, $D(\alpha, \beta, \gamma) = D(\Phi, \Theta, 0)$, and the eigenfunction for the Hamiltonian H_{rot} in Eq. (2.3) can be written as

$$Y_{j m_j}(\hat{R}) = Y_{j m_j}(\Theta, \Phi) = \sqrt{\frac{2j + 1}{4\pi}}\, D^{j*}_{m_j 0}(\Phi, \Theta). \tag{2.5}$$

In order to formulate the theory of electron scattering from a rigid rotating diatomic molecule in a space-frame, Arthurs and Dalgarno[3] developed a basis set which is an eigenfunction of the square of the total angular momentum $\vec{J}$ and its projection M along the polar axis of this frame. According to the Hund's coupling scheme (d)[20(a)] the orbital angular momentum $\vec{\ell}$ of the incident electron is coupled with the angular momentum $\vec{j}$ of the nuclear rotation to form the constant of the motion $\vec{J} = \vec{j} + \vec{\ell}$ whose eigen-functions are given by

$$\mathcal{Y}^{JM}_{j\ell}(\hat{R}, \hat{r}) = (-1)^{\ell - j - M} \sqrt{\frac{(2j + 1)(2J + 1)}{4\pi}} \sum_{m_j m_\ell} \begin{pmatrix} j & \ell & J \\ m_j & m_\ell & -M \end{pmatrix} D^{j*}_{m_j 0}(\hat{R}) Y_{\ell m_\ell}(\hat{r}). \tag{2.6}$$

(For the definitions of 3-j, 6-j symbols, etc., see, for example, Rotenberg et al.[21]) Note that

$$\mathcal{Y}^{JM}_{j\ell}(-\hat{R},-\hat{r}) = (-1)^{j+\ell}\,\mathcal{Y}^{JM}_{j\ell}(\hat{R},\hat{r}) \tag{2.7}$$

have a well defined parity.

We now substitute the following expansion

$$\Psi^{JM}(\vec{r}_1,\ldots\vec{r}_N,\vec{r};\vec{R}) = \Phi_0(\vec{r}_1,\ldots\vec{r}_N;\vec{R})\,r^{-1}\sum_{j'\ell'} u^J_{j',\ell'}(r)\,\mathcal{Y}^{JM}_{j'\ell'}(\hat{R},\hat{r}) \tag{2.8}$$

for the total wavefunction (see Ref. 2 for the antisymmetrization of this wavefunction in $e^- - H_2$ scattering) in Eq. (2.1) and derive a set of coupled radial scattering equations by using the orthogonality of the ground electronic state wavefunction Φ_0 and of the basis set $\mathcal{Y}^{JM}$:

$$\left[\frac{d^2}{dr^2} - \frac{\ell(\ell+1)}{r^2} + 2\{E_T - \epsilon_0 - Bj(j+1)\}\right] u^J_{j\ell}(r)$$

$$= 2\sum_{j'\ell'}\left\langle \mathcal{Y}^{JM}_{j\ell}\,|V(\vec{r};\vec{R})|\,\mathcal{Y}^{JM}_{j'\ell'}\right\rangle u^J_{j',\ell'}(r), \tag{2.9}$$

where

$$V(\vec{r};\vec{R}) = \left\langle \Phi_0(\vec{r}_1,\ldots\vec{r}_N;\vec{R})\,|V(\vec{r}_1,\ldots\vec{r}_N,\vec{r};\vec{R}|\,\Phi_0(\vec{r}_1,\ldots\vec{r}_N;\vec{R})\right. \tag{2.10}$$

and E_T is the total energy of the colliding particles. The right hand side of Eq. (2.9) is diagonal in J and M and also independent of M because the interaction potential given by Eq. (2.10) is invariant under rotation of all co-ordinates.

One can always write Eq. (2.10) as a multipole expansion[22]

$$V(\vec{r};\vec{R}) = \sum_{\mu} V_{\mu}(r)\, P_{\mu}(\hat{r};\hat{R}) \tag{2.11}$$

of the molecular charge distribution about the center of mass of the molecule. Here P is the Legendre polynomial of order ℓ. The summation index μ will have both even and odd integral values for molecular systems which belong to the $C_{\infty v}$ point group, e.g., the heteronuclear diatomic molecules like CO; but only even integral values for $D_{\infty h}$ symmetry group molecules which possess a center of symmetry (e.g., N_2, CO_2, etc.). In Eq. (2.11) we have not shown the parametric dependence of $V_{\mu}(r)$ over the inter-nuclear separation R.

After substituting (2.11), the right hand side of Eq. (2.9) can be simplified.[3] The final form of the radial equations for scattering in a space-frame will then become

$$\left[\frac{d^2}{dr^2} - \frac{\ell(\ell+1)}{r^2} + k_j^2\right] u^J_{j,\ell}(r)$$

$$= 2 \sum_{j'\ell'} \sum_{\mu} (-1)^{-J-\mu} \sqrt{(2j+1)(2\ell+1)(2j'+1)(2\ell'+1)} \begin{pmatrix} j & j' & \mu \\ 0 & 0 & 0 \end{pmatrix}$$

$$\begin{pmatrix} \ell & \ell' & \mu \\ 0 & 0 & 0 \end{pmatrix} \begin{Bmatrix} j' & \ell' & J \\ \ell & j & \mu \end{Bmatrix} V_{\mu}(r)\, u^J_{j',\ell'}(r), \tag{2.12}$$

where

$$k_j^2 = 2\,[E_T - \epsilon_0 - Bj(j+1)]\,. \tag{2.13}$$

For the same value of J, this system of equations splits up into two different sets according to the parity $(-1)^{j+\ell}$. One solves the coupled Eqs. (2.12), subject to the following boundary conditions

$$u^J_{j',\ell',j\ell}(r) \underset{r\to 0}{\sim} 0$$

$$\underset{r\to 0}{\sim} k_{j'}^{-1/2} \left[\sin\left(k_{j'} r - \frac{1}{2}\ell'\pi\right) \delta_{jj'}\,\delta_{\ell\ell'} + \cos\left(k_{j'} r - \frac{1}{2}\ell'\pi\right) K^J_{j',\ell',j\ell}\right] \quad \text{for} \quad k^2_{j'} > 0$$

$$\underset{r\to\infty}{\sim} |k_{j'}|^{-1/2} \exp(-|k_{j'}|\, r) \quad \text{for} \quad k^2_{j'} < 0, \tag{2.14}$$

in order to calculate the scattering matrix

$$\underline{S}^J = (1 + i\underline{K}^J)\,(1 - i\underline{K}^J)^{-1} \tag{2.15}$$

and the transition matrix

$$\underline{T}^J = \underline{S}^J - 1 = 2i\underline{K}^J(1 - i\underline{K}^J)^{-1}. \tag{2.16}$$

The first set of (j',ℓ') subscript on u^J in Eq. (2.14) refers to the outgoing channel while the second set (j,ℓ) is for the incident channel.

The formulae for various cross-sections for a transition from molecular rotational state j to j' have been derived by Arthurs and Dalgarno in the original

paper.[3] However, these expressions can be further simplified[23] by using the concept of angular momentum transfer, $\vec{\ell}_t = \vec{j}' - \vec{j} = \vec{\ell} - \vec{\ell}'$ (where $\vec{J} = \vec{j} + \vec{\ell} = \vec{j}' + \vec{\ell}'$), introduced by Fano and Dill.[24] In this simplified form the differential cross-section for (j→j') transition becomes

$$\frac{d\sigma_{j\to j'}}{d\Omega} = \frac{k_j^{-2}}{4(2j+1)} \sum_L A_L^{(jj')} P_L(\cos\theta) \tag{2.17}$$

where

$$A_L^{(jj')} = (-1)^L (2L+1) \sum_{\ell_1 \ell_2 \ell_1' \ell_2'} {}_i\ell_1' - \ell_1 - \ell_2' + \ell_2$$

$$\sqrt{(2\ell_1'+1)(2\ell_1+1)(2\ell_2'+1)(2\ell_2+1)} \begin{pmatrix} \ell_1' & \ell_2' & L \\ 0 & 0 & 0 \end{pmatrix} \begin{pmatrix} \ell_1 & \ell_2 & L \\ 0 & 0 & 0 \end{pmatrix}$$

$$\sum_{\ell_t} (-1)^{\ell_t} (2\ell_t+1) \begin{Bmatrix} \ell_1' & \ell_2' & L \\ \ell_2 & \ell_1 & \ell_t \end{Bmatrix} \mathfrak{I}^{\ell_t}_{j'\ell_1', j\ell_1} \mathfrak{I}^{\ell_t^*}_{j'\ell_2', j\ell_2} \tag{2.18}$$

The new $\underline{\mathfrak{I}}^{\ell_t}$ matrix is obtained from the transition matrix $\mathbf{T}^J$ by the following relation

$$\mathfrak{I}^{\ell_t}_{j'\ell', j\ell} = \sum_J (-1)^J (2J+1) \begin{Bmatrix} j' & j & \ell_t \\ \ell & \ell' & J \end{Bmatrix} T^J_{j'\ell', j\ell}. \tag{2.19}$$

The advantage of relation (2.19) compared to that given by Arthurs and Dalgarno in Eq. (19) of their paper[3] is that two infinite sums over J, present in their expression, have now been replaced by a single sum over ℓ_t whose values are restricted by the inequality

$$\text{larger of } (|\ell-\ell'|, |j-j'|) \le \ell_t \le \text{ smaller of } (\ell+\ell', j+j').$$

The scattering cross-section for the transition (j→j') is given by

$$\sigma_{j\to j'} = \frac{\pi\ k_j^{-2}}{2j+1}\ A_0^{(jj')} = \frac{\pi k_j^{-2}}{2j+1} \sum_{\ell_t \ell\ell'} (2\ell_t + 1)\ |\mathfrak{I}^{\ell_t}_{j'\ell',j\ell}|^2$$

$$= \frac{\pi k_j^{-2}}{2j+1} \sum_{J\ell\ell'} (2J+1)\ |T^J_{j'\ell',j\ell}|^2. \tag{2.20}$$

And the momentum transfer cross-section for (j→j') transition becomes

$$\sigma^m_{j\to j'} = \int \frac{d\sigma_{j\to j'}}{d\Omega}\ (1 - \cos\theta)\, d\Omega$$

$$= \frac{\pi k_j^{-2}}{2j+1} \left[A_0^{(jj')} - \frac{1}{3} A_1^{(jj')}\right] \tag{2.21}$$

However, the total scattering and the momentum transfer cross-sections,

$$\sigma(j) = \sum_{j'} \sigma_{j\to j'} \tag{2.22}$$

and

$$\sigma^m(j) = \sum_{j'} \sigma^m_{j\to j'} \tag{2.23}$$

respectively, are nearly independent of the initial rotational state j of the molecule[25] except close to threshold.

The coupled radial scattering Eqs. (2.12) are exact and their solution should, in principle, give the correct results for electron impact rotational transitions

in a diatomic molecule. However, slow convergence in the basis channel $(j\ell)$ in the presence of the strong non-central forces makes the solution of these equations numerically an arduous task.

B. Electron Scattering in a Molecule-Fixed Frame of Reference

In a co-ordinate system fixed to the nuclei, i.e. the body-fixed frame of reference, the internuclear axis becomes the quantization axis and the component λ of the total angular momentum $\vec{J}$ along this axis comes entirely from the orbital angular momentum of the incident electron, because

$$\vec{J} \cdot \hat{R} \equiv J_{z'} = (\vec{j} + \vec{\ell}) \cdot \hat{R} = \vec{\ell} \cdot \hat{R} = \lambda,$$

if the target molecule is in its $^1\Sigma$ electronic state. This basically corresponds to the Hund's coupling scheme (a)[20(b)] where the electron orbital angular momentum $\vec{\ell}$ is coupled with the inter-nuclear axis. The eigenfunctions of J_z; will now form a natural choice for the basis set. These basis functions are a linear combination of the products of $Y_{\ell\lambda}(\hat{r}')$ and $D^{J^*}_{M\lambda}(\hat{R})$. The former of these two components belongs to the single-center expansions of the continuum electron orbital about the center of mass of the molecule while the latter is a symmetric top wavefunction[26] used for the nuclei as the angular momentum component λ along the internuclear axis is now not necessarily zero. Therefore, following Chang and Fano[8], these basis function for a diatomic molecule can be written as

$$X^{JM\eta}_{\ell\lambda}(\hat{r},\hat{R}) = \sqrt{\frac{2J+1}{8\pi(1+\delta_{0\lambda})}}\ [Y_{\ell\lambda}(\hat{r}')\, D^{J\,*}_{M\lambda}(\hat{R}) + Y_{\ell,-\lambda}(\hat{r}')\, D^{J\,*}_{M,-\lambda}(\hat{R})]. \qquad (2.24)$$

In a linear molecule any plane through the inter-nuclear axis is a plane of symmetry. The variable η in Eq. (2.24), which can have only +1 or -1 values, determines the symmetry of the wavefunction upon reflection through this plane. In order to determine the parity of this function, an inversion of all (electronic plus nuclear) co-ordinates through the origin (the center of mass in present case) can be visualized[27] as (i) a reflection σ_v of the electronic co-ordinates in the symmetry plane passing through the inter-nuclear axis and (ii) the inversion of the nuclear co-ordinates. The successive application of these two operations gives rise to the following relation

$$X^{JM\eta}_{\ell\lambda}(-\hat{r}',-\hat{R}) = \eta(-1)^J\, X^{JM\eta}_{\ell\lambda}(\hat{r}',\hat{R}). \qquad (2.25)$$

Thus the parity of the body frame basis functions (2.24) is $\eta(-1)^J$. Since J is a constant of the motion, the parity of the lab frame basis functions (2.6) can also be considered as $(-1)^{j+\ell+J}$ instead of $(-1)^{j+\ell}$ [see Eq. (2.7)] and then $\eta = (-1)^J$

The two basis functions of space- and molecule-fixed frames of reference, given by Eqs. (2.6) and (2.24) respectively, can be related to each other by an orthogonal operator

$$\Omega_{j\lambda}^{(\ell J \eta)} = (-1)^{-j+\ell+\lambda} \sqrt{2j+1} \begin{pmatrix} j & \ell & J \\ 0 & \lambda & -\lambda \end{pmatrix} \frac{1+\eta(-1)^{J-}}{\sqrt{2(1+\delta_{0\lambda})}} \tag{2.26}$$

such that

$$X_{\ell\lambda}^{JM\eta} = \sum_{J} y_{j\ell}^{JM} \Omega_{j\lambda}^{(\ell J \eta)} \tag{2.27}$$

and

$$y_{j\ell}^{JM} = \sum_{\lambda} X_{\ell\lambda}^{JM\eta} \Omega_{\lambda j}^{(\ell J \eta)^T}, \tag{2.28}$$

where a superscript T denotes a transpose of the operator. Other properties of the transformation operator (2.26) have been discussed in detail in Ref. 8 as well by Fano in his two earlier papers.[28]

The total wavefunction for the Hamiltonian (2.1) in a molecule-fixed frame of reference can now be expanded as

$$\Psi^{JM\eta}(\vec{r}_1', \ldots \vec{r}_N', \vec{r}'; \vec{R}) = \Phi_0(\vec{r}_1', \ldots \vec{r}_N'; \vec{R})\, r^{-1} \sum_{\ell'\lambda'} f_{\ell'}^{\lambda'}(r)\, X_{\ell'\lambda'}^{JM\eta}(\hat{r}', \hat{R}) \tag{2.29}$$

and the radial scattering equation, equivalent to (2.9), becomes

$$\left[\frac{d^2}{dr^2} - \frac{\ell(\ell+1)}{r^2} + 2(E_T - \epsilon_0)\right] f_\ell^\lambda(r) = 2 \sum_{\ell'} \left\langle Y_{\ell\lambda} \left| V \right| Y_{\ell'\lambda} \right\rangle f_{\ell'}^{\lambda}(r)$$

$$+ 2B \sum_{\lambda' j} \Omega_{\lambda j}^{(\ell J \eta)^T} j(j+1)\, \Omega_{j\lambda'}^{(\ell J \eta)} f_\ell^{\lambda'}(r). \tag{2.30}$$

(Note that in the molecule-fixed frame of reference D^{J*} are not eigenfunctions of H_{rot}). After substituting the multipole expansion (2.11), the integral in the first term on the right hand side of the above equation can be simplified to the following form

$$\langle Y_{\ell\lambda} |V| Y_{\ell'\lambda} \rangle = \sum_{\mu} V_{\mu}(r) \int Y^{*}_{\ell\lambda}(\hat{r}') P_{\mu}(\hat{r}') Y_{\ell'\lambda}(\hat{r}') d\hat{r}'$$

$$= (-1)^{\lambda} \sqrt{(2\ell + 1)(2\ell' + 1)} \sum_{\mu} \begin{pmatrix} \ell & \ell' & \mu \\ 0 & 0 & 0 \end{pmatrix} \begin{pmatrix} \ell & \ell' & \mu \\ \lambda & -\lambda & 0 \end{pmatrix} V_{\mu}(r). \tag{2.31}$$

Eq. (2.30) is diagonal in J and η. While the first term on the right hand side of Eq. (2.30) is diagonal in λ but the second term, which is diagonal in ℓ, represents the coupling of the incident electron's motion with nuclear rotation. This term comes from H_{rot}, present in the Hamiltonian (2.1), operating on D^{J*} of the basis function (2.25).

Eqs. (2.9) and (2.30) present an exact description of the same physical situation in two geometrically different frames of reference. One can indeed write

$$u^{J\eta}_{j\ell}(r) = \sum_{\lambda} f^{\lambda\eta}_{\ell}(r) \Omega^{(\ell J\eta)^{T}}_{\lambda j} \tag{2.32}$$

and

$$f^{\lambda\eta}_{\ell}(r) = \sum_{j} u^{J\eta}_{j\ell}(r) \Omega^{(\ell J\eta)}_{j\lambda}. \tag{2.33}$$

[In these two equations we have introduced a superscript η on functions u and f to denote their parities explicitly.] A transformation from a body- to the space-frame, or vice versa, does not change the dynamics of the collision problem.

C. Fixed-Nuclei Approximation and the Frame-Transformation Theory

The body-frame scattering Eq. (2.30) can be further simplified by making an approximation. On comparing the two terms on the right hand side of this equation, one will notice that owing to the smallness of the rotational constant B ($\simeq 7.30 \times 10^{-3}$ eV for the lighter most molecule H_2) there will be a region of the configuration space close to the nuclei where first of these two terms will dominate the whole scattering process. The multipole terms V_μ of Eq. (2.31) are usually very strong in the neighborhood of the nuclei for higher values of μ (See Fig. 1 of I and Ref. 29). The neglect of those terms which contain the rotational constant B should have very little effect on the solutions of the body-frame equations in this inner part of the configuration space.

After dropping H_{rot} in the molecular core-region the Hamiltonian (2.1) then describes merely the electronic motion of the colliding systems. This essentially means invoking the zeroth-order (fixed-nuclei) approximation in the Born-Oppenheimer separation[30] of the electronic and nuclear motions. The body-frame radial scattering equation (2.30) takes up the following simple form

$$\left[\frac{d^2}{dr^2} - \frac{\ell(\ell+1)}{r^2} + k^2\right] f^{\lambda}_{\ell}(r)$$

$$= 2(-1)^{\lambda} \sqrt{2\ell+1} \sum_{\ell' \mu} \sqrt{2\ell'+1} \begin{pmatrix} \ell & \ell' & \mu \\ 0 & 0 & 0 \end{pmatrix} \begin{pmatrix} \ell & \ell' & \mu \\ \lambda & -\lambda & 0 \end{pmatrix} V_{\mu}(r)\, f^{\lambda}_{\ell'}(r), \tag{2.34}$$

where $k^2 = 2(E_T - \epsilon_0)$, in the fixed-nuclei approximation. In addition to being independent of J and η, it now becomes diagonal in λ which is the projection of ℓ ($|\lambda| \leq \ell$) along the internuclear axis.

Although the fixed-nuclei approximation has been used very successfully in calculating the bound electronic state properties of the molecules since the publication of the classic paper of Born and Oppenheimer [31]. But it was only recently that a single-channel formulation of the electron-diatomic molecule scattering in this approximation was developed by Temkin and Vasvada[32] and later generalized to multichannel theory independently by Temkin et al[33] and Burke and Chandra.[10] (A relationship in between these two formulations has been discussed in Ref. 17.) Burke et al[11] have also formulated the multichannel scattering theory in the fixed-nuclei approximation for non-linear molecular target systems. All these formulations are based upon the single-center expansion

$$\phi_{\alpha}(\vec{r}') = r^{-1} \sum_{\ell} \varphi^{\alpha}_{\ell}(r)\, Y_{\ell m_{\alpha}}(\hat{r}') \tag{2.35}$$

of the bound and

$$F^{\lambda}(\vec{r}\,') = r^{-1} \sum_{\ell} f^{\lambda}_{\ell}(r)\, Y_{\ell\lambda}(\hat{r}') \tag{2.36}$$

of the continuum molecular orbitals about the center of mass of the molecule. Starting from different basis sets than that given in Eq. (2.29), all these workers derive the coupled radial Eqs. (2.34) for scattering of an electron from a diatomic molecule in a body-fixed frame of reference in the fixed-nuclei approximation. [Henry and Change[15] and Burke and Sinfailam[34] have generalized these equations to include the exchange effects in e^--H_2 and e^--N_2 scattering, respectively, by antisymmetrizing the total wavefunction of the (electron+molecule)-system.]

While in the inner-molecule core-region one can use the fixed-nuclei approximation but in the outer-region, away from the nuclei where short-range terms of the interaction potential are not so strong and the long-range terms (e.g., permanent and induced dipole moments, quadurpole moment, etc.) take up the scattering, the nuclear vibration and/or rotation can no longer be neglected. Also, in this region the coupling between the angular momentum $\vec{\ell}$ of the incident electron and the internuclear axis $\hat{R}$ is weak while between $\vec{\ell}$ and $\vec{j}$ is strong. A natural way of including the effects of the nuclear rotation in the collision process in the outer-region will, therefore, be to work in a space-fixed frame of reference using the formulation of Authurs and Dalgarno[3] and solve the scattering Eq. (2.12). If the inner-region is defined by $0 \leq r \leq r_t$,

then in the outer region for $r \geq r_t$ the highly anistropic short-range terms and the exchange effects have become negligibly small and the long-range terms are not so non-central and strong in their nature, it is, therefore, expected that the convergence problem in the basis set $(j\ell)$ will not be so severe now. At the same time by using a fixed-nuclei approximation for $r \leq r_t$, one will be able to include the local and non-local short-range terms of the electron-molecule interaction in the scattering equations in this region to a satisfying degree of accuracy without increasing the complexity of the numerical work.

A molecule-fixed frame of reference, however, does not necessarily mean a fixed-nuclei approximation unless one neglects the splitting of the rotational levels of the molecule, i.e., the nuclei become infinitely massive. The neglect of the nuclear rotation in the inner-region in a body-frame have changed the physics of the problem in this region. The inner- and outer-regions describe the electron-molecule scattering in body- and space-fixed frames of reference respectively where two entirely different physical situations prevail. Although a transformation from one frame to the other is still carried out by the energy independent operator (2.26) but it is no longer merely a geometrical transformation as the word frame-transformation may imply. Instead in going from inner (body)- to the outer-region (lab-frame) the dynamical approximations describing the collision problem also change.

The essential approximation which one makes in deriving the fixed-nuclei Eq. (2.34) from the body-frame Eq. (2.30) is that the effect of the rotational

energy terms of the molecule [second term on the right hand side of Eq. (2.30)] can be neglected from the energy k^2 (in Ryd.) of the incident electron. Although the correct energy factor in a given channel should be $k^2(J,\ell)$ [in the lab-frame $k^2(J,\ell) = k_j^2$ from Eq. (2.13)] but in the fixed-nuclei approximation this quantity simply becomes k^2. The effect of this difference on the electron scattering in any region will be a minimal if the potential energy on the right hand side of the fixed nuclei Eq. (2.34) is large compared to $k^2 - k^2(J,\ell)$. If the value of the inner molecular core radius r_t becomes so big that this condition is not satisfied then the fixed-nuclei approximation in that region will certainly break down. One shall have to terminate the inner-region at smaller values of r_t and introduce the space frame treatment in the outer region for $r \geq r_t$.

However, under certain circumstances (e.g., when the impact energy of the incident electron is so high that owing to the smallness of B the difference in between k^2 and $k^2(J,\ell)$ itself becomes negligible and/or the long-range terms of the interaction potential fall off rapidly) it is possible that the integration of the lab-frame Eq. (2.12) in the outer-region may not make a significant contribution to the scattering. (A situation similar to this was discovered by Henry and Chang[15] and Chang[16] in their study of the simultaneous vibration-rotation excitation in e^--H_2 scattering.) The phase shift obtained by considering the scattering only in the inner-region in a body-frame in fixed-nuclei approximation will be accurate enough and a space-frame treatment in the outer-region will not be required, i.e., most of the phase accumulation will take place from the

solution of the fixed-nuclei equations in the region $o \leq r \leq r_t$. The adiabatic-nuclei approximation[2] can now be used to calculate the cross-sections for electron impact vibration-rotation transitions in a diatomic molecule.

The frame-transformation theory of electron-molecule scattering is, therefore, particularly useful when the energy of the incident electron is low and/or the interaction potential consists of sufficiently long-range (e.g., r^{-1}, r^{-2}, etc., type) terms which do not fall off very rapidly.

III. METHOD OF IMPLEMENTATION OF THE FRAME-TRANSFORMATION THEORY

A. Definition and Calculation of R-Matrix

In formulating the f.-t. theory of electron-molecule scattering, Chang and Fano[8] have suggested the transformation of the solutions and derivatives of the body-frame fixed-nuclei Eqs. (2.34) at point r_t to the lab-frame in going from inner- to the outer-region. Consequently, one has to perform two separate transformations. Recently, the R- matrix theory, developed by Wigner and Eisenbud[14] for nuclear reactions,[35] has been used very extensively in electron-atom scattering calculations.[36] Here, while considering the scattering only in one (usually laboratory) frame of reference, the interior part ($r \leq r_t$) includes both the local and non-local short-range interactions and the outer part ($r \geq r_t$) consists of only the long-range terms of the local potential. This natural division of the whole interaction space in two parts, supplemented merely by a similarity transformation of a matrix from body- to lab-frame in going from

inner- to the outer-region, makes it very convenient to use the $\underline{R}$-matrix method for studying electron-molecule scattering in the context of the f.-t. theory.

We adopt the same definition of the $\underline{R}$-matrix as given by Burke and Robb,[36] namely

$$\underline{R}(r_t) = [\underline{w}(r) \{r\underline{w}'(r) - b\underline{w}(r)\}^{-1}]_{r=r_t} \tag{3.1}$$

where $\underline{w}(r)$ and $\underline{w}'(r)$ are a set of linearly independent solutions of Eq. (2.34) and their derivatives respectively and $\underline{b}$ is an arbitrary constant matrix. If $\underline{b}$ is taken to be a null matrix the expression (3.1) can be looked upon as the lograthmic derivate matrix of the solutions at $r = r_t$. A set of linearly independent solutions of (2.34) can be related to another set by a transformation

$$\underline{v}(r) = \underline{A}\underline{w}(r) \tag{3.2}$$

where $\underline{A}$ is a non-singular matrix which is independent of r. After substituting (3.2) into (3.1) we find

$$\underline{R}(r_t) = [\underline{v}(r) \{r\underline{v}'(r) - b\underline{v}(r)\}^{-1}]_{r=r_t},$$

i.e., the $\underline{R}$-matrix of Eq. (3.1) is independent of the choice of the set of linearly independent solutions of an equation.

In order to form the sets $\underline{w}(r)$ and $\underline{w}'(r)$, we integrate the fixed-nuclei Eqs. (2.34) in the region from 0 to r_t with the following boundary conditions

$$f^{\lambda}_{\ell\ell'} \underset{r\to 0}{\sim} r^{\ell+1}\delta_{\ell\ell'}$$

$$f^{\lambda'}_{\ell\ell'}(r_t) = k^{-1/2}\left[j_\ell(kr_t)\,\delta_{\ell\ell'} + \eta_\ell(kr_t)\,K^{\lambda}_{\ell\ell'}\right] r_t. \tag{3.3}$$

Here $j_\ell(x)$ and $n_\ell(x)$ are respectively the regular and irregular spherical Bessel functions such that

$$j_\ell(x) \underset{x\to\infty}{\sim} \frac{1}{x}\sin\left(x - \frac{1}{2}\ell\pi\right)$$

and

$$\eta_\ell(x) \underset{x\to\infty}{\sim} \frac{1}{x}\cos\left(x - \frac{1}{2}\ell\pi\right)$$

[Note that in the fixed-nuclei approximation all channels will be open and degenerate.] The second subscript on f^{λ} in Eq. (3.3) stands for the incident channel. The K^{λ}-matrix calculated from Eq. (3.3) is not the correct $\underline{K}$-matrix as no account has been taken of the long-range terms in the inner-region ($0 \le r \le r_t$) in the solution of the fixed-nuclei equations. Instead, the calculation of K^{λ} is based completely upon the inclusion of the short-range terms of local and non-local electron-molecule interaction potential in the scattering Eq. (2.34) in the molecular core region.[37]

The convergence of the eigenphase sum

$$\delta^{\lambda}_{Sum} = Tr\left[\tan^{-1}(\underline{B}\,\underline{K}^{\lambda}\,\underline{B}^{-1})\right] \tag{3.4}$$

will now completely depend upon the inclusion of the highly anisotropic short-range terms and the two nuclear singularities in the fixed-nuclei Eqs. (2.34). In Eq. (3.4) $\underline{B}$ is an orthogonal matrix which diagonalizes the real symmetric K^{λ}-matrix. The convergence of δ^{λ}_{sum} will, in fact, determine whether the single-center expansion (2.36) in ℓ of the continuum molecular orbital and the multipole expansion (2.11) in μ of the molecular charge distribution have converged.

The solution elements $f^{\lambda}_{\ell\ell'}$, and their derivatives $f^{\lambda'}_{\ell\ell'}$, are now linearly combined

$$w^{\lambda}_{ij}(r) = \sum_{k=1}^{n_e} a_{ik} f^{\lambda}_{kj}(r),$$

$$w^{\lambda'}_{ij}(r) = \sum_{k=1}^{n_e} a_{ik} f^{\lambda'}_{kj}(r), \qquad (3.5)$$

$(i, j = 1, \ldots n_e$ the no. of coupled equations),

to form a set of linearly independent solutions $\underline{w}^{\lambda}(r)$ and their derivatives $\underline{w}^{\lambda'}(r)$. The generic program[38] written by us describes in detail the method of solving and matching a set of coupled homogeneous (or inhomogeneous) scattering equations to the asymptotic scattering boundary conditions. This program could be readily adapted to the choice of the boundary conditions given in Eq. (3.3). The matching procedure, needed to calculate K^{λ} matrix, also yields[38] the coefficients of linear combination a's used in Eqs. (3.5). These sets of $\underline{w}^{\lambda}(r)$

and $\underline{w}^{\lambda}(r)$ can now be employed for calculating the $\underline{R}^{\lambda}$-matrix at point r = in a molecule-fixed frame of reference in fixed-nuclei approximation:

$$\underline{R}^{\lambda}(r_t) = [\underline{w}^{\lambda}(r)\ \{\underline{r}\,\underline{w}^{\lambda'}(r) - \underline{b}\,\underline{w}^{\lambda}(r)\}^{-1}]_{r=r_t} \tag{3.6}$$

This matrix will obviously be diagonal in λ and have the dimensions equal to the number of ℓ values of the single-center expansion (2.36) that are coupled in Eq. (2.34).

B. Transformation of $\underline{R}^{\lambda}$-Matrix and Calculation of $\underline{S}^{J}$-Matrix

In the outer-region ($r_t \leq r \leq \infty$) the space-fixed frame treatment of the scattering process is described by Eq. (2.12). The terms V_μ of the electron-molecule interaction potential now consist of only a first few long-range multipole moments, permanent or induced, of the molecular charge distribution. The coupled radial Eqs. (2.12) are integrated inward from $r = \infty$ to $r = r_t$. The asymptotic forms given in Eqs. (2.14) determine the boundary conditions to be used to start an inward integration from $r = \infty$ in order to generate a family of solutions. If n_0 is the number of open channel basis sets ($j\,\ell \equiv p$) out of the total number n_t coupled in Eq. (2.12), a set of n_0 linearly independent solutions and derivatives is obtained from the following combinations

$$\begin{aligned} v_{pr}^{J\eta} &= \sum_{q=1}^{n_t+n_0} c_{pq}\, u_{qr}^{J\eta}, \\ v_{pr}^{J\eta'} &= \sum_{q=1}^{n_t+n_0} c_{pq}\, u_{qr}^{J\eta'}, \end{aligned} \tag{3.7}$$

of the elements of solutions of Eq. (2.12) and their derivatives respectively. Here we have introduced the superscript $\eta = (-1)^{j+\ell} = (-1)^{j'+\ell'}$ specifying the parity $[= (-1)^J \eta]$ of the basis set coupled in Eq. (2.12). In order to determine the coefficients c's in Eq. (3.7) we form the $\underline{R}^{J\eta}$ -matrix at $r = r_t$, i.e.,

$$\underline{R}^{J\eta}(r_t) = [\underline{v}^{J\eta} \{\underline{r}\, \underline{v}^{J\eta'}(r) - \underline{b}\, \underline{v}^{J\eta}(r)\}^{-1}]_{r=r_t}, \tag{3.8}$$

where constant matrix $\underline{b}$ is the same as used in Eq. (3.6).

This matrix should be equal to the $\mathcal{R}^{J\eta}(r_t)$-matrix obtained by transforming to the space-frame the $\underline{R}^{\lambda}(r_t)$-matrix of Eq. (3.6) which has been calculated in the body-frame of reference in fixed-nuclei approximation. Therefore

$$\underline{v}^{J\eta}(r_t) = \mathcal{R}^{J\eta}(r_t)\ [\underline{r}\, \underline{v}^{J\eta'}(r) - \underline{b}\, \underline{v}^{J\eta}(r)]. \tag{3.9}$$

The elements of $\mathcal{R}^{J\eta}(r_t)$-matrix are given by a similarity transformation of the $\underline{R}^{\lambda}(r_t)$-matrix carried out by the orthogonal transformation operator Ω of Eq. (2.26). Therefore,

$$\mathcal{R}^{J\eta}_{j\ell,j'\ell'} = \sum_{\lambda \geq 0}^{\ell_{min}} \Omega^{(\ell J\eta)^T}_{\lambda j}\ R^{\lambda}_{\ell\ell'}\ \Omega^{(\ell' J\eta)}_{j'\lambda}$$

$$= 2\sqrt{(2j+1)(2j'+1)} \sum_{\lambda \geq 0}^{\ell_{min}} \begin{pmatrix} j & \ell & J \\ 0 & \lambda & -\lambda \end{pmatrix} \frac{R^{\lambda}_{\ell\ell'}}{1+\delta_{0\lambda}} \begin{pmatrix} j' & \ell' & J \\ 0 & \lambda & -\lambda \end{pmatrix}, \tag{3.10}$$

where ℓ_{min} = smaller of (ℓ, ℓ', J). Because for linear molecules $\underline{R}^{-\lambda} = \underline{R}^{\lambda}$ [see Eq. (2.34)], this transformation can also be written as[39]

$$\mathcal{R}^{J\eta}_{j\ell, j'\ell'} = \sqrt{(2j+1)(2j'+1)} \sum_{\lambda=-\ell_{min}}^{\ell_{min}} \begin{pmatrix} j & \ell & J \\ 0 & \lambda & -\lambda \end{pmatrix} R^{\lambda}_{\ell\ell'} \begin{pmatrix} j' & \ell' & J \\ 0 & \lambda & -\lambda \end{pmatrix}. \quad (3.11)$$

The matrix of Eq. (3.11) is now substituted on the right hand side of Eq. (3.9). Burke et al[40] have discussed in detail the solution of the matching equation (3.9) in their formulation of the $\underline{R}$-matrix theory of electron-atom scattering. They have also derived the appropriate expressions relating the $\underline{K}$-matrix to the coefficients of linear expansion used in Eqs. (3.7). Once $\underline{K}^{J\eta}$-matrix is known one can always compute the $\underline{S}^{J\eta}$-matrices from Eqs. (2.15) and (2.16) respectively in order to calculate the differential and integrated cross-sections[41] for electron impact rotational transitions in a diatomic molecule.

The whole procedure of employing the f.-t. theory to study electron-molecule scattering can, therefore, be divided into five following steps:

(1) study the convergence of the fixed-nuclei Eq. (2.34) in the inner-region $(0 \leq r \leq r_t)$ in ℓ and μ,

(2) compute body frame $\underline{R}^{\lambda}$-matrix at $r = r_t$ for all values of $\lambda \leq \ell_{min}$,

(3) transform the $\underline{R}^{\lambda}$-matrix to $\underline{\mathcal{R}}^{J\eta}$-matrix,

(4) solve the space-frame Eqs. (2.12) in the outer-region $(r \geq r_t)$ by integrating inward from $r = \infty$ to $r = r_t$ and match the solutions and derivatives with $\underline{\mathcal{R}}^{J\eta}$-matrix for calculting the $\underline{K}^{J\eta}$-matrix,

(5) calculate the $\underline{S}^{J\eta}$-matrix from Eq. (2.15) and then the cross-sections for different rotational transitions.

In addition to this, one will also have to study the dependence of the final cross-sections on the choice of the boundary point r_t where the inner- and the outer-region are separated from each other. This will involve trying a number of different values for r_t and then deciding upon that particular value where the results are fairly 'stabilized'. This point has been further discussed at length in Sec. IV B(iii).

The last three steps, out of the above five required for the successful implementation of the f.-t. theory, have to be carried out both for even and odd parities, i.e., for η = +1 and -1 values, for the same value of J. However, it may also be necessary to study the convergence of the lab-frame Eqs. (2.12) in the number of coupled channels ($j\ell$) in the outer-region ($r \geq r_t$). In that case, steps (3) to (5) will have to be repeated each time by increasing the number of coupled rotational states in the outer-region for each J and η values.

IV. NUMERICAL CALCULATIONS

A. Test Study: Application to a Model Calculation

The practical application of the f.-t. theory is a multistep process which becomes an arduous task. We, therefore, thought it to be extremely useful to apply this theory first to some model calculation of e^--CO scattering before using it in more fundamental and complex situations. This test study will also

make the physics of the problem more transparent and at the same time provide a good check on our whole numerical procedure.

Crawford and Dalgarno[18] have studied the scattering of thermal-energy electrons from carbon monoxide using the close-coupling (c.c.) formulation of Arthurs and Dalgarno[3]. (The method has accordingly been called rotational close coupling.) Their whole calculation has been done in the space-fixed frame by solving the Eq. (2.12). They employ a semi-empirical potential which is a combination of the dipole, quadrupole, and polarization potentials of carbon monoxide. This potential, in the notation of Eq. (2.11), can be written as

$$V_0(r) = -\frac{\alpha_0}{2(r^2 + r_0^2)^2},$$

$$V_1(r) = \begin{cases} 0 & r \leq r_d \\ \dfrac{D}{r^2}\,\dfrac{(r - r_d)^2}{b_d^2 + (r - r_d)^2} & r \geq r_d, \end{cases}$$

and

$$V_2(r) = V_2^{(q)}(r) + V_2^{(p)}(r) \tag{4.1}$$

where

$$V_2^{(q)}(r) = \begin{cases} 0 & r \leq r_q \\ \dfrac{Q}{r^3}\,\dfrac{(r - r_q)^2}{b_q^2 + (r - r_q)^2} & r \geq r_q, \end{cases}$$

and

$$V_2^{(p)}(r) = \begin{cases} 0 & r \le r_p \\ -\dfrac{\alpha_2}{2(r^2 + r_0^2)^2} \dfrac{(r - r_p)^2}{b_p^2 + (r - r_p)^2} & r \ge r_p. \end{cases}$$

In this expansion (all quantities are in atomic units, unless specified otherwise)

$$\begin{aligned} D &= 0.044, \qquad Q = -1.859, \\ \alpha_0 &= 13.342, \quad \alpha_2 = 2.396 \end{aligned} \tag{4.2}$$

are respectively the dipole moment, quadrupole moment, spherical and the non-spherical components of the polarizability of CO molecule. The values of other seven parameters (r_0, r_d, b_d, r_q, b_q, r_p, and b_p), given in Ref. 18, were adjusted so that this potential, when used in Eq. (2.12), could reproduce the experimentally measured[9] momentum transfer cross-section in the energy range from 0.005 eV to 0.1 eV. The asymptotic form of the potential (4.1) is

$$\begin{aligned} V_0(r) &\sim -\frac{\alpha_0}{2r^4}, \\ V_1(r) &\sim \frac{D}{r^2}, \end{aligned} \tag{4.3}$$

and

$$V_2(r) \sim \frac{Q}{r^3} - \frac{\alpha_2}{2r^4}.$$

Before using the f.-t. theory, we first used this potential to study the electron scattering in the fixed-nuclei approximation in the whole region of configuration space. We employed the program of Chandra[38] to solve Eq. (2.34) in the region ($0 \leq r \leq \infty$). The solution of these equations will now give us the exact $\underline{K}^{\lambda}$-matrix of the body-frame in fixed-nuclei approximation. This matrix was then used to compute the eigenphase sum defined in Eq. (3.4) for studying the convergence of the single-center expansion (2.36) in ℓ for $^2\Sigma$ ($\lambda=0$), $^2\Pi$ ($\lambda=1$), and $^2\Delta$ ($\lambda=2$) states of the (e^-+CO)-system. We found that 8 or 9 values of ℓ were sufficient to achieve satisfactory convergence of the single-center expansion when the model potential of Eq. (4.1) was used. The converged eigenphase sums for these three cases are shown in Fig. 1. There is known to be a shape resonance[42] at about 1.75 eV for electron scattering from CO in $^2\Pi$ state. We notice from Fig. 1 that the eigenphase sums calculated using the Crawford and Dalgarno portential,[18] given in Eq. (4.1), does not reproduce this resonance. However, there is a resonance behavior shown by the $^2\Sigma$ state eigenphase sum at about 1.40 eV. Similarly the $^2\Pi$ eigenphase sum too shows a very broad resonance at a higher energy.

In order to employ the f.-t. theory the potential (4.1) should be used in the inner region ($o \leq r \leq r_t$) in the fixed-nuclei approximation. If point r_t is far enough from the center of mass of the molecule then one is always justified in using the asymptotic form (4.3) of this potential in the lab-frame treatment in the outer-region. However, as the potential (4.1) is in a very simple form, we

have used the exact potential even in the region for $r \geq r_t$. In order to calculate the cross-sections for different rotational transitions from f.-t. theory we have carried the five step process mentioned at the end of Sec. III.

A sampling of our partial cross-sections, $\sigma^J_{j\to j'}$, for transitions (0→0), (0→1), (1→1), and (2→2) is shown in Table I for five different values of the incident electron energy. In the fourth column of this table the exact rotational c.c. results, which we have calculated and agree very well with those of Ref. 18, are also given. In the last five columns the cross-sections calculated from the f.-t. theory for five different values of r_t are tabulated. [The value $\underline{b} = 1$ was used in Eqs. (3.6) and (3.9) in the definition of $\underline{R}$-matrix.]

The very first thing which one should expect from these results is that smaller the value of r_t better should be the agreement between the rotational c.c. and f.-t. results. This is due to the fact that the potential used in two regions of the f.-t. theory is exactly the same and it is only the rotational level spacing which has been neglected in the inner-region in fixed-nuclei approximation. A decrease in the size of this region will, therefore, mean that the lab-frame rotational c.c. treatment is being introduced closer to the origin. Our results of Table I confirm this general conclusion.

We also notice from the enteries of this table that the partial cross-sections which vary most with the values of r_t are those in which ($\ell=0$, $\ell'=0$) partial wave coupling is present, namely σ^J ($j=J\to j'=J$). On the other hand, the $\sigma^0(0\to0)$ cross-section is almost invariant with the values of r_t considered in this table

and at the same time in good agreement with the exact rotational c.c. results. The major contribution to the (0→0) transition with J = 0 will basically come from V_0 term of potential (4.1). The form of this term used by Crawford and Dalgarno[18] is such that it has already assumed its asymptotic form much before the space-frame treatment is introduced at r_t = 4.466 (a.u.) [see Eqs. (4.1) and (4.2), r_0 = 1.310 (a.u.) from Ref. 18] and therefore goes off as r^{-4}. As a result the V_0 term has become so small in the outer-region that most of the phase accumulation occurs from the solution of the fixed-nuclei equations in the inner region and a lab-frame treatment in the outer-region does not make any significant contribution to the scattering. The cross sections for other values of j, j', and J are almost constant for all values of r_t and they agree very well with those calculated from rotational c.c. method. This kind of behavior of the results calculated from f.-t. theory will, however, very much depend upon the nature of the short-range terms, which are not very strong in the present case.

It will probably not be too late to mention at this stage that such a good agreement in between the rotational c.c. and f.-t. results is subject to the accuracy to which the fixed-nuclei Eqs. (2.34) are solved in the inner-region in order to calculate the $\underline{R}^{\lambda}$-matrix at $r = r_t$. The accuracy of the solutions in the present case simply means that the sufficient values of ℓ are coupled in Eq. (2.34) for the single-center expansion (2.36) of the continuum orbital to converge for each value of λ. However, such a satisfactory solution of the inner-region equation in a body-frame of reference in fixed-nuclei approximation is a

pre-requisite for a successful application of the f.-t. theory for studying the electron-molecule scattering.

B. Application to the Single-Center Pseudo-Potential Method

(i) Adaptation of the pseudo-potential method to the frame-transformation theory

The pseudo-potential method, originally introduced in our e $-N_2$ study,[10] has been found to work very well even for electron scattering from CO in the fixed nuclei approximation. In this method the exchange effects between the incident and the molecular electrons are simulated by orthogonalizing the continuum scattering orbital to the bound molecular orbitals of the same symmetry. The body-frame fixed-nuclei Eq. (2.34) are now replaced by the following coupled inhomogeneous equations:

$$\left[\frac{d^2}{dr^2} - \frac{\ell(\ell+1)}{r^2} + k^2\right] f_\ell^\lambda(r)$$

$$= 2(-1)^\lambda \sqrt{2\ell+1} \sum_{\mu\ell'} \sqrt{2\ell'+1} \begin{pmatrix} \ell & \ell' & \mu \\ 0 & 0 & 0 \end{pmatrix} \begin{pmatrix} \ell & \ell' & \mu \\ \lambda & -\lambda & 0 \end{pmatrix} V_\mu(r)\, f_{\ell'}^\lambda(r)$$

$$+ \sum_{\alpha=1}^{n_b} \xi_\alpha \varphi_\ell^\alpha(r). \qquad (4.4)$$

Here $\varphi_{\ell}{}^{\alpha}$ (r) are the radial coefficients in the single-center expansion (2.35) of the molecular core orbitals $\phi_{\alpha}(\vec{r}')$ which have the same symmetry as the continuum orbital $F^{\lambda}(\vec{r}')$ in Eq. (2.36). ξ_{α} are the lagrange multipliers determined by the requirement that

$$\left\langle \phi^{\alpha} \right| F^{\lambda} \rangle = 0 \tag{4.5}$$

for $\alpha = 1, \ldots n_b$, the number of such bound orbitals of a particular symmetry.

As discussed in I, the program of Faisal and Tench[43] was employed to convert the two-center ground electronic state wave-function of CO, given by McLean and Yoshimine,[44] into a one-center expansion about the center of mass of the molecule. These single-center expansions of the molecular orbitals were then used to calculate the multipole expansion (2.11) of the molecular charge distribution.

[We will like to point out to the reader that there is an error in Eq. (17) of Ref. 22 where the electron-nuclei contribution {terms enclosed in the parenthesis on the right hand side of Eq. (2.4)} to the static potential has been expanded into the Legendre polynominals about the center of mass of the molecule. As the program of Faisal and Tench[43] has used this expression to compute the multipole expansion of the molecular charge distribution, the corresponding correction should, therefore, also be made in this program. This error and the correct form of the expression are given in I.]

The highly anistropic short-range terms, nuclear singularities, and the exchange effects are properly represented in the Eq. (4.4) by achieving satisfactory convergences in the expansions (2.11), (2.35), and (2.36) simultaneously. We have shown in I that these three expansions converge very well even for low symmetry molecules like CO.

In order to have a resonance in the $^2\Pi$ eigenphase sum calculated from (4.4) at about 1.75 eV, the static potential in I was augmented by a polarization potential of the form

$$V_{pol}(\vec{r}) = -\frac{1}{2r^4}\ [\alpha_0 + \alpha_2 P_2(\hat{r}\cdot\hat{R})]\ [1 - \exp\{-(r/r_0)^6\}], \quad (4.5)$$

where

$$\alpha_0 = 13.342, \qquad \alpha_2 = 2.396. \quad (4.6)$$

The adjustable parameter $r_0 = 1.605$ (a.u.) was found to give a resonance in $^2\Pi$ state at $E_r = 1.753$ eV. The calculated values of the width (Γ_r) and background phase shift (δ_r) for this resonance are given in Table III.

In the context of f.-t. theory, we solve Eqs. (4.4), together with the polarization potential (4.5), in the molecular core-region ($0 \le r \le r_t$). The method of solving the inhomogenous equations together with the requirements of orthogonality has been discussed in detail in our previous paper of Ref. 38. This program could be easily adapted to calculate the fixed-nuclei $\underline{R}^\lambda$-matrix defined in Eq. (3.6). In the outer-region ($r \ge r_t$), on the other hand, we assume that

$\varphi_\ell^\alpha(r) \simeq 0$ and both the static and the polarization potentials, Eqs. (2.11) and (4.5) respectively, have taken up their asymptotic forms. Therefore, for the space-frame Eq. (2.12) in the outer-region the potential will be given by

$$V_0(r) = -\frac{\alpha_0}{2r^4}, \qquad V_1 = \frac{D}{r^2},$$

$$V_2(r) = \frac{Q}{r^3} - \frac{\alpha_2}{2r^4}, \tag{4.7}$$

and

$$V_3(r) = \frac{O}{r^4},$$

where O is that octopole moment of the CO molecule. The values of α_0 and α_2 are given in Eq. (4.6). But

$$D = -0.105, \qquad Q = -1.547, \tag{4.8}$$

and

$$O = 4.380.$$

were obtained from the multipole expansion (2.11) of the CO static potential whose calculation has been described elsewhere.[1]

(ii) Selection of the inner-molecular core radius r_t

The partial cross-sections $\sigma^J_{j\to j'}$, obtained by using the single-center pseudo-potential in context of the f.-t. theory are given in Table II for six

different values of r_t. According to the test study of Sec. IV(A), we find that the $\sigma^J_{j \to j'}$ for (j, j' = J) cross-section varies most with r_t. This is associated with the fact that in this case the s-wave is coupled with both initial and final rotational states.

We have said above, while discussing the adaptation of the pseudo-potential to f.-t. theory, that in going from inner- to the outer-region we completely neglect the short-range parts of the local and non-local electron molecule interactions. A selection of a smaller value of r_t will, therefore, mean that more of these potential terms are being neglected in performing a frame-transformatic even though they have not become small enough. On the other hand, performing the transformation at a large distance from the center of mass of the molecule corresponds to the fact that although the potential, which is still non-negligible due to the long-range terms, has become comparable to the rotational level spacings but the latter has not been introduced yet into the scattering equations. The size of the inner molecular core-region, where the fixed-nuclei approximation is being used, has now become so big that the difference in between $[k^2 - k^2(J, \ell)]$ is no longer smaller than the potential energy terms and therefore the nuclear rotation can no longer be neglected from the scattering equations. In Table II there corresponds a region between r_t = 10.150 (a.u.) to r_t = 13.398 (a.u.) where the partial cross-sections for all transitions seem to have "stabilized".

Chang and Fano° do not give any rigorous criterion for the selection of the boundary point r_t which divides the interaction region into two parts where two physically different treatments of the scattering process are to be carried out. All their statements concerning the choice of this point are qualitative. We do not see any quantative way for defining the range of the inner molecular core-region other than carrying out the f.-t. treatment at a number of different values of r_t and then selecting that value where the various cross-sections have become fairly 'stationary'. From our test study, discussed in the preceding subsection, one will conclude that if the scattering equations in the inner-region in fixed-nuclei approximation are solved accurately enough then the final cross-sections for electron impact rotational transitions in a molecule will be very close to the exact values provided a transformation from molecule- to the space-frame is performed at a point where the results are 'stabilized'.

In the following calculations we have, therefore, used $r_t = 11.774$ (a.u.) for the inner-molecular core radius. Note that this value of the core radius is almost six times of the equilibrium inter-nuclear separation (= 2.132 a.u.) in the ground electronic state of carbon monoxide.

The existence of the boundary point r_t is the central aspect of the f.-t. theory. Selection of two different limiting values for r_t will reduce the f.-t. theory to two well known formulations of the electron-molecule scattering—for $r_t = 0$ it will reduce to the rotational c.c. theory of Authurs and Dalgarno[3] and

for $r_t = \infty$ become equivalent[17] to the adiabatic-nuclei theory[2]. The existence of a value of r_t in between these two limits, therefore, becomes a vital point for the applicability of the f.-t. theory. But at the same time the absence of a rigorous criterion for deciding upon the inner-molecular radius r_t makes this theory less fundamental than, say, the rotational c.c. formulation of Arthurs and Dalgarno[3]. The stabilization requirement used by us in choosing a value for r_t when performing a transformation from molecule- to a space-fixed frame of reference constitutes probably the best criterion under the existing circumstances. Although this condition too lacks an element of rigorousness, it is nevertheless significant that one can obtain more accurate and reliable results with it.

An alternative way for finding a value for the core-radius will be to try to fit the cross-sections computed from the f.-t. theory to the experimental measurements. Although this fitting procedure will be free from all sorts of uncertainties which may be embeded in the stabilization criterion but at the same time it will make the whole theory more phenomenological.

However, under certain circumstances—e.g., when the information about the molecular core-region can be extracted from the experimental data—it is possible to bypass the difficulties associated with the selection of a proper value for r_t. Fano[28(b)] while analyzing the high resolution photoabsorption spectrum of H_2 and Atabek et al[45] calculating the spectrum of Π_u^- Rydberg levels of

H_2, using the f.-t. theory, have obtained the information about the core-region of hydrogen molecule from the multichannel quantum defect methods developed by Seaton.[46]

We have now specified all the necessary quantities for the inner- and outer-region required to apply the f.-t. theory to study the e^--CO scattering using the pseudo-potential method. The thermal energy momentum transfer cross-section, $\sigma^m(0)$ [Eq. 2.23)], calculated from this method is shown by (dash-dot) curve D in Fig. 3. The ratio of the theoretical results to that experimentally measured (curve A) drops from a factor of five at 0.005 eV to about a factor of two at 0.1 eV. We have given in I an analytic proof to show that, unlike the total scattering cross-section, the momentum transfer cross-section, averaged over all molecular orientations, is finite even for electron scattering from a polar molecule in a body-fixed frame of reference in the fixed-nuclei approximation. Therefore at higher energies the momentum transfer cross-section calculated from the pseudo-potential using the f.-t. theory should be the same as given in Fig. 8 of I where it was computed in the fixed-nuclei approximation. One will also notice that our calculated results in I does reproduce the 1.75 eV $^2\Pi$ resonance.

(iii) Re-normalization of the dipole-term in the static potential of CO molecule

The electron-polar molecule scattering at sufficiently low-energies is very much dominated by the long-range electron-dipole interaction.[47] The values of

the dipole, quadrupole, and octopole moments which we have used in our pseudo-potential method are given in Eq. (4.8). (These values are in good agreement with those computed in Ref. 44; D = -0.1007, Q = -1.634.) McLean and Yoshimine[44] have employed an extended basis set in the expansion of their two-center wave function with seventeen STAO centered on each of the carbon and oxygen nuclei. This sophisticated wave-function reproduces the correct ground electronic state energy for the equilibrium inter-nuclear separation of CO, the theoretical quadrupole moment (-1.547 a.u.) is about 83% of the experimental value (-1.859 a.u.) but the magnitude of the dipole moment (0.105 a.u.) obtained from this wave-function is about 2.4 times higher than the experimentally measured value (0.044 a.u.) [cf. Eqs. (4.2) and (4.8)] . (Also, the theoretically calculated dipole moment has a sign opposite to that of the experimentally measured. This discrepancy in sign is related to the polarity of CO molecule and the direction of the inter-nuclear axis which have been discussed in Ref. 44) It will make a difference in the thermal-energy electron scattering cross-sections for $j \rightarrow j\pm1$ transitions approximately by a factor of $(2.4)^2$ [See Eqs. (A12) and (A13) in the Appendix].

We, therefore, thought that the easiest way to rectify the shortcoming of the present wave function, without affecting its other properties which are in conformity with the experiments, would be to scale down the dipole-term in the multipole expansion (2.11) by a factor of

$$\zeta_d = \frac{|D_{theory}|}{D_{exp}} = 2.386. \qquad (4.9)$$

This re-normalization of only the dipole-term will ensure its continuity over the whole range of the interaction space while other multipole terms will remain unchanged. The multipole expansion (2.11) of the static potential will now be replaced by

$$V(\vec{r};\vec{R}) = \sum_{\mu} \frac{V_{\mu}(r)}{[1 + (\zeta_d - 1)\,\delta_{\mu 1}]}\, P_{\mu}(\hat{r}\cdot\hat{R}) \qquad (4.10)$$

in the fixed-nuclei Eq. (4.4). This re-scaling of the V_1 -term should not alter significantly the short-range nature of the charge distribution of carbon-monoxide computed from the wave function of McLean and Yoshimine.[44]

To consider the constant ζ_d as a parameter in the usual sense of the word perhaps will not constitute a correct description of the present situation. The value $\zeta_d = 2.386$ has not been arrived at by fitting our results to any of the quantities which we intend to calculate finally. The circumstances, on the other hand, have forced us to re-scale the dipole-term of the static potential by ζ_d in order to correct, rather in a phenomenological way, the deficiency of the ground electronic state wave-function of CO molecule whose calculation in itself is a major field of research in the domain of quantum chemistry and not the aim of the present study.

Although re-normalization of only the dipole-term will not affect the convergence properties of the single-center expansions (2.35) and (2.36) and also of the multipole expansion (4.10) in the fixed-nuclei Eq. (4.4), which we have

discussed in detail in I. But it will certainly require a new value for the parameter r_0 used in the polarization potential (4.5) in order to have a resonance in the $^2\Pi$ state eigenphase sum at about 1.75 eV. The procedure described in I was repeated again but this time only for the $^2\Pi$ state. The new value of this parameter obtained was $r_0 = 1.541$ (a.u.) which is not very much different than the old one (1.605). The new eigenphase sum have been plotted in Fig. 2 and the values of the resonance parameters in the present case are given in Table III. One will notice that the effect of renormalization of the dipole term on the values of δ_0 and Γ_r is very insignificant indeed. Also this re-scaling will not affect the value of the molecular core-radius $r_t = 11.774$ (a.u.) defining the inner-region of the f.-t. theory. Moreover, the new values of the multipole moments required to specify the potential (4.7) in the outer-region in a lab-frame are now given by

$$\begin{aligned} D &= -0.044, \qquad Q = -1.547, \qquad O = 4.380, \\ \alpha_0 &= 13.342, \qquad \alpha_2 = 2.396, \end{aligned} \tag{4.11}$$

which differ from the old constants, given in Eq. (4.8), in the magnitude of the dipole moment only.

(IV) Convergence in the outer-region

The last thing to be considered is the convergence of the space-frame Eq. (2.12) in the outer-region in the basis set $(j\ell)$ for each value of J and parity.

The calculation of the cross-section for transitions involving higher rotational states will require the solutions of equations for large values of J. At the same time the number of coupled channels (j,ℓ) will increase [by min (J,j) + 1 for even parity $\{(-1)^{J+j+\ell} = 1\}$ and by min (J,j) for add parity $\{-1^{J+j+\ell} = -1\}$] with the introduction of each new rotational state j. The consideration of higher values of J will also mean that one has to calculate the fixed-nuclei $\underline{R}^{\lambda}$-matrix [Eq. (3.6)] at the boundary point r_t for higher values of λ, since $|\lambda| \leq$ min (ℓ,J) from Eq. (3.11). In addition to this, because of r^{-2} type behavior of the electron-dipole interaction potential, the solutions of the lab-frame Eq. (2.12) assume their free-wave asymptotic forms at a large distance (say $r=r_\infty$) from the center of mass of the molecule. In the outer-region, therefore, one would have to integrate a large set of coupled equations over a wider range of r ($r_t \leq r \leq r_\infty$). All these factors combined together require large machine size and the computational time. Hence the solution of Eq. (2.12) in the outer-region in a space-frame becomes economically quite prohibitive.

We, therefore, restricted ourselves to the calculation of the cross-sections for transitions (0→j') and (1→j'). In the present case, unlike for the homonuclear diatomic molecules, final rotational state quantum number j' can take both even and odd values. Thus, in Eq. (2.12) for each J we coupled only those rotational states which were necessary for the convergence of the partial cross-sections $\sigma^J_{0\to j'}$ and $\sigma^J_{1\to j'}$ in even and odd parities separately. In Tables IV and V we have tabulated $\sigma^J_{0\to j'}$ and $\sigma^J_{1\to 1'}$ respectively with the coupling of each new

rotational state in even parity. These cross-sections correspond to 1.75 eV of the incident electron energy. The convergence of the partial cross-sections for odd parity has been shown in Table VI.

We find that maximum number of rotational states are needed to be coupled in even parity with J= 2, 3, and 4. It is probably due to the fact that because $^2\Pi$ is a resonating state therefore maximum contribution to the cross section will come from the coupling of the ℓ = 1,2, and 3 partial waves. For values of J=2, 3, and 4 the first six or seven rotation states of the molecule can be coupled to these values of the orbital angular momenta.

One will also notice from these three tables that the slowest rate of convergence in J is for $j \to j \pm 1$ and j+2 transitions. [Actually for electron impact energies $\leq$ 0.10 eV as many as 100 values of J were required for $\Delta j = \pm 1$ transitions.] The cross-sections for these transitions are directly dominated by contribution(s) coming from the long-range electron dipole (and electron-octopole if $j+j' \geq 3$) and the electron-quadrupole interactions respectively. We also found that, for all incident electron energies, the $\underline{T}^J$ -matrix elements for $\Delta j = \pm 1$ and 2 transitions for values of J higher than 10, obtained from the f.-t. theory were in good agreement with those calculated from the Born approximation considering merely the V_1, V_2 (only the quadrupole part), and V_3 terms of the interaction potential (4.7). In order to calculate the differential scattering cross-section for $j \to j \pm 1$ and j+2 transitions, we, therefore, replace the exact $\underline{T}^J$ -matrix elements in Eq. (2.19) for J > 10 by the corresponding

elements calculated from the Born approximation. This will also mean that one has to calculate the fixed nuclei $\underline{R}^{\lambda}$ -matrix at $r = r_t$ only for eleven (λ=0, . . 10) values of λ.

The differential scattering cross-section for a j→j' transition can be calculated by recasting the Eq. (2.17) in the following form

$$\frac{d\sigma_{j\to j'}}{d\Omega} = \frac{d^{B}\sigma_{j\to j'}}{d\Omega} + \frac{k_j^{-2}}{4(2j+1)} \sum_{L} [A_L^{(jj')} - {}^{B}A_L^{(jj')}] P_L(\cos\theta) \qquad (4.12)$$

In this relation $d^{B}\sigma_{j\to j'}/d\Omega$ is the differential cross-section calculated from Born approximation and the coefficients A_L are defined by Eq. (2.18) where maximum value of J in (2.19) is J_{max} beyond which the exact $\underline{T}^{J}$ -matrix can be replaced by those calculated from the Born-approximation. ${}^{B}A_L$ is also calculated from Eq. (2.18) by using the Born $\underline{T}^{J}$ -matrix in Eq. (2.19) up to J_{max}. [The relevant formulae of Born approximation are given in the Appendix.] Consequently, the scattering and the momentum transfer cross-sections for transitions j → j±1 and j+2 are calculated from

$$\sigma_{j\to j'} = {}^{B}\sigma_{j\to j'} + \frac{\pi k_j^{-2}}{2j+1} [A_0^{(jj')} - {}^{B}A_0^{(jj')}] . \qquad (4.13)$$

and

$$\sigma^{m}_{j\to j'} = {}^{B}\sigma^{m}_{j\to j'} + \frac{\pi k_j^{-2}}{2j+1} \left[\left\{A_0^{(jj')} - \frac{1}{3}A_1^{(jj')}\right\} - \left\{{}^{B}A_0^{(jj')} - \frac{1}{3}{}^{B}A_1^{(jj')}\right\}\right] \qquad (4.14)$$

respectively. ${}^{B}\sigma_{j\to j'}$ is the scattering and ${}^{B}\sigma^{m}_{j\to j'}$ the momentum transfer cross section for (j→j') transition calculated from the Born approximation [see Eqs. (A12 and A13)].

C. Final Results

The momentum transfer cross-section inferred from swarm experiments by Hake and Phelps[9] in the energy range between 10^{-3} to 1.0 eV is shown by curve A in Fig. 3. The dotted curve A' above 1.0 electron Volts, which peaks at about 1.50 eV, was chosen by these experimentalists to extrapolate smoothly to their derived curve A at lower energies.

We have extended the rotational c.c. calculation of Crawford and Dalgarno[18] in a space-fixed frame of reference to higher energies. The total momentum transfer cross-section σ^{m} (0) [Eq. (2.23)] obtained from this calculation is marked B in Fig. 3. Although the authors of Ref. 18 used seven parameters in their potential (4.1) in order to reproduce the momentum transfer cross section of Hake and Phelps[9], but we notice from Fig. 3 that the theoretical results (curve B) begin to deviate from the inferred values (curve A) at about 0.20 eV. These computed results also show a very broad peak near 1.50 eV ranging from about 0.60 to 5.0 eV. On the basis of the eigenphase sums obtained by using the potential (4.1) in the fixed-nuclei Eq. (2.34) and shown in Fig. 1, one will conclude that it is probably the combination of $^{2}\Sigma$ and $^{2}\Pi$ resonances which is responsible for this broad peak in curve B (Fig. 3).

The momentum transfer cross-section calculated by an application of our methodology, developed in the preceding sections to e^--CO scattering is shown by curve D of Fig. 3. These results are obtained with the re-normalized value of the dipole-term in the static potential [Eq. (4.10)]. On comparing these new results with those computed from the original V_1-term in the multipole expansion, which are marked C in Figure 3, we find that re-scaling of this term has maximum effect on thermal-energy electron scattering momentum transfer cross-section. The electron-polar molecule scattering in this energy range is very much dominated by the long-range electron-dipole interaction.[47] Therefore a decrease in the magnitude of the dipole moment by ζ_d [Eq. (4.9)] has suppressed the contribution of $\sigma^m_{0\to 1}$ to $\sigma^m(0)$ [Eq. (2.23)] approximately by a factor of ζ_d^2 [see Eq. (A13)]. For higher incident electron energies the dipole potential becomes less important and the short-range forces take up the scattering process. We, therefore, find that the momentum transfer cross-section calculated with the original-dipole-term-static-potential (curve C) decreases very rapidly with the increasing incident electron velocity and by the time the impact energy becomes 0.10 electron Volts the results of curve C are only 18% higher than those of curve D.

The re-scaling of the dipole-term has, therefore, mainly affected the extremely low-energy electron scattering from CO molecule. The small differences in the values of the momentum transfer cross-sections at higher incident electron energies calculated with two different magnitudes of the V_1-term

support our argument of Sec. IV B(iii) that a rather phenomenological re-normalization of only the dipole-term in the multipole expansion of the static potential does not have a serious effect on the short-range terms of the electron-CO interaction potential.

The new momentum transfer cross-section (curve D), on the other hand, is in very good agreement with the inferred values[9] (curve A). (Hake and Phelps do not give any error limits for their results in Ref. 9.) Also, the results of curve D reproduce the 1.75 eV $^2\Pi$ resonance very well. In addition to this, our calculated momentum transfer cross-section beyond 2 eV is indistinguisable from that of dotted curve A' which Hake and Phelps[9] has obtained by an extrapolation of their inferred results below 1 eV (curve A). These extrapolated results have their maximum value around 1.50 eV which is about 0.25 electron volts lower than the position of the maxima in the calculated curve D. Although one can always adjust the resonance position in our pseudo-potential method by finding an appropriate value for the parameter r_0 in the polarization potential (4.5) but the magnitude of the cross-section, which is about 44% higher than the extrapolated values of curve A' in the resonance energy region, is not controlled by any disposable parameter in our calculation. Hake and Phelps[9] do not discuss the accuracy or reliability of their extrapolated results of the momentum transfer cross-section in this sensitive resonance region. A better comparison in between the theory and experiment will, therefore, require further measurements of the momentum transfer cross-section in this energy domain. However,

our computed momentum transfer cross-section, which is obtained by using a single parameter in the polarization potential, is in satisfactorily good agreement with the experimental measurements over the whole range of energy.

Fig. 4 contains the elastic scattering cross-section for (0→0) rotational transition. The continuous curve shows the results which were obtained from an application of the f.-t. theory to the single-center pseudo-potential method with re-normalized dipole-term while the broken curve corresponds to our extension of the rotational c.c. calculation of Crawford and Dalgarno.[18] The pseudo-potential results of the continuous curve reproduce the 1.75 eV resonance very well. On the other hand the broken curve results not only fail to go through this resonance properly but they are in considerable disagreement with those represented by the continuous curve over the whole range of energy. The cross-section for elastic scattering will basically be determined by the short-range terms. A discrepancy between the two curves of Fig. 4, therefore, simply means that the model potential (4.1) used by Crawford and Dalgarno[18] does not represent the behavior of the e^--CO interaction potential at short-distances from the center of mass of the molecule correctly.

The excitation cross section $\sigma_{0\to1}$ calculated from two different potentials have been plotted in Fig. 5. Because of the presence of a long-range electron-dipole interaction the distant collisions in electron scattering from polar molecules become quite important. The electron scattering for $\Delta j = \pm 1$ transitions

will very much depend upon the dipole potential. The cross-section for these inelastic transitions in a polar molecule, therefore, will always be large at very low incident electron energies for reasonably large values of dipole moment. A very good agreement between the two curves of Fig. 5 at low energies is in accordance with our contention that the re-normalization of the dipole-term in the multipole expansion of the static potential [Eq. (4.10)] of the CO molecule has improved the asymptotic behavior of this potential without making any significant change in its short-range nature. We again notice that, unlike the continuous curve, the broken curve results do not show the 1.75 eV resonance.

The rotational excitation cross-sections for (0→2) and (0→3) transitions are shown in Fig. 6. [We found that the cross-sections obtained from Crawford and Dalgarno potential for transitions higher than (0→2) were negligibly small.] The $\sigma_{0\to 2}$ results calculated from two different potentials are again in good agreement up to 1.0 eV. The cross-section for this transition in the low-energy domain will, however, depend upon the quadrupole moment and the non-spherical component (α_2) of the induced dipole polarizability of the target molecule. For CO molecule the value of α_2 is very small [Eq. (4.11)] and it gives rise to an interaction potential which goes off as r^{-4} [Eq. (4.7)], therefore, it is primarily the electron-quadrupole interaction which will determine the $\sigma_{0\to 2}$ cross-section for low-energy electrons. As we see from Fig. 6 that this interaction gives rise to almost an energy independent cross-section.[48] [A difference in the magnitude of the quadrupole moment used in the model potential {Eq. (4.2)}

and the pseudo-potential {(Eq. 4.11)} is probably giving rise to a slight difference in the cross-sections for (0→2) transition of the broken and continuous curves at these very low-energies.] At higher impact energies, however, other short-range terms become important and therefore while the pseudo-potential results both for (0→2) and (0→3) transitions go through the resonance but the cross-section calculated from the model potential (4.1) does not show this behavior.

The rotational excitation cross-section for (0→4) transition calculated from the pseudo-potential method is shown in Fig. 7. (The cross-sections for transitions higher than $\Delta j = 4$ were negligibly small.) Since both $\sigma_{0\to3}$ and $\sigma_{0\to4}$ are non-zero only in the resonance energy region (see Figs. 6 and 7), it is, therefore, mainly the short-range terms of the interaction potential which are responsible for these transitions. On comparing the magnitudes of the various cross-sections at the resonance energy 1.75 eV one will notice that $\sigma_{0\to4}$, although smaller than $\sigma_{0\to0}$, is largest among the excitation cross-sections for the transitions which start from the ground rotational state of CO molecule. This result seems to be in striking similarity with the rotational excitation in $e^- - N_2$ scattering where we found[10,23,49] that $\sigma_{0\to4}$, although smaller than $\sigma_{0\to0}$, was larger compared to $\sigma_{0\to2}$ in the resonance energy region.

The total scattering cross-section $\sigma(0)$, defined by Eq. (2.22), is shown in Fig. 8. The good agreement between the broken and the continuous curves at extremely low energies begins to disappear as the short-range interaction becomes important at higher energies. Although the pseudo-potential results

have a large spike at 1.75 electron Volts, but those calculated from Crawford and Dalgarno[18] potential (4.1) show a wide resonance type behavior around 3.00 eV. Also there is a big difference in the maximum values of the cross-section obtained from these two different calculations.

A comparison of Figs. 3 and 8 will also reveal that $\sigma^m(0)$ and $\sigma(0)$ calculated from the model potential of Crawford and Dalgarno have their maxima at two different energies, 1.50 and 3.00 eV respectively. While in the case of the pseudo-potential method both of these quantities peak at 1.75 eV, which is the position of the resonance in $^2\Pi$ state of the (e^-+CO)-system.[42]

Such a detailed comparison of the various cross-sections computed using these two different potentials in the scattering equations makes two very important points about the nature of these interactions. The semi-empirical potential (4.1) of Crawford and Dalgarno[18] is good only for describing the electron collisions with carbon monoxide at extremely low energy where the scattering is primarily determined by various long-range terms (e.g., electron-dipole, electron quadrupole, etc.) of the e^--CO interaction. This model fails to represent the short-range forces. It should therefore, not be used to calculate either the low-energy elastic scattering cross-sections or to study the e^--CO scattering at higher energies. The re-normalization of the dipole-term in the multipole expansion of the charge distribution of carbon monoxide used in our pseudo-potential method, on the other hand, has improved its asymptotic behavior without altering the short-range nature of this potential is any apparent way.

The individual contributions to $\sigma(0)$ and $\sigma^m(0)$ are given in Tables VII and VIII respectively. Tables IX and X contain, respectively, the rotationally elastic and inelastic scattering cross-sections $\sigma_{1\to j'}$ and the momentum transfer cross-sections $\sigma^m_{1\to j}$, for $j' = 0$ to 5. In all these tables both the scattering and the momentum transfer cross-sections for $\Delta j = \pm 1$ transitions are largest in the thermal-energy region. These tables also show that all our results for individual transitions reproduce the 1.75 eV $^2\Pi$ resonance very well. In addition to this, one would also notice that in the resonance energy region—unlike the $0\to j'$ transitions where $\sigma_{0\to 4}$ and $\sigma^m_{0\to 4}$ have the largest values for excitation cross-sections—$\sigma_{1\to 3}$ and $\sigma^m_{1\to 3}$, although smaller than the elastic $\sigma_{1\to 1}$ and $\sigma^m_{1\to 1}$ respectively, are maximum among the cross-sections for inelastic transitions which start from the first excited rotational state of carbon monoxide. This feature is again the same which was found both in the pure rotational excitation[10,23] and the simultaneous vibration-rotation excitation[49] in e^--N_2 scattering. The last thing which we will like to point out from these tables is the fact that, except for extremely-low energy values, $\sigma(0)$ is almost equal to $\sigma(1)$ (Tables VII and IX) and so is the case with $\sigma^m(0)$ and $\sigma^m(1)$ (Tables VIII and X). These agreements between these cross-sections are in accordance to the statements made in Eqs. (2.22) and (2.23) respectively.

The differential scattering cross-sections for $(0\to j')$ and $(1\to j')$ transitions at 0.01 eV are shown by continuous curves in Figs. 9 and 10 respectively.

These results were obtained from the pseudo-potential method, with the re-normalized dipole-term, combined with the f.-t. theory. The scattering process for this value of the incident electron energy will basically be determined by the asymptotic forms of the various long-range permanent and induced multipole potential terms [Eq. (4.7)]. The angular distribution for both elastic transitions (0→0) and (1→1) in Figs. 9 and 10 respectively has its maximum value in the backward direction. The $d\sigma_{j\to j\pm1}/d\Omega$ peaks, on the other hand, in the forward direction because of the importance of the long-distance collisions due to the electron-dipole interaction, and vanishes almost completely in the backward direction. At this impact energy the electron-quadrupole interaction dominates the scattering for $\Delta j = 2$ transitions and thus giving rise to an almost isotropic angular distribution.[48] The differential cross-section for higher transitions from the ground and first rotational states were negligibly small for this value of the incident electron energy and are not shown in Figs. 9 and 10, respectively.

In Fig. 9 we have also shown by the broken curves the angular distribution obtained by using the semi-empirical potential (4.1) of Crawford and Dalgarno[18] in the rotational c.c. Eq. (2.12). The results computed from this potential for (0→1) transition were indistinguishable from those of the continuous curve on the scale of Fig. 9. As for other two transitions [(0→0) and (0→2)], apart from a difference in their magnitudes, general behavior of the cross-sections

represented by the continuous and broken curves as a function of the scattering angle is almost identical. Note that the elastic differential scattering cross-section for (0→0) transition, which will depend upon the short-range terms even at 0.01 eV, vanishes in the forward direction when computed from the model potential (4.1). A slight difference in the values of the (0→2) differential cross-section of the continuous and broken curves in Fig. 9 is associated with the difference in the magnitudes of the quadrupole moment used in two potentials [cf. Eqs. (4.2) and (4.11)].

The angular distributions for (0→j') and (1→j') transitions at 1.50 electron Volts are drawn in Figs. 11 and 12 respectively. The continuous curves of these figures were obtained from the single-center pseudo-potential method, with re-normalized dipole-term, in the context of the f.-t. theory. Although the magnitudes of the cross-sections for the same Δj values in these two figures are different but their general behavior as a function of the scattering angle is almost identical. Here again we find that the curves for $\Delta j = \pm 1$ transitions peak in the forward direction. But, unlike those shown in Figs. 9 and 10, the differential cross-section for these transitions now does not vanish in the backward direction. We also notice from Figs. 11 and 12 respectively that (0→2) and (1→3) angular distributions are no longer isotropic. All these things simply mean that it is not the long-range interactions which now determine the scattering but the short-range forces too play an important role at this impact energy even for these transitions.

The broken curves in Fig. 11 are the differential scattering cross-sections calculated from the model potential (4.1) of Crawford and Dalgarno[18] at 1.50 eV [The cross-sections obtained from this potential for transitions higher than $(0 \rightarrow 2)$ were negligibly small.] $d\sigma_{0\rightarrow 2}/d\Omega$ of the broken curve is still isotropic. Although the angular distribution for $(0 \rightarrow 1)$ transition obtained from this potential (broken curve in Fig. 11) peaks in the forward direction but vanishes almost completely beyond 45°. This kind of behavior of the broken curves, which is quite different from that of the continuous curves of the pseudo-potential and shown in the same Fig. 11, implies that the short-range forces represented in the semi-empirical potential (4.1) of Crawford and Dalgarno[18] are so weak that even for scattering of 1.50 eV incident energy electrons the asymptotic forms of the electron-dipole and electron-quadrupole interaction potentials dominate the cross-sections for $(0 \rightarrow 1)$ and $(0 \rightarrow 2)$ transitions respectively.

The broken curves for the $(0 \rightarrow 0)$ transitions in Fig. 11 has two peaks of almost equal heights in the forward and backward directions. The single minimum of this curve lies between 55° and 65°. The continuous curve for the angular distribution of the pseudo-potential, on the other hand, has a crest at about 90° with two, almost equidistant, troughs on either sides. These differences in $d\sigma_{0\rightarrow 0}/d\Omega$ calculated from two different potentials exemplifies the fact that the nature of the short-range forces represented by the Crawford and Dalgarno[18] potential (4.1) is entirely different than that of the pseudo-potential.

The definition of the momentum transfer cross-section involves a weighting factor of $(1-\cos\theta)$ [see Eq. (2.21)] which takes away the forward scattering contribution. A broad peak in the momentum transfer cross-section at about 1.50 eV (curve B in Fig. 3) calculated from the model potential is, therefore, exclusively due to the rotationally elastic electron scattering from carbon monoxide.

In Figs. 13 and 14 are shown the angular distributions for $(0 \rightarrow j')$ and $(1 \rightarrow j')$ transitions calculated from the pseudo-potential at the $^2\Pi$ resonance energy 1.75 eV [Both the momentum transfer cross-section $\sigma^m(0)$ (curve D in Fig. 3) and the total integrated scattering cross-section $\sigma(0)$ (continuous curve in Fig. 8) obtained from this potential have a well defined resonance at this energy.] We notice that the 90° crest in the elastic differential cross-sections (0→0) and (1→1) at 1.50 eV, shown in Figs. 11 and 12 respectively, have flattened out in Figs. 13 and 14 increasing the cross-section in the backward and forward directions at 1.75 eV. This distribution of the elastic cross-section as a function of the scattering angle at the resonance energy is very similar to what we found in e^--N_2 scattering.[10,23,49]

An additional interesting feature of these results is that the angular distribution for $\Delta j = \pm 1$ transitions—which is absent in e^--N_2 scattering—although still has the forward scattering peak, oscillates around 90° giving rise to a crest and trough on either side of this angle at almost symmetric positions.

This behavior of the differential cross-section for angular distribution for ($j \rightarrow j \pm 1$) transitions is the manifestation of basically a p-wave nature of the $^2\Pi$ resonance present in electron scattering from carbon monoxide. The differential scattering cross-sections for $\Delta j = 2$ and 4 transitions are, however, almost symmetric about 90° and again very similar to the N_2 case[10,23,49] where they have a peak and a broad minima in the ($j \rightarrow j+2$) and ($j \rightarrow j+4$) transitions respectively. The $d\sigma_{j \rightarrow j+3}/d\Omega$, on the other hand, increases monotomically in going from forward to the backward direction.

In the end we show the differential scattering cross-section at 3.00 eV. The ($0 \rightarrow j'$) results are drawn in Fig. 15 while those for ($1 \rightarrow j'$) in Fig. 16. The continuous curves in these two figures again correspond to the pseudo-potential method combined with the f.-t. theory and the re-normalized dipole term. The cross-sections for $\Delta j = \pm 1$ transitions have lost their crest and trough around 90° which was present in the resonance energy (1.75 eV) angular distributions shown in Figs. 13 and 14. As a matter of fact, the differential cross-section for this transition, although still peaking in the forward direction, has a very broad crest at about 90°. However, the $d\sigma_{j \rightarrow j'}/d\Omega$ for $j' = j + 2$, $j + 3$, and $j + 4$, although smaller in magnitude, but basically have the same shape as at 1.75 eV.

The angular distributions for ($0 \rightarrow j'$) transitions calculated from the Crawford and Dalgarno[18] potential (4.1) at 3.00 eV are shown by the broken

curves in Fig. 15. [The total integrated scattering cross-section calculated from this potential has a broad resonance at this energy value (broken curve in Fig. 8)]. The behavior of the broken curves in Fig. 15 is entirely different than those of the continuous curves. The short-range terms of this model potential fail to show any oscillations either in the $(0 \rightarrow 1)$ or $(0 \rightarrow 2)$ angular distributions. On the other hand, the differential scattering cross-section for all three transitions—(0→0), (0→1), and (0→2)—calculated from the model potential (4.1) of Crawford and Dalgarno[18] at 3.0 eV peaks in the forward direction.

V. CONCLUSION

The work presented here probably constitutes the very first study of electron scattering from such a complex system as carbon monoxide using ab-initio methods. Although, to check the accuracy of the various cross-sections given here more experimental measurements will be required in future but the basic fact that the computed momentum transfer cross-section over the whole energy range is in very good agreement with the values inferred from swarm experiments is assuring enough that the other results too should be in satisfactorily good agreement with the future measurements.

As regard to the f.-t. theory, which has formed the basis of the present study, our opinion is that it provides a good formalism for studying the electron-molecule scattering from first principles. The convenience with which the short-range forces can be included by working in a fixed-nuclei approximation in the

inner-region and at the same time allowing the introduction of nuclear degrees of freedom in the outer-region makes this theory quite attractive. We have shown here how our single-center pseudo-potential method—combined with the R-matrix—can be adapted to the f.-t. theory.

Our experience, however, is that inspite of all its glamour the practical implementation of the f.-t. theory is an extremely arduous task. As we have pointed out elsewhere in this article, it is a multistep process. The absence of a rigorous criterion for the selection of a value for the inner-molecular core radius, where a transformation from a molecule- to a space-fixed frame of reference should be performed, introduces an element of uncertainty in its application. In addition to this, considerable effort has to be made in solving the scattering problem in the outer-region in a space-fixed frame of reference.

This complexity will increase further when one wants to include both the nuclear vibration and rotation in the outer-region. A great disparity in the time period of these motions will now require two different points in the configuration space in order to introduce in the scattering equations the Hamiltonians associated with these two modes of nuclear motion. This in turn will also mean that one has to perform two separate transformations—one each for the vibration and rotation. Inspite of the availability of high speed and large memory computing machines, it seems to us that one should make a very careful judicious study of the problem at hand before deciding to use the f.-t. theory.

ACKNOWLEDGEMENTS

The realization that the frame-transformation theory, combined with the R-matrix method, should be employed to study electron scattering from polar molecules came about from very long discussions with Professor P. G. Burke almost four years ago. I am very much grateful to Professor Burke for several of his illuminating suggestions in the incipient stages of this work and for supplying his R-matrix theory notes. Many useful discussions with Dr. A. Temkin and his continuous encouraging supervision during the course of a very involved calculation has been very conducive in bringing this project to a successful end. I am also indebted to other members of the Theoretical Studies Group intermittent discussions with whom have benefitted me on several occasions. It would probably not have been possible to finish this calculation without a generous use of the excellent computing facilities at Goddard Space Flight Center and the co-operation of the computer center personnel.

APPENDIX

The Born approximation theory of electron-molecule scattering is very well formulated.[25,48] In this Appendix we give the relevant formulae and put them in a form directly applicable to the present study.

The $T^J_{j'\ell',j\ell}$ matrix element for a transition from the initial rotational state j to the final state j' calculated in Born approximation from a set of coupled scattering Eqs. (2.12) is given by[50]

$$^{B}T^J_{j'\ell',j\ell} = -2i\pi \sum_{\mu=1} f_\mu(j'\ell', j\ell; J) \int_0^\infty J_{\ell'+1/2}(k_{j'}r)\, V_\mu(r)\, J_{\ell+1/2}(k_j r)\, r\,dr, \tag{A1}$$

where coefficient

$$f_\mu(j'\ell', j\ell; J) = \left\langle \mathcal{Y}^{JM}_{j'\ell'} \middle| P_\mu(\hat{r}\cdot\hat{R}) \middle| \mathcal{Y}^{JM}_{j\ell} \right\rangle$$

$$= (-1)^{-J-\mu} \sqrt{(2j'+1)(2\ell'+1)(2j+1)(2\ell+1)} \begin{pmatrix} j & j' & \mu \\ 0 & 0 & 0 \end{pmatrix} \begin{pmatrix} \ell & \ell' & \mu \\ 0 & 0 & 0 \end{pmatrix} \begin{Bmatrix} j & \ell & J \\ \ell' & j' & \mu \end{Bmatrix} \tag{A2}$$

has already been introduced on the right hand side of Eq. (2.12). $J_{\ell+1/2}(x)$ is a Bessel function related to the regular spherical Bessel function of Eq. (3.3) by the following relation

$$J_{\ell+1/2}(x) = \sqrt{\frac{2x}{\pi}}\, j_\ell(x).$$

If the multipole expansion (2.11) of the electron-molecule electrostatic interaction (2.4) is replaced by its asymptotic form, namely

$$V(\vec{r};\vec{R}) = \sum_{\mu} v_{\mu}\, r^{-\mu-1}\, P_{\mu}(\hat{r}\cdot\hat{R}), \tag{A3}$$

where v_1, v_2, v_3, . . ., etc. are respectively the dipole, quadrupole, octopole, . . ., etc. moments of the molecular charge distribution, the relation (A1) will then become

$${}^{B}T^{J}_{j',\ell',j,\ell} = -2i\pi \sum_{\mu=1} f_{\mu}(j'\ell', j\ell; J)\, v_{\mu} \int_0^{\infty} J_{\ell'+1/2}(k_{j'} r)\, \frac{dr}{r^{\mu}}. \tag{A4}$$

The radial integral (A4) can be evaluated analytically. There are two different cases to be considered:

$$k_j = k_{j'} = k_0 \quad (\text{Say}) > 0,$$

$$\int_0^{\infty} J_{\ell'+1/2}(k_0 r)\, J_{\ell+1/2}(k_0 r)\, \frac{dr}{r^{\mu}}$$

$$= \frac{k_0^{\mu-1}\, \Gamma(\mu)\, \Gamma(S-\mu)}{2^{\mu}\Gamma(S)\, \Gamma\left(S-\ell-\frac{1}{2}\right)\, \Gamma\left(S-\ell'-\frac{1}{2}\right)}, \qquad [\mu > 0] \tag{A5}$$

and

$$k_j > k_j' > 0$$

$$\int_0^\infty J_{\ell'+1/2}(k_j' r)\, J_{\ell+1/2}(k_j r)\, \frac{dr}{r^\mu}$$

$$= \frac{k_j'^{\ell'+1/2}\,\Gamma(S-\mu)}{2^\mu\, k_j^{\ell'-\mu+3/2}\,\Gamma\left(\ell'+\frac{3}{2}\right)\Gamma\left(S-\ell'-\frac{1}{2}\right)}\, F\left(S-\mu, \ell'-S+\frac{3}{2}, \ell'+\frac{3}{2}; \frac{k_j'^2}{k_j^2}\right), \quad [\mu > -1] \tag{A6}$$

where we have defined

$$S = \frac{1}{2}(\ell + \ell' + \mu) + 1 \tag{A7}$$

and F (a,b,c;z) is a hypergeometric function.[51]

For expressions (A5) and (A6) to be finite the arguments of the Gamma functions present in the numerator of these relations should be greater than zero, i.e.,

$$S - \mu > 0$$

Or, from (A7),

$$\ell + \ell' + 2 > \mu. \tag{A8}$$

The second 3-j symbol on the right hand side of Eq. (A2) will be zero unless $|\ell - \ell'| \leq \mu \leq \ell + \ell'$. The Born radial integral present in Eq. (A4) will,

therefore, always converge as long as the values of ℓ, ℓ', and μ satisfy the triangular relation $\Delta(\ell, \ell', \mu)$. The Born $\underline{T}^J$-matrix elements can now be computed by substituting the expression (A5) or (A6), as the case may be, in Eq. (A4). For those values of ℓ, ℓ', and μ which do not satisfy the inequality (A8), the ${}^B\underline{T}^J$-matrix element will automatically vanish because of the 3-j symbol present in Eq. (A2).

Crawford et al[25] have derived an expression for the differential scattering cross-section for a $(j \rightarrow j')$ transition. For an electron-molecule interaction of the form (A3), one can write

$$\frac{d\,{}^B\sigma_{j\rightarrow j'}}{d\Omega} = 4(2j'+1)\frac{k_{j'}}{k_j}\sum_{\mu=1}\frac{v_\mu^2}{2\mu+1}\begin{pmatrix} j' & j & \mu \\ 0 & 0 & 0 \end{pmatrix}^2\left[\int_0^\infty j_\mu(Kr)\frac{dr}{r^{\mu-1}}\right]^2 \qquad \text{(A9)}$$

where $\hat{k}_j$ and $\hat{k}_{j'}$ specify the directions of the initial and final momentum respectively and $\vec{K} = \vec{k}_j - \vec{k}_{j'}$ defines the momentum transfer during the collision such that

$$K_{min} = |k_j - k_{j'}|, \quad K_{max} = k_j + k_{j'}. \qquad \text{(A10)}$$

Because

$$\int_0^\infty j_\mu(Kr)\frac{dr}{r^{\mu-1}} = \frac{\sqrt{\pi}\,K^{\mu-2}}{2^\mu\,\Gamma\left(\mu+\frac{1}{2}\right)}$$

the differential scattering cross-section is, therefore, given by

$$\frac{d\,{}^{B}\sigma_{j\to j'}}{d\Omega} = 4\pi(2j'+1)\frac{k_{j'}}{k_j}\sum_{\mu=1}\left[\frac{v_\mu}{2^\mu\,\Gamma\left(\mu+\frac{1}{2}\right)}\begin{pmatrix} j & j' & \mu \\ 0 & 0 & 0\end{pmatrix}\right]^2 \frac{K^{2\mu-4}}{2\mu+1}.$$

The integrated cross-section for an inelastic transition $(j \to j')$, defined by,

$${}^{B}\sigma_{j\to j'} = \int \frac{d\,{}^{B}\sigma_{j\to j'}}{d\Omega}\, d\hat{k}_{j'}$$

will now become

$$\begin{aligned} {}^{B}\sigma_{j\to j'} &= \frac{8\pi(2j'+1)}{3k_j^2}\, D^2 \begin{pmatrix} j & j' & 1 \\ 0 & 0 & 0\end{pmatrix}^2 \ln\frac{K_{max}}{K_{min}} \\ &+ \frac{4\pi^2(2j'+1)}{k_j^2}\sum_{\mu\geq 2}\left[\frac{v_\mu}{2^\mu\,\Gamma\left(\mu+\frac{1}{2}\right)}\begin{pmatrix} j & j' & \mu \\ 0 & 0 & 0\end{pmatrix}\right]^2 \frac{K_{max}^{2\mu-2} - K_{min}^{2\mu-2}}{(\mu-1)(2\mu+1)}, \end{aligned} \tag{A12}$$

where we have replaced v_1 by D for the permanent dipole moment of the target molecule. The first term on the right hand side of Eq. (A12) will obviously be absent for electron scattering from homonuclear diatomic systems.

The momentum transfer cross-section

$${}^{B}\sigma^{m}_{j\to j'} = \int \frac{d\,{}^{B}\sigma^{m}_{j\to j'}}{d\Omega}\,(1 - \hat{k}_j\cdot\hat{k}_{j'})\, d\hat{k}_{j'}$$

is given by

$$B\sigma^{m}_{j\to j'} = \frac{8\pi(2j'+1)}{3k_j^2} D^2 \begin{pmatrix} j & j' & 1 \\ 0 & 0 & 0 \end{pmatrix}^2 \left[1 - \frac{K_{min}^2}{2k_j k_{j'}} \ln \frac{K_{max}}{K_{min}} \right]$$

$$+ \frac{2\pi^2(2j'+1)}{k_{j'} k_j^3} \sum_{\mu \geq 2} \left[\frac{v_\mu}{2^\mu \Gamma\left(\mu + \frac{1}{2}\right)} \begin{pmatrix} j & j' & \mu \\ 0 & 0 & 0 \end{pmatrix} \right]^2 \frac{K_{min}^{2\mu} - K_{max}^{2\mu} + 4\mu k_j k_{j'} K_{max}^{2\mu-2}}{(\mu-1)\mu(2\mu+1)} . \tag{A13}$$

The K_{min} and K_{max} are defined in Eq. (A10) and again the first term on the right hand side will be present only for electron scattering from polar molecules.

REFERENCES

1. N. Chandra, Phys. Rev. A. 12, 2342 (1975).
2. For detailed discussions of fixed- and adiabatic-nuclei approximations see, for example, D. E. Golden, N. F. Lane, A. Temkin, and E. Gerjury, Rev. Mod. Phys. 43, 642 (1971).
3. A. M. Arthurs and A. Dalgarno, Proc. Roy. Soc. A. 256, 540 (1960).
4. A good compilation of references on this work is given by K. Takayanagi, in The Physics of Electronic and Atomic Collisions, edited by J. S. Risley and R. Geballe (University of Washington Press, Seattle, 1976), pp. 219 ff.
5. R. J. W. Henry, Phys. Rev. A. 2, 1349 (1970).
6. N. Chandra and A. Temkin, Phys. Rev. A 13, 188 (1976).
7. A. Herzenberg, in Fundamental Interaction in Physics, edited by B. Kursunognu and A. Perlmutter (Plenum, New York, 1973), pp. 261 ff.
8. E. S. Chang and U. Fano, Phys. Rev. A 6, 173 (1972).
9. R. D. Hake and A. V. Phelps, Phys. Rev. 158, 70 (1967).
10. P. G. Burke and N. Chandra, J. Phys. B 5, 1696 (1972).
11. P. G. Burke, N. Chandra, and F. A. Gianturco, J. Phys. B 5, 2212 (1972).
12. N. Chandra and F. A. Gianturco, Chem. Phys. Lett. 24, 326 (1974).
13. N. Chandra, Bull. Am. Phys. Soc. 20, 1470 (1975); ibid 21, 575 (1976).
14. E. P. Wigner and L. Eisenbud, Phys. Rev. 72, 29 (1947).
15. R. J. W. Henry and E. S. Chang, Phys. Rev. A 5, 276 (1972).
16. E. S. Chang, Phys. Rev. Lett. 33, 1644 (1974).

17. N. Chandra, J. Phys. B 8, 1953 (1975).

18. O. H. Crawford and A. Dalgarno, J. Phys. B. 4, 494 (1971).

19. M. E. Rose, Elementary Theory of Angular Momentum (Wiley, New York, 1957), pp. 49 ff.

20. G. Herzberg, Molecular Spectra and Molecular Structure I. Spectra of Diatomic Molecules (van Nostrand, New York), (a) pp. 225; (b) pp. 219 ff.; (c) pp. 237 ff.

21. M. Rotenberg, R. Bivins, N. Metropolis, and J. K. Wooten, Jr., The 3-j and 6-j Symbols, (MIT Press, Cambridge, 1959).

22. F. H. M. Faisal, J. Phys. B. 3, 636 (1971).

23. N. Chandra, J. Phys. B. 8, 1338 (1975).

24. U. Fano and D. Dill, Phys. Rev. A 6, 185 (1972).

25. O. H. Crawford, A. Dalgarno, and P. B. Hays, Mol. Phys. 13, 181 (1967).

26. The definition of the symmetric top wavefunctions is the same as given by Rose on page 55 of Ref. 19. However, there is an error in this definition which has been discussed by us in Ref. 10.

27. This parity operation of the total wavefunction, which classifies a molecular state as positive or negative in the nominclature of the molecular spectroscopy, has been discussed in detail in Ref. 20(c). The reader should, however, be reminded that in the present case the electronic wavefunction of the target molecule is not affected by this inversion operation as we are considering the scattering from a $^1\Sigma^+$ state.

28. U. Fano, [a]Comments At. Mol. Phys. 2, 47 (1970); [b]Phys. Rev. A. 2, 353 (1970).

29. P. G. Burke, N. Chandra, and F. A. Giaturco, Mol. Phys. 27, 1121 (1974).

30. M. Born and K. Huang, Dynamical Theory of Crystal Lattices (Clarendon Press, Oxford, 1954), pp. 165 ff.

31. M. Born and R. Oppenheimer, Ann. Phys. (Leipzig) 84, 457 (1927).

32. A. Temkin and K. V. Vasvada, Phys. Rev. 160, 109 (1967).

33. A Temkin, K. V. Vasvada, E. Chang, and A. Silver, Phys. Rev. 186, 57 (1969).

34. P. G. Burke and A.-L. Sinfailam, J. Phys. B 3, 641 (1970).

35. A. Comprehensive review on the R-matrix theory and its application in nuclear physics has been written by A. M. Lane and R. G. Thomas, Rev. Mod. Phys. 30, 257 (1958).

36. For a recent review on the application of the R-matrix method to various electron-atom collision problems see P. G. Burke and W. D. Robb, Adv. At. Mol. Phys. 11, 143 (1975).

37. An approach similar to this for atomic case has been discussed by P. G. Burke, in Lectures in Theoretical Physics (Gordon and Beach, New York) vol. 11 C, pp. 34 ff.

38. N. Chandra, Comput. Phys. Commun. 5, 417 (1973).

39. Here we would like to refer the reader to the footnote given on page 1342 of Ref. 23 in order to explain the relationship between the transformation (3.11) and the one given earlier by the authors of Ref. 34.

40. P. G. Burke, A. Hibbert, and W. D. Robb, J. Phys. B. 4, 153 (1972).

41. The $\underline{T}^J$-matrix of Eqs. (2.19) and (2.20) will include both even and odd parity elements.

42. J. N. Bardsley, F. Mandl, and A. R. Woods, Chem. Phys. Lett. 1, 359 (1967).

43. F. H. M. Faisal and A. L. V. Tench, Comput, Phys. Commun. 2, 261 (1971)

44. A. D. McLean and M. Yoshimine, IBM J. Res. Dev., Suppl. 12, 206 (1967); J. Chem. Phys. 46, 3862 (1967).

45. O. Atabek, D. Dill, and Ch. Jungen, Phys. Rev. Lett. 33, 123 (1974).

46. M. J. Seaton, Monthly Notices Roy. Astron. Soc. 118, 504 (1958); Proc. Phys. Soc. (London) 88, 801 (1966).

47. K. Takayanagi, Comments At. Mol. Phys. 3, 95 (1972).

48. K. Takayanagi and Y. Itikawa, Adv. At. Mol. Phys. 6, 105 (1970).

49. N. Chandra and A. Temkin, Phys. Rev. A (1976), in press.

50. M. J. Seaton, Proc. Phys. Soc. 77, 174 (1961). Eq. (A1) has an additional minus sign because we have $\underline{T} = \underline{S} - 1$ [see Eq. (2.16)] which is opposite to the definition used by Seaton.

51. M. Abramowitz and I. A. Stegun, Handbook of Mathematical Functions (Dover, New York 1972), pp. 556.

FIGURE CAPTIONS

Fig. 1 – Eigenphase sum calculated in the fixed-nuclei approximation from the model potential (4.1) of Crawford and Dalgarno (Ref. 18).

Fig. 2 – Eigenphase sum calculated in the fixed-nuclei approximation using the single-center pseudo-potential method. The dipole-term in the static potential has been re-normalized by ζ_d [Eq. (4.10)] and $r_0 = 1.541$(a.u.) in the polarization potential (4.5). (The values of the resonance parameters are given in Table III.)

Fig. 3 – Comparison of the momentum transfer cross-section $\sigma^m(0)$ [Eq. (2.23)] versus incident electron energy obtained from different methods. A are the results of Hake and Phelps (Ref. 9) inferred from the swarm experiments with the dotted curve A' obtained so that it extrapolates smoothly to the derived results of A below 1.00 eV. B is calculated by solving the rotational close-coupling Eqs. (2.12) with the potential (4.1) of Crawford and Dalgarno (Ref. 18). C and D represent the results obtained by using the single center pseudo-potential method with the frame-transformation theory: the broken curve C corresponds to the original dipole-term in the static potential; the continuous curve D shows the final results of the re-normalized dipole-term in the static potential.

Fig. 4 – The elastic scattering cross-section for (0→0) rotational transition. The broken curve was computed by solving the rotational close-coupling Eqs. (2.12) with the model potential (4.1) of Crawford and Dalgarno (Ref. 18). The final results, shown by the continuous curve, were obtained by combining the single-center pseudo-potential method with the frame-transformation theory and re-normalized dipole-term in the static potential.

Fig. 5 – Same as Fig. 4 but for (0→1) rotational transition.

Fig. 6 – Same as Fig. 4 but for (0→2) and (0→3) rotational transitions. [The broken curve results for (0→3) transition were negligibly small.]

Fig. 7 – Same as Fig. 4 but for (0→4) rotational transition. (The broken curve results for this transition were negligibly small).

Fig. 8 – The total scattering cross-section $\sigma(0)$ [Eq. (2.22)]. The broken curve was computed by solving the rotational close-coupling Eq. (2.12) with the model potential (4.1) of Crawford and Dalgarno (Ref. 18). The final results, shown by the continuous curve, were obtained by combining the single-center pseudo-potential method with the frame transformation theory and re-normalized dipole term in the static potential.

Fig. 9 – Differential scattering cross-section for (0→0,1,2) rotational transitions at 0.01 eV. The broken curves were computed by solving the rotational close-coupling Eqs. (2.12) with the model potential (4.1)

of Crawford and Dalgarno (Ref. 18). The final results, shown by the continuous curves, were obtained by combining the single center pseudo-potential method with the frame-transformation theory and re-normalized dipole-term in the static potential.

Fig. 10 – Differential scattering cross-sections for (1→0,1,2) rotational transitions at 0.01 eV. These results were obtained by combining the single-center pseudo-potential method with the frame-transformation theory and re-normalized dipole term in the static potential.

§ See foot note to Table IX.

Fig. 11 – Same as Fig. 9 but for (0→0,1,2,3,4) rotational transitions at 1.50 eV. [The broken curve results for transitions higher than (0 → 2) were negligibly small.]

Fig. 12 – Same as Fig. 10 but for (1→0,1,2,3,4,5) rotational transitions at 1.50 eV.

§ See foot note to TableIX.

Fig. 13 – Same as Fig. 10 but for (0→0,1,2,3,4) rotational transitions at the resonance energy 1.75 eV.

Fig. 14 – Same as Fig. 10 but for (1→0,1,2,3,4,5) rotational transitions at the resonance energy 1.75 eV.

§ See foot note to Table IX.

Fig. 15 – Same as Fig. 9 but for (0→0,1,2,3,4) rotational transitions at 3.00 eV. [The broken curve results for transitions higher than (0→2) were negligibly small.]

Fig. 16 – Same as Fig. 10 but for (1→0,1,2,3,4,5) transitions at 3.00 eV.

§ See foot note to Table IX.

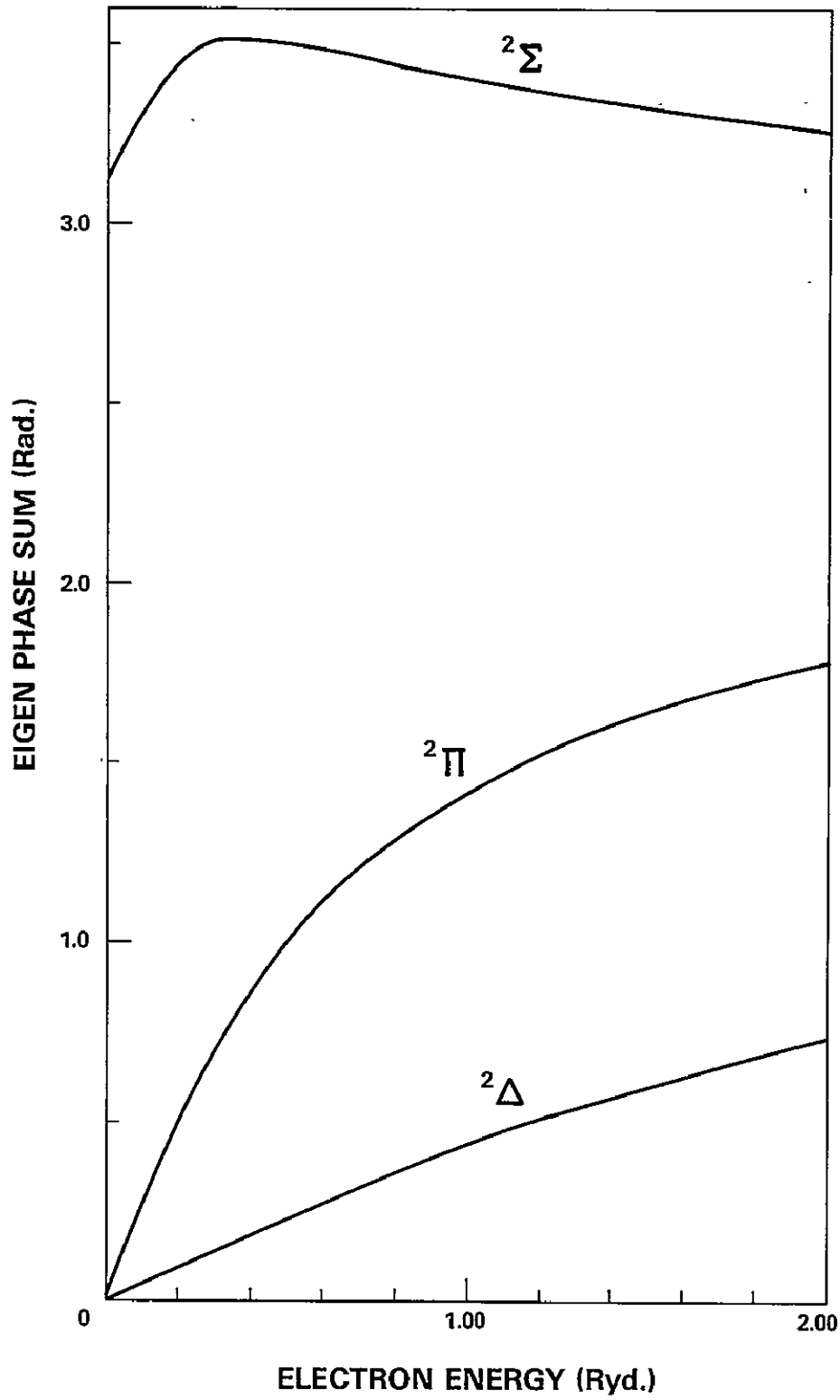

Figure 1. Eigenphase sum calculated in the fixed-nuclei approximation from the model potential (4.1) of Crawford and Dalgarno (Ref. 18).

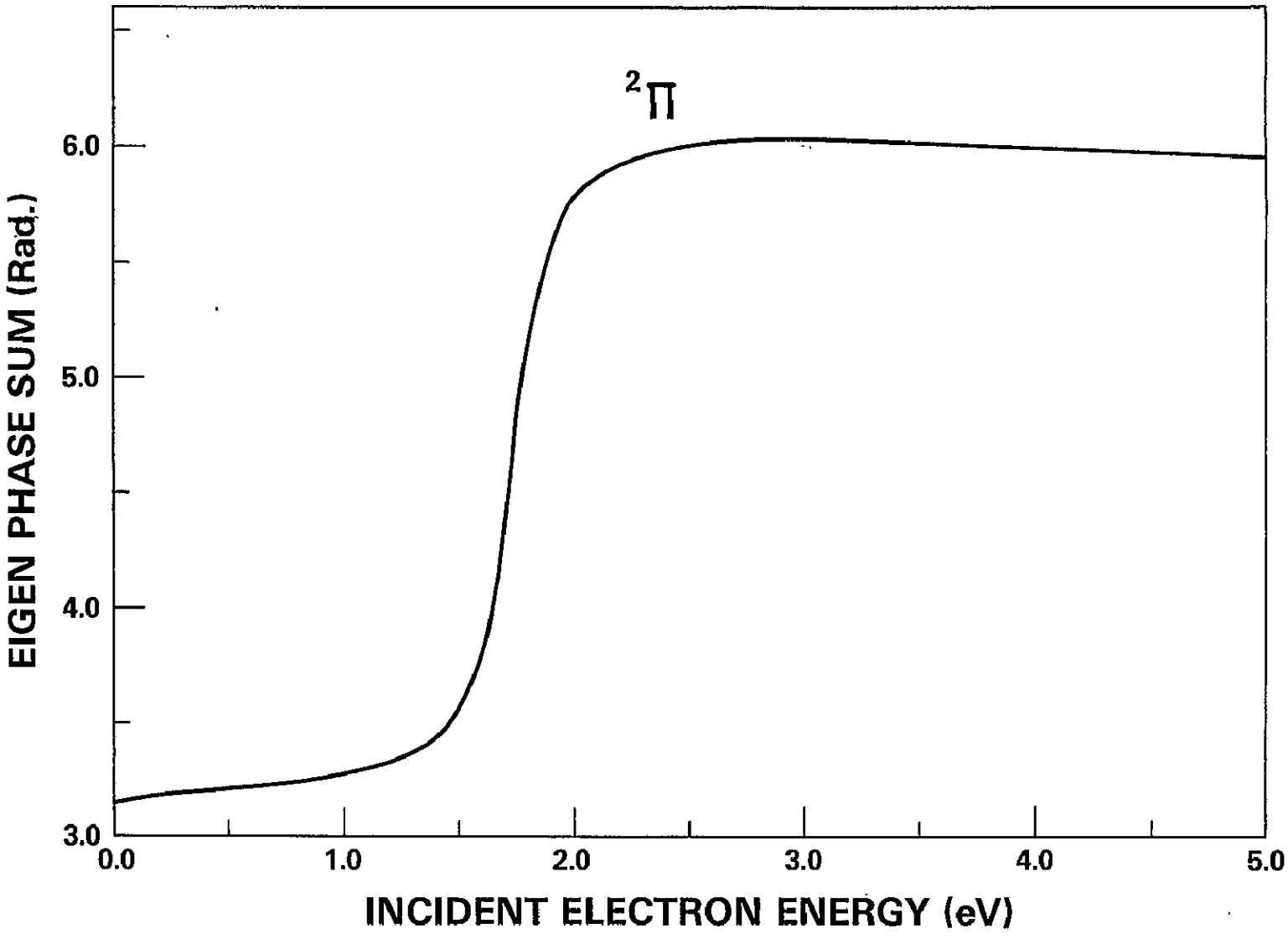

Figure 2. Eigenphase sum calculated in the fixed-nuclei approximation using the single-center pseudo-potential method. The dipole-term in the static potential has been re-normalized by ζ_d [Eq. (4.10)] and r_0 = 1.541 (a.u.) in the polarization potential (4.5). (The values of the resonance parameters are given in Table III.)

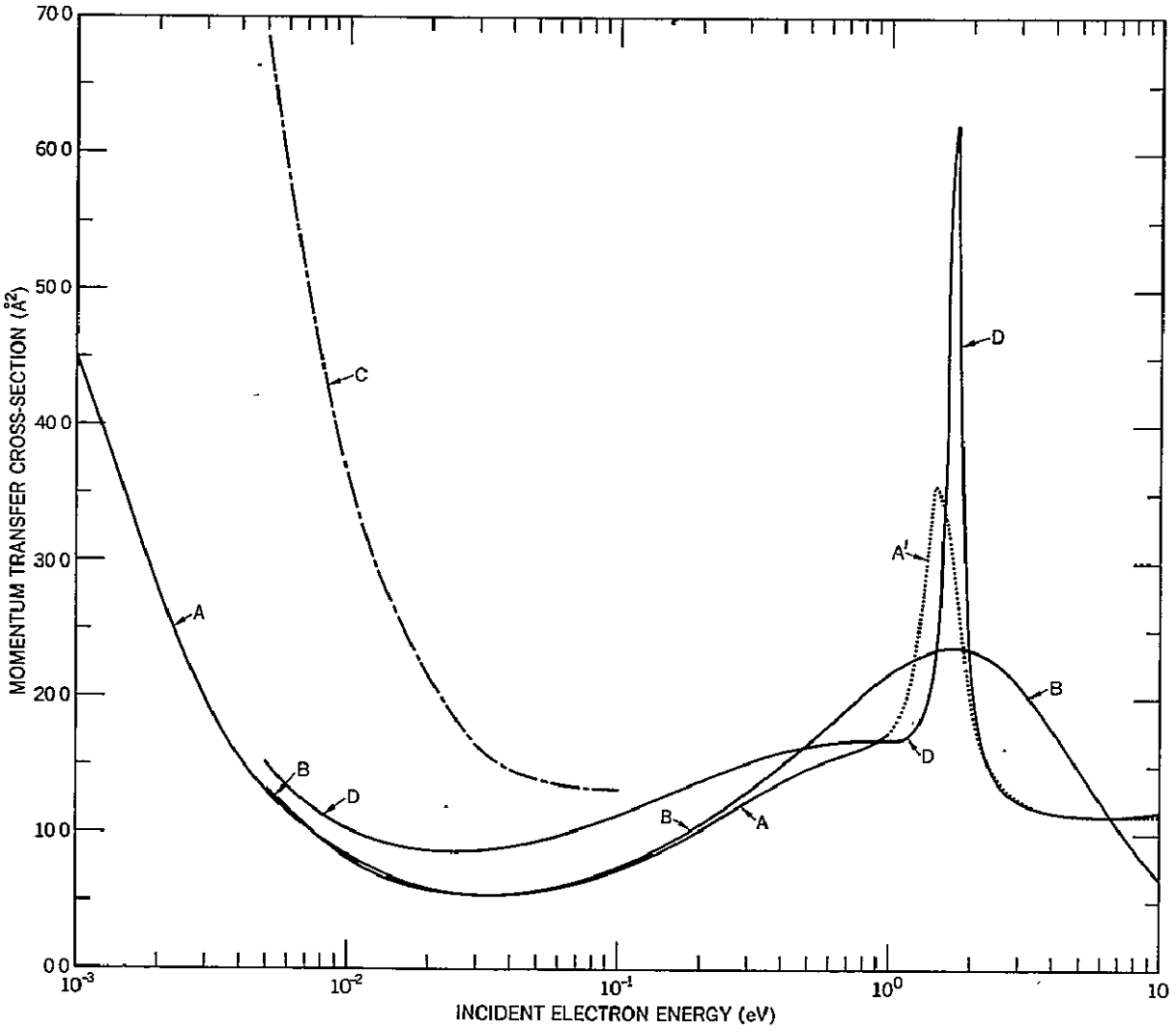

Figure 3. Comparison of the momentum transfer cross-section σ^m (0) [Eq. (2.23)] versus incident electron energy obtained from different methods. A are the results of Hake and Phelps (Ref. 9) inferred from the swarm experiments with the dotted curve A' obtained so that it extrapolates smoothly to the derived results of A below 1.00 eV. B is calculated by solving the rotational close-coupling Eqs. (2.12) with the potential (4.1) of Crawford and Dalgarno (Ref. 18). C and D represent the results obtained by using the single center pseudo-potential method with the frame-transformation theory: the broken curve C corresponds to the original dipole-term in the static potential; the continuous curve D shows the final results of the re-normalized dipole-term in the static potential.

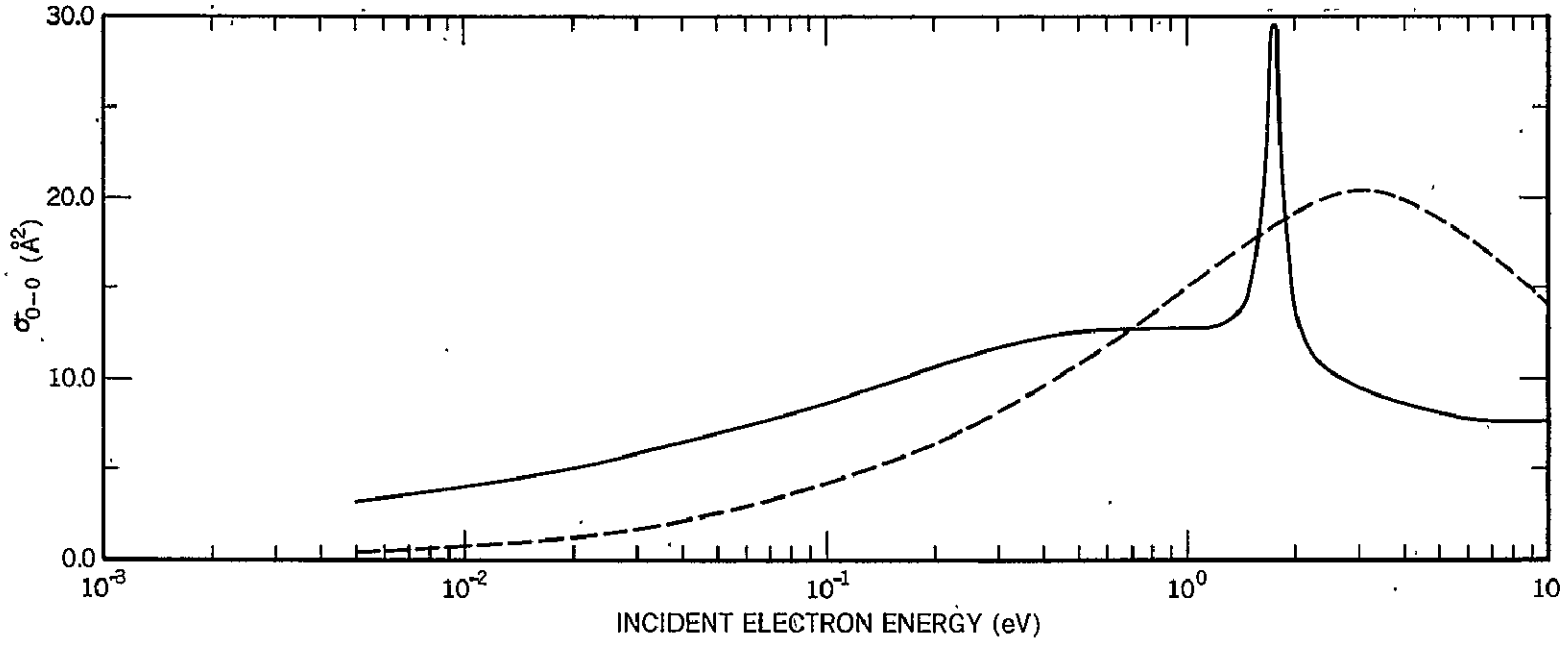

Figure 4. The elastic scattering cross-section for (0→0) rotational transition. The broken curve was computed by solving the rotational close-coupling Eqs. (2.12) with the model potential (4.1) of Crawford and Dalgarno (Ref. 18). The final results, shown by the continuous curve, were obtained by combining the single-center pseudo-potential method with the frame-transformation theory and re-normalized dipole-term in the static potential.

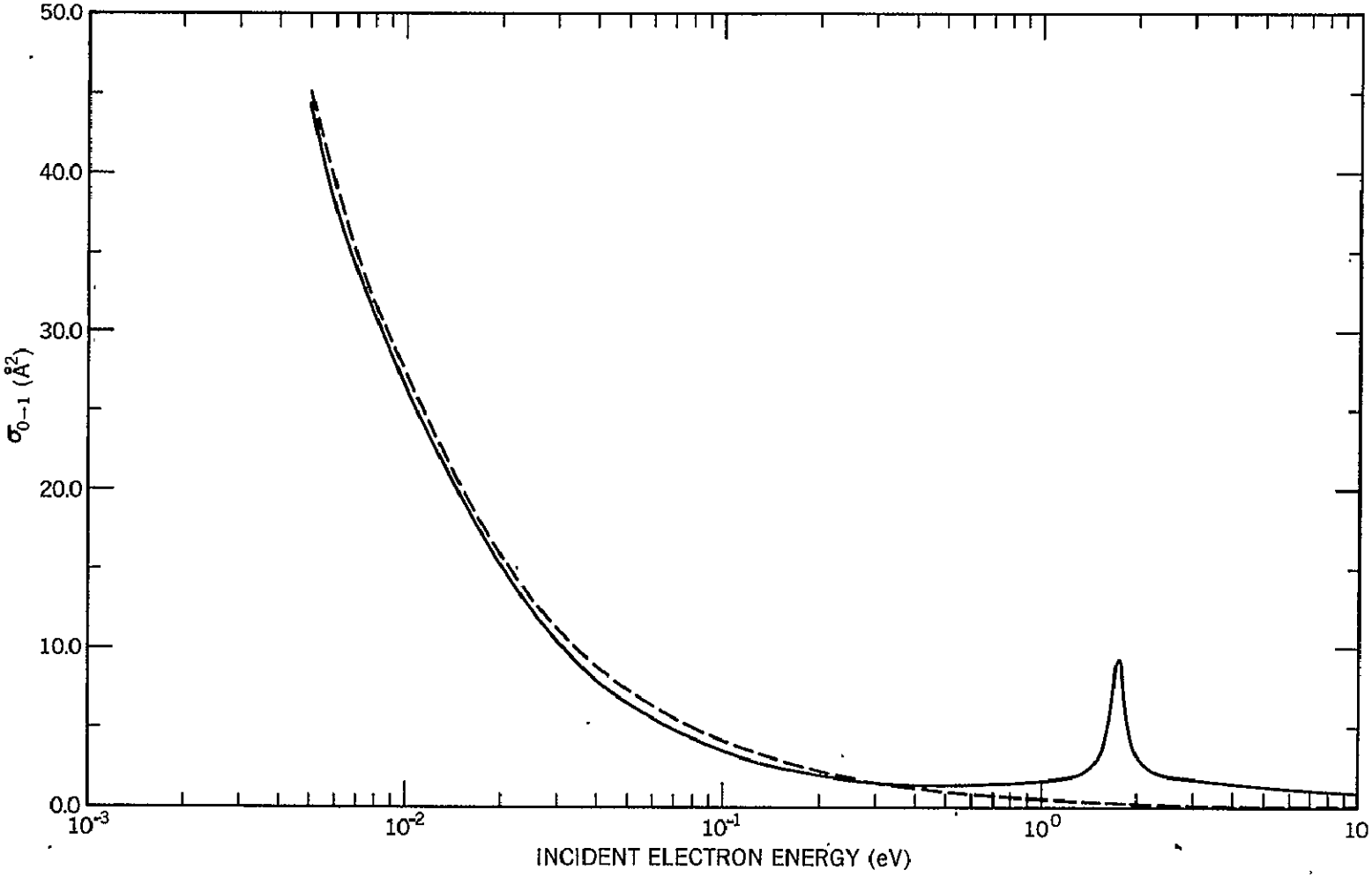

Figure 5. Same as Fig. 4 but for (0→1) rotational transition.

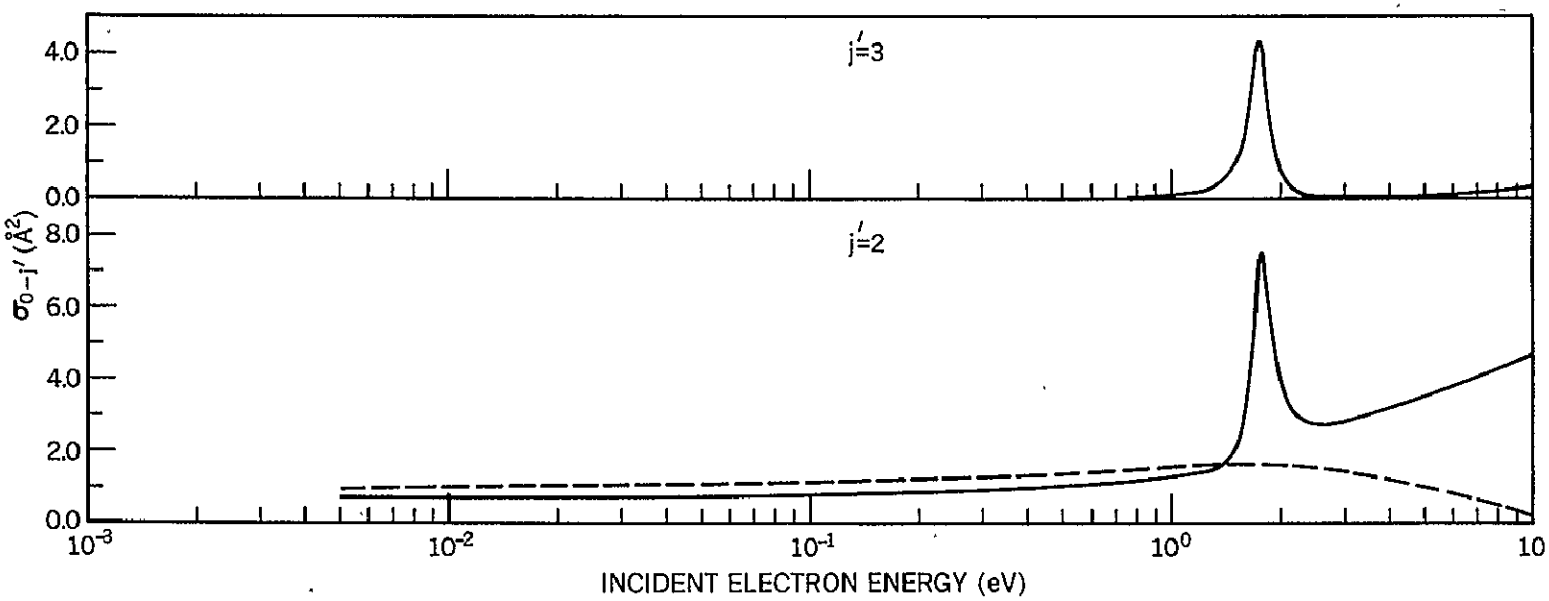

Figure 6. Same as Fig. 4 but for (0→2) and (0→3) rotational transitions. [The broken curve results for (0→3) transition were negligibly small.]

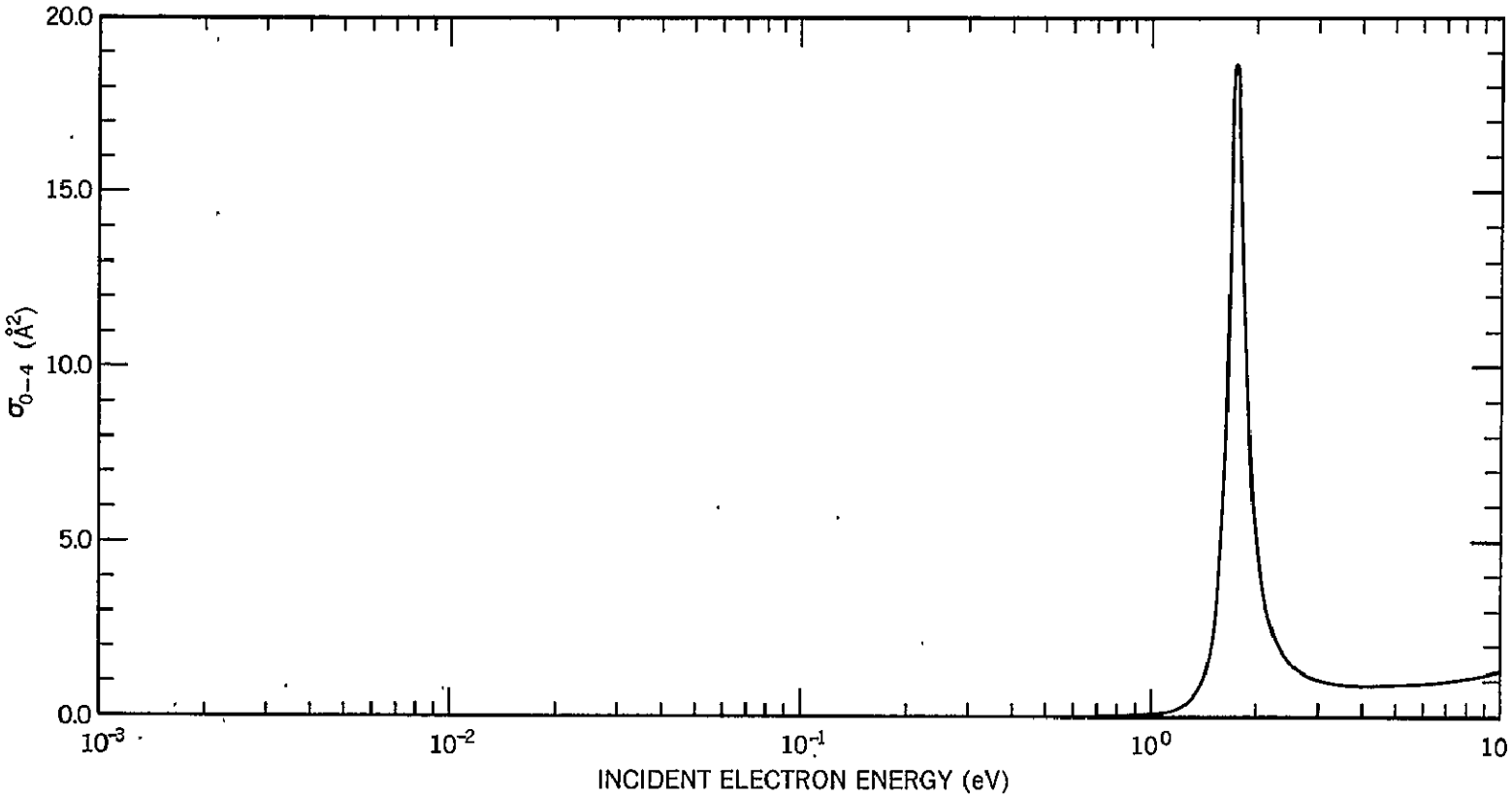

Figure 7. Same as Fig. 4 but for (0→4) rotational transition. (The broken curve results for this transition were negligibly small).

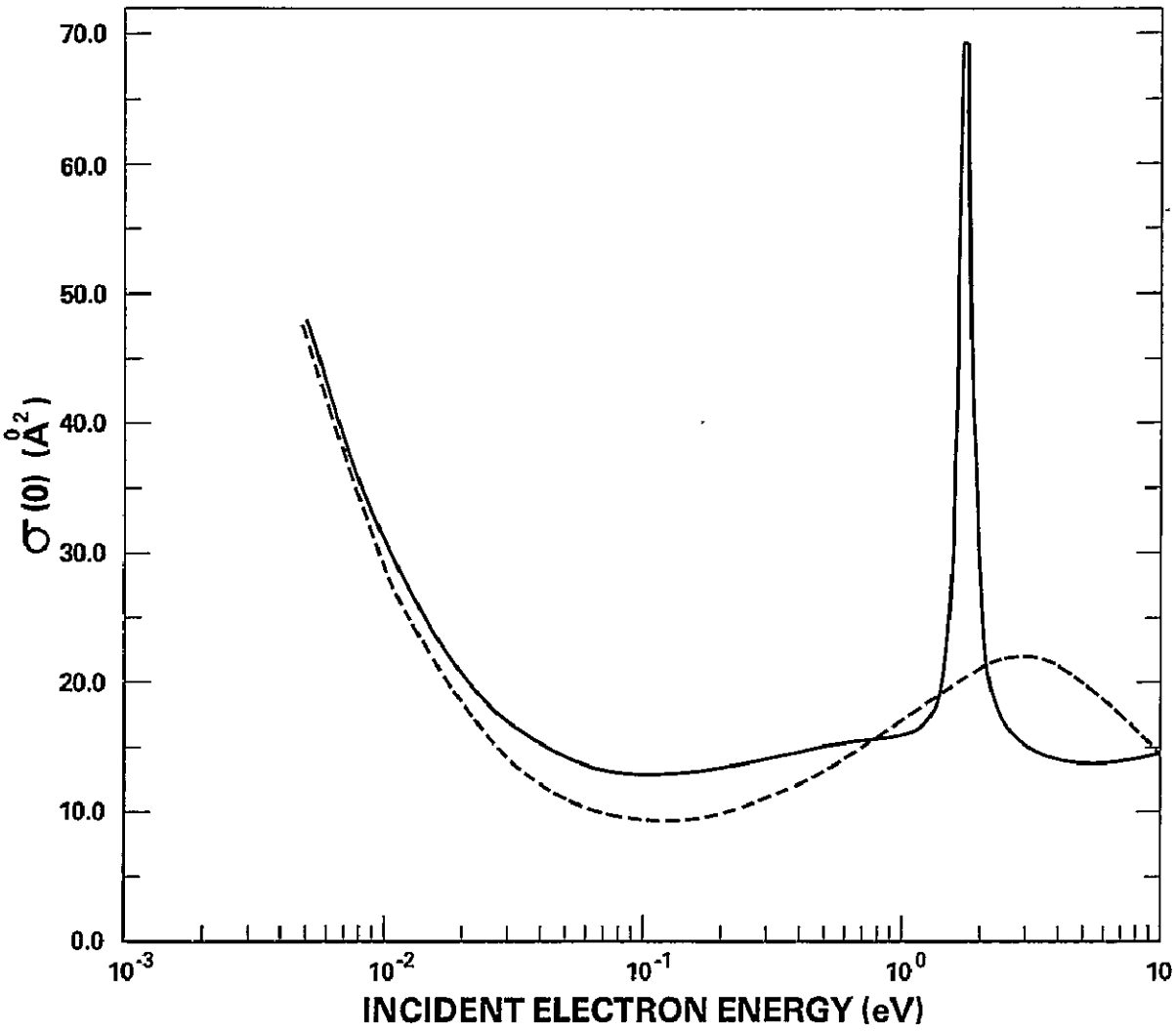

Figure 8. The total scattering cross-section $\sigma(0)$ [Eq. (2.22)]. The broken curve was computed by solving the rotational close-coupling Eq. (2.12) with the model potential (4.1) of Crawford and Dalgarno (Ref. 18). The final results, shown by the continuous curve, were obtained by combining the single-center pseudo-potential method with the frame transformation theory and re-normalized dipole term in the static potential.

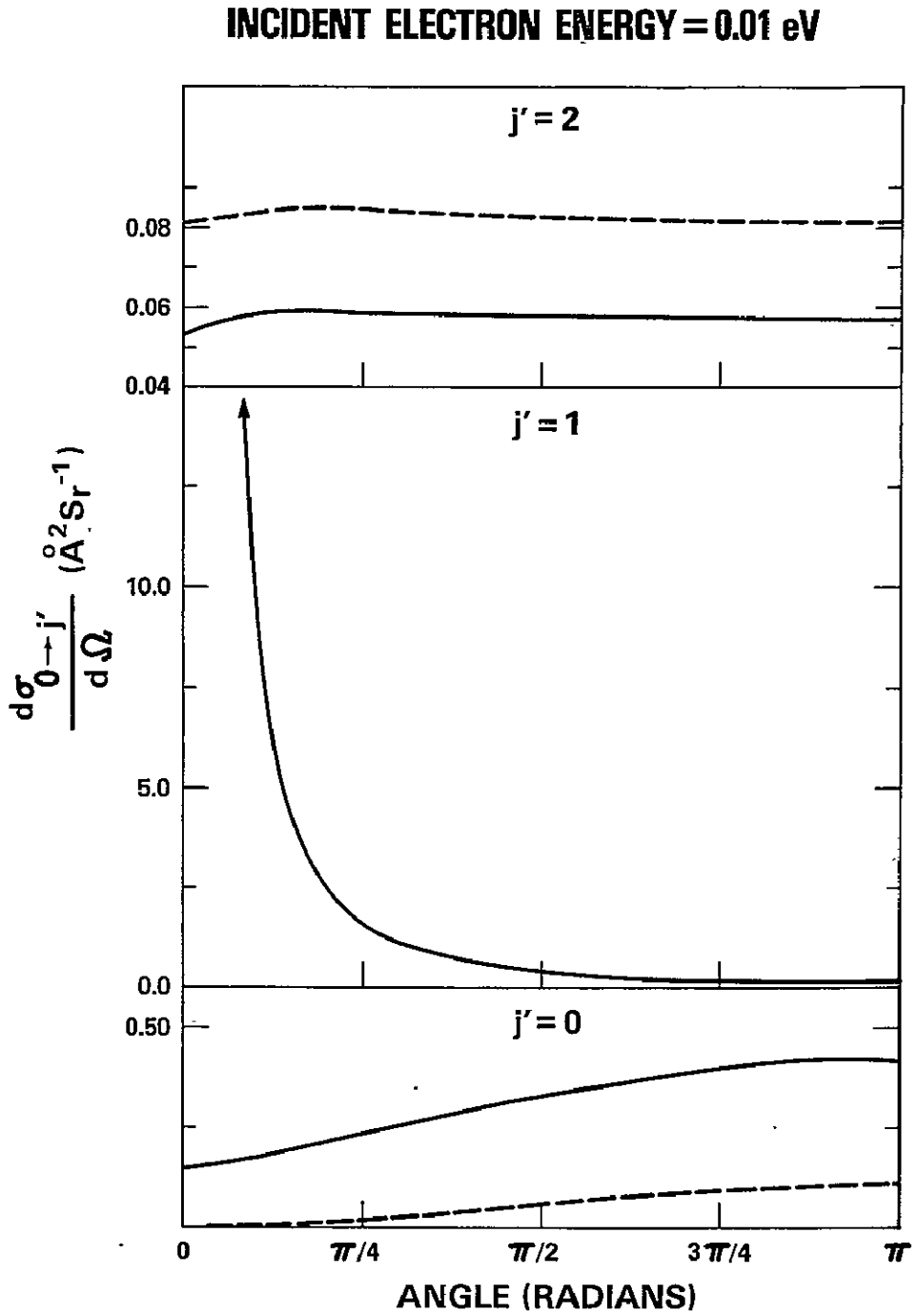

Figure 9. Differential scattering cross-section for (0→0,1,2) rotational transitions at 0.01 eV. The broken curves were computed by solving the rotational close-coupling Eqs. (2.12) with the model potential (4.1) of Crawford and Dalgarno (Ref. 18). The final results, shown by the continuous curves, were obtained by combining the single center pseudo-potential method with the frame-transformation theory and re-normalized dipole-term in the static potential.

C.2

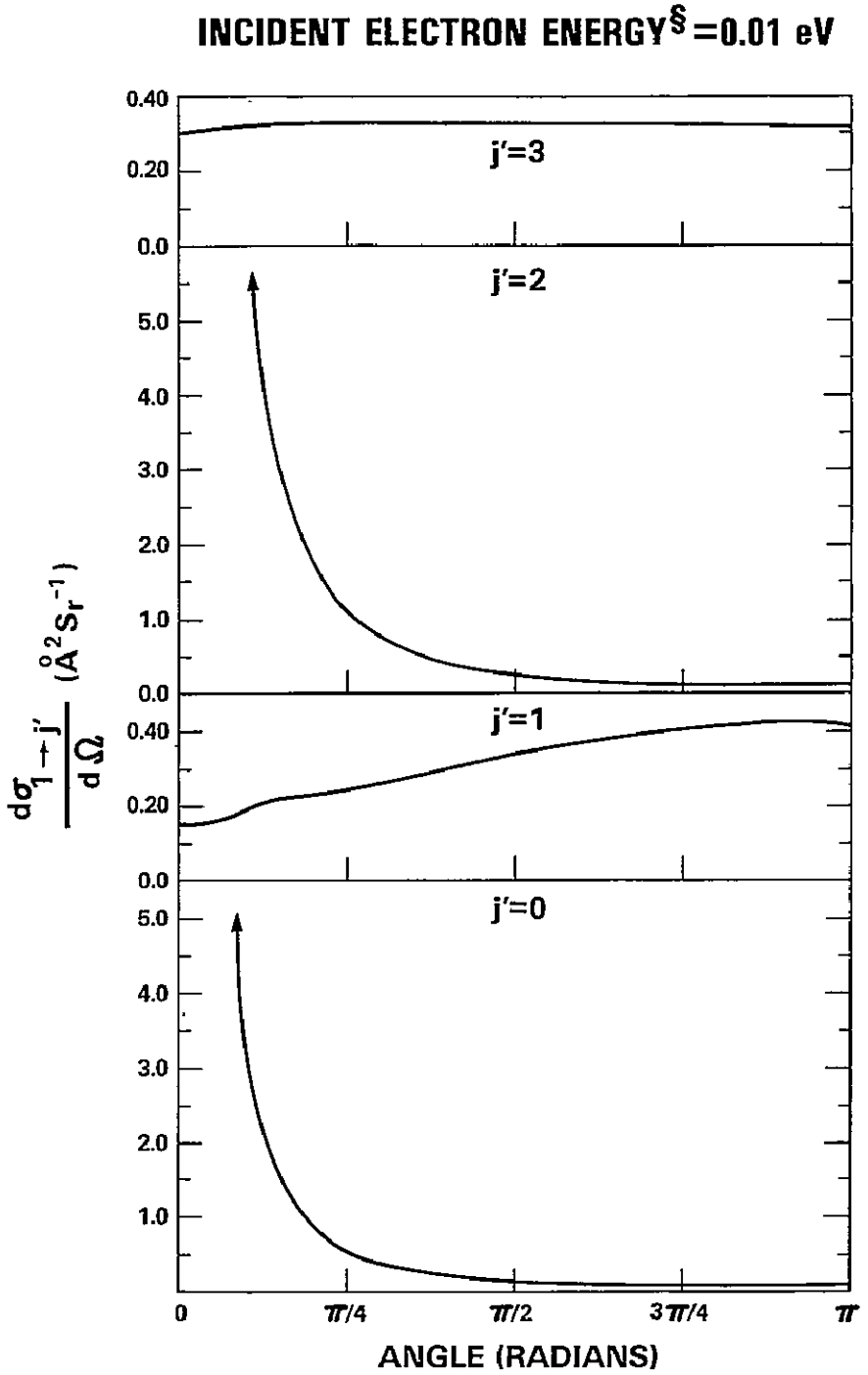

Figure 10. Differential scattering cross-sections for (1→0,1,2) rotational transitions at 0.01 eV. These results were obtained by combining the single-center pseudo-potential method with the frame-transformation theory and re-normalized dipole term in the static potential.

§See footnote to Table IX.

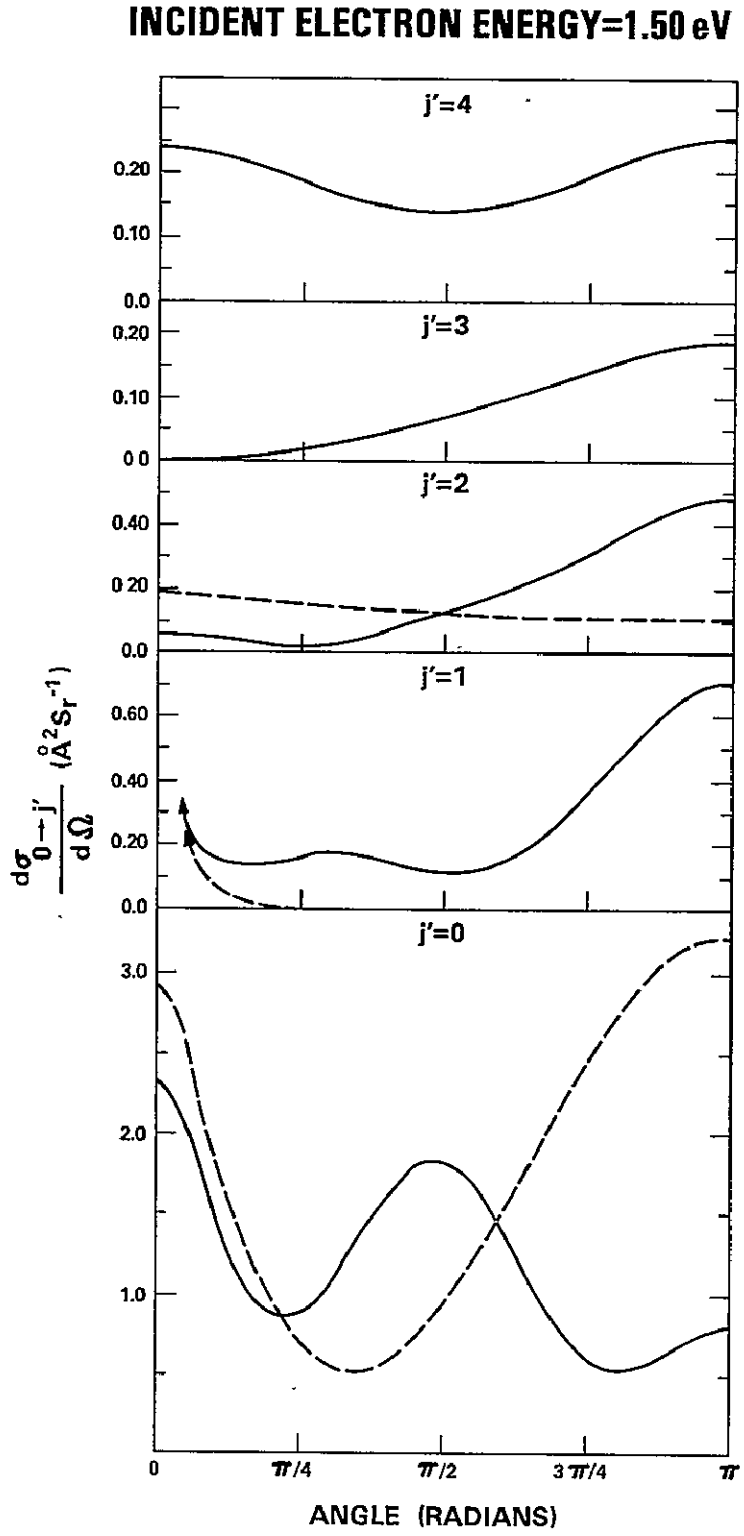

Figure 11. Same as Fig. 9 but for (0→0,1,2,3,4) rotational transitions at 1.50 eV. [The broken curve results for transitions higher than (0→2) were negligibly small.]

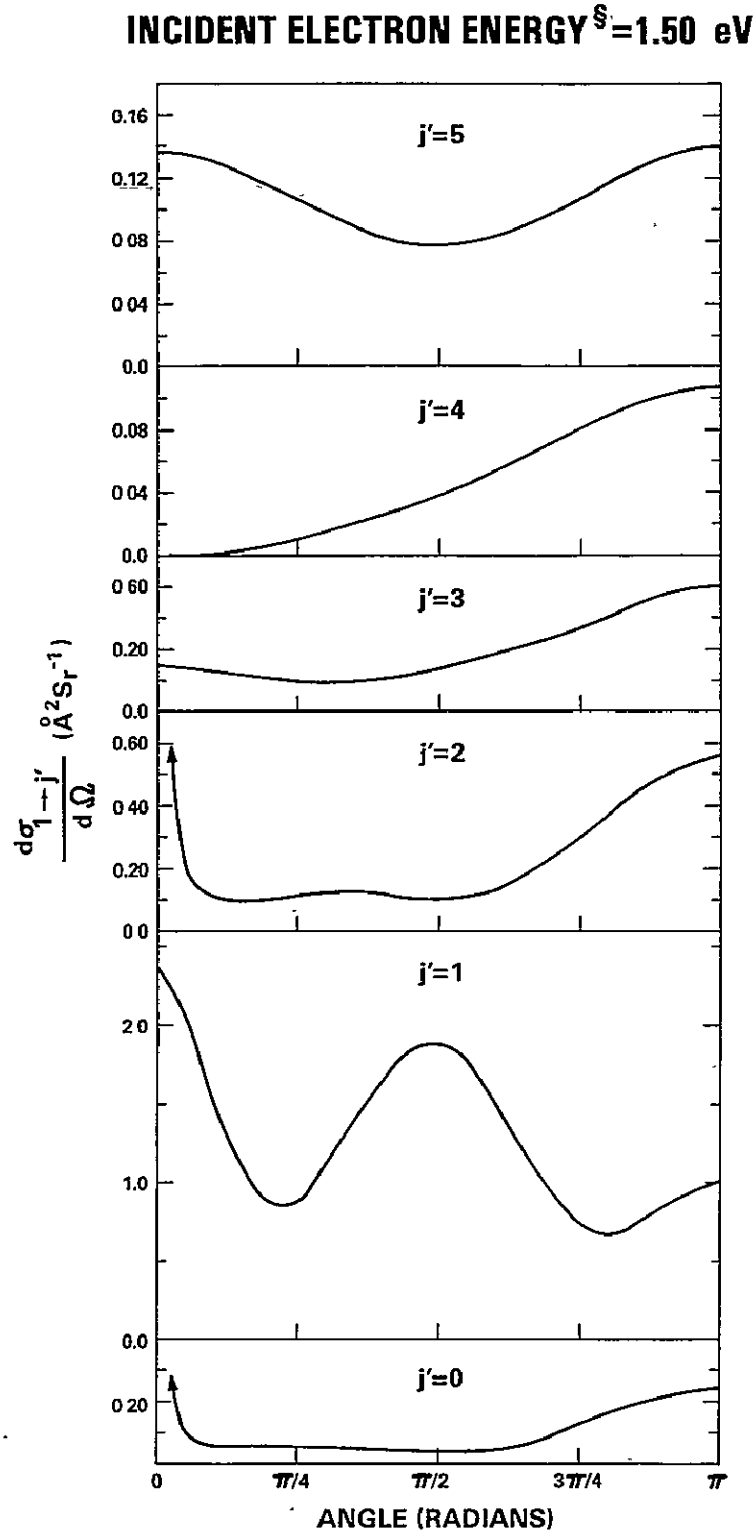

Figure 12. Same as Fig. 10 but for (1→0,1,2,3,4,5) rotational transitions at 1.50 eV.
§See footnote to Table IX.

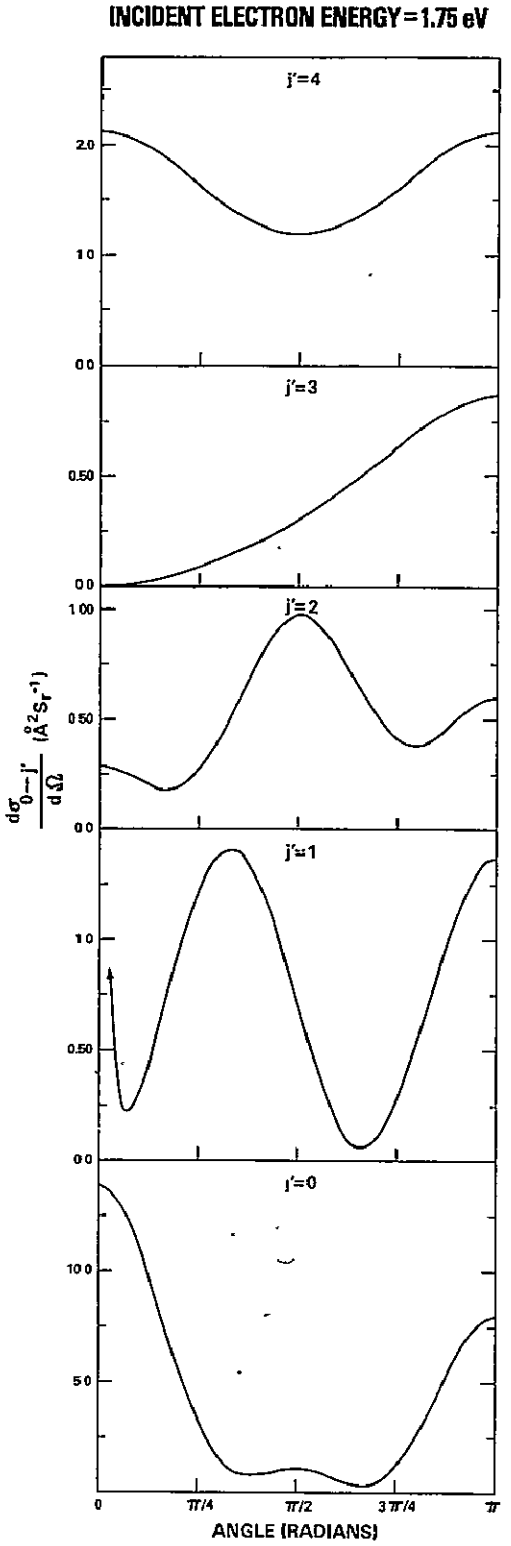

Figure 13. Same as Fig. 10 but for (0→0,1,2,3,4) rotational transitions at the resonance energy 1.75 eV.

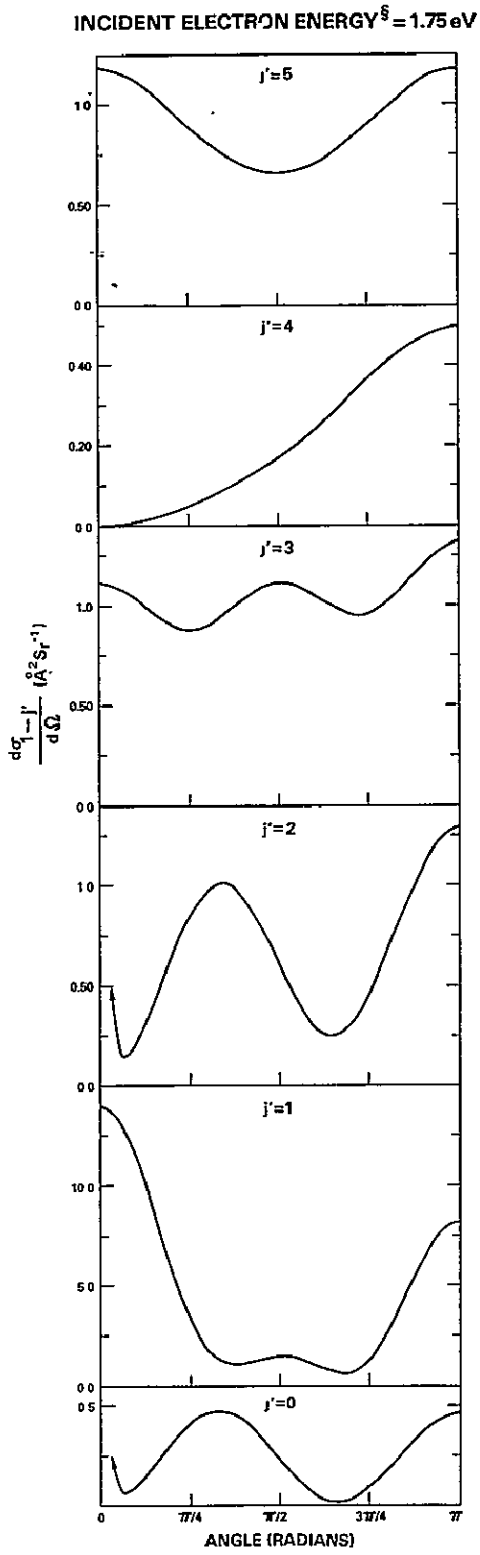

Figure 14. Same as Fig. 10 but for (1→0,1,2,3,4,5) rotational transitions at the resonance energy 1.75 eV.

§ See footnote to Table IX.

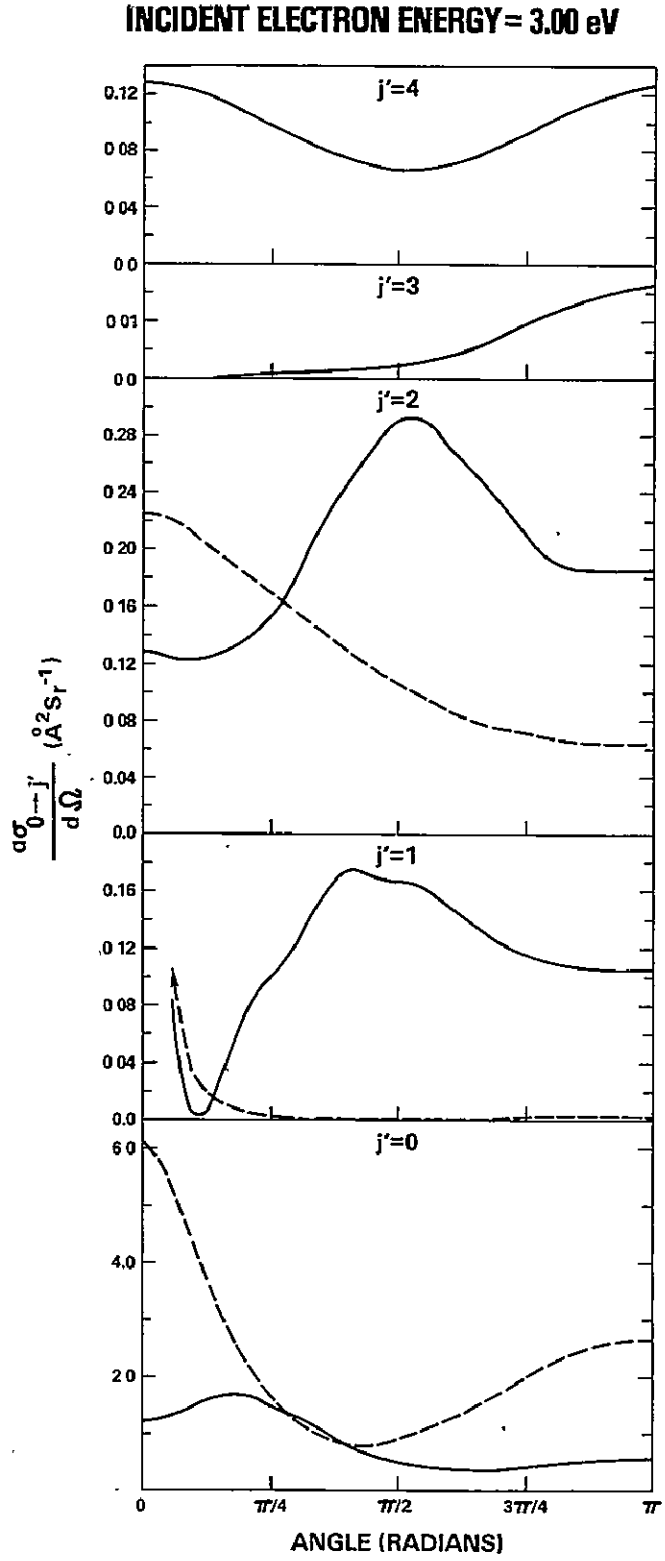

Figure 15. Same as Fig. 9 but for (0→0,1,2,3,4) rotational transitions at 3.00 eV. [The broken curve results for transitions higher than (0→2) were negligibly small.]

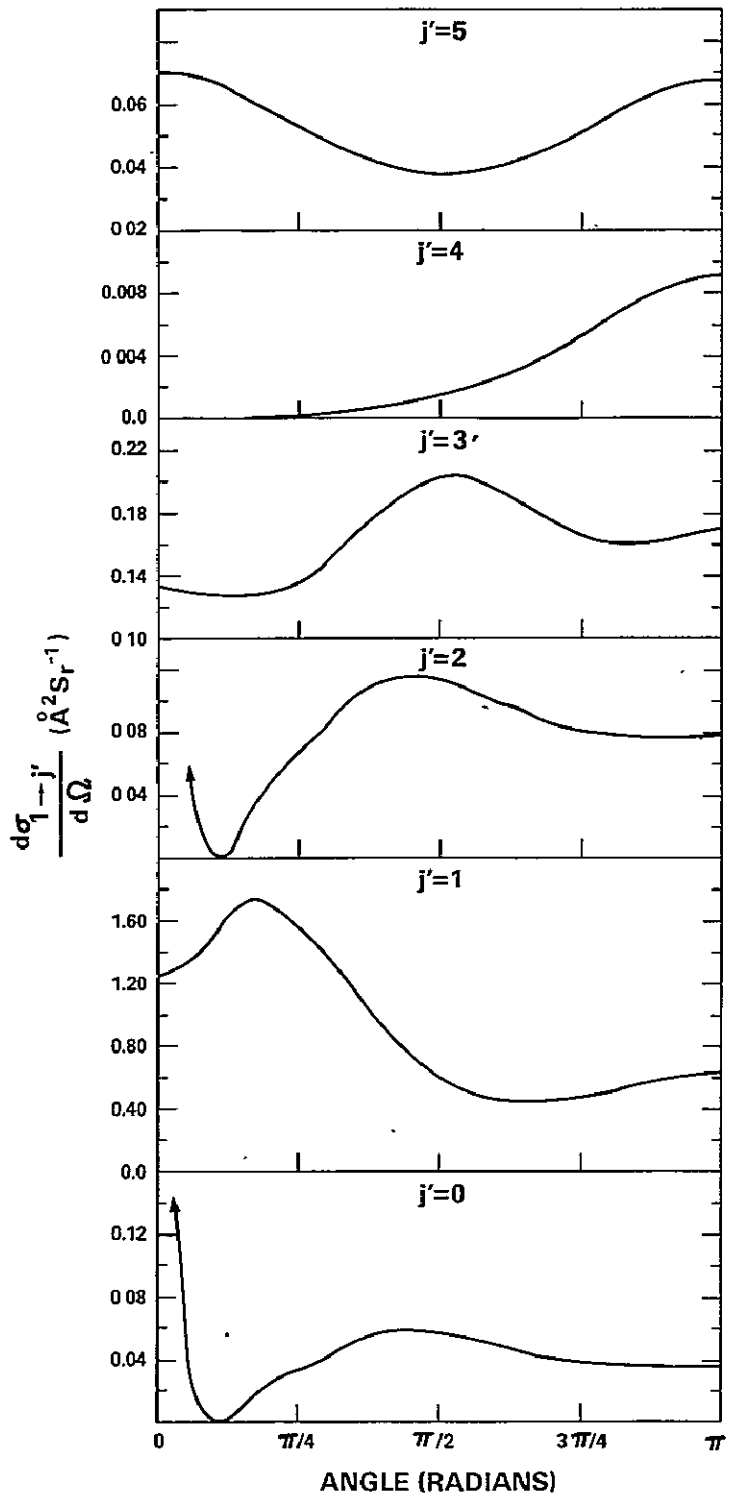

Figure 16. Same as Fig. 10 but for (1 → 0,1,2,3,4,5) transitions at 3.00 eV.
§See footnote to Table IX.

Table I

Comparison of $\sigma^{J}_{j\to j'}$, ($\mathring{A}^2$) Calculated from the Frame-Transformation Theory with the Close-Coupling Results Obtained Using Crawford and Dalgarno (Ref. 18) Potential

Energy (eV)	j → j'	J	Exact (c.c)*	Frame-transformation ($b^{\S}$=1.0), $r_t^{\S\dagger}$ = 4.466	6.090	7.714	9.338	10.150
0.005	0 → 0	0	0.356	0.352	0.352	0.352	0.352	0.352
		1	0.037	0.037	0.037	0.037	0.037	0.037
		2	0.002	0.002	0.002	0.002	0.002	0.002
	0 → 1	0	4.142	4.142	4.142	4.142	4.142	4.142
		1	9.669	9.670	9.670	9.670	9.671	9.671
		2	5.603	5.603	5.603	5.603	5.603	5.603
	1 → 1	0	0.134	0.134	0.134	0.134	0.134	0.134
		1	0.479	0.464	0.446	0.429	0.412	0.404
		2	0.020	0.020	0.020	0.020	0.020	0.020
	2 → 2	0	0.005	0.005	0.005	0.005	0.005	0.005
		1	0.056	0.056	0.056	0.056	0.056	0.056
		2	0.511	0.494	0.472	0.445	0.412	0.393
0.05	0 → 0	0	2.251	2.243	2.243	2.243	2.242	2.242
		1	0.328	0.328	0.328	0.328	0.328	0.328
		2	0.009	0.009	0.009	0.009	0.009	0.009
	0 → 1	0	0.532	0.532	0.532	0.532	0.533	0.533
		1	0.874	0.874	0.874	0.874	0.874	0.874
		2	0.519	0.519	0.519	0.519	0.519	0.519
	1 → 1	0	0.052	0.051	0.051	0.051	0.051	0.051
		1	2.466	2.430	2.388	2.349	2.311	2.292
		2	0.111	0.114	0.115	0.116	0.117	0.117
	2 → 2	0	0.003	0.003	0.003	0.003	0.003	0.003
		1	0.004	0.004	0.003	0.003	0.003	0.003
		2	2.482	2.445	2.397	0.338	2.265	2.223
0.10	0 → 0	0	3.468	3.458	3.458	3.458	3.458	3.458
		1	0.667	0.667	0.667	0.667	0.667	0.667
		2	0.021	0.021	0.021	0.021	0.021	0.021
	0 → 1	0	0.270	0.270	0.270	0.270	0.270	0.270
		1	0.430	0.430	0.430	0.430	0.430	0.430
		2	0.258	0.258	0.258	0.258	0.258	0.258
	1 → 1	0	0.024	0.023	0.023	0.023	0.023	0.023
		1	3.698	3.656	3.606	3.560	3.516	3.494
		2	0.249	0.258	0.261	0.264	0.267	0.269
	2 → 2	0	0.002	0.002	0.002	0.002	0.002	0.002
		1	0.007	0.007	0.007	0.007	0.007	0.007
		2	3.709	3.666	3.609	3.540	3.457	3.409

* c.c. = rotational close-coupling;
§ see Eq. (3.6);
† in atomic units.

Table II

$\sigma^{J}_{j\to j'}$, ($\mathring{A}^2$) Calculated from the Frame-Transformation Using the Pseudo-Potential

Energy (eV)	j → j'	J	Frame-transformation ($b^{\dagger}$=1.0), $r_c^{\dagger *}$ = 6.902	8.526	10.150	11.774	13.398	15.022
0.005	0 → 0	0	0.990	1.341	1.452	1.485	1.495	1.497
		1	0.142	0.138	0.137	0.137	0.137	0.137
		2	0.024	0.023	0.023	0.023	0.023	0.023
	0 → 1	0	23.319	22.867	22.820	22.812	22.810	22.810
		1	54.900	53.848	53.744	53.727	53.723	53.721
		2	32.352	31.787	31.745	31.742	31.742	31.742
	1 → 1	0	0.189	0.188	0.187	0.187	0.187	0.187
		1	0.987	1.343	1.448	1.457	1.435	1.397
		2	0.172	0.166	0.166	0.165	0.165	0.165
	2 → 2	0	0.008	0.008	0.008	0.008	0.008	0.008
		1	0.122	0.121	0.120	0.120	0.120	0.120
		2	1.816	2.345	2.489	2.463	2.352	2.185
0.05	0 → 0	0	5.614	6.305	6.519	6.582	6.600	6.605
		1	0.211	0.208	0.207	0.207	0.207	0.207
		2	0.011	0.011	0.011	0.011	0.011	0.011
	0 → 1	0	2.397	2.307	2.286	2.280	2.278	2.278
		1	4.340	4.206	4.179	4.171	4.167	4.166
		2	3.008	2.955	2.951	2.951	2.951	2.951
	1 → 1	0	0.054	0.054	0.054	0.054	0.054	0.054
		1	5.551	6.284	6.487	6.513	6.474	6.406
		2	0.074	0.073	0.073	0.074	0.075	0.076
	2 → 2	0	0.003	0.003	0.003	0.003	0.003	0.003
		1	0.011	0.011	0.011	0.011	0.011	0.010
		2	5.656	6.491	6.719	6.692	6.540	6.311
0.10	0 → 0	0	7.588	8.324	8.550	8.615	8.634	8.638
		1	0.327	0.320	0.318	0.317	0.317	0.317
		2	0.022	0.022	0.022	0.022	0.022	0.022
	0 → 1	0	0.919	0.862	0.846	0.840	0.839	0.839
		1	1.843	1.764	1.744	1.738	1.735	1.734
		2	1.502	1.475	1.473	1.473	1.474	1.474
	1 → 1	0	0.033	0.034	0.034	0.034	0.034	0.033
		1	7.507	8.292	8.508	8.537	8.500	8.438
		2	0.120	0.118	0.119	0.121	0.124	0.129
	2 → 2	0	0.002	0.002	0.002	0.002	0.002	0.002
		1	0.002	0.002	0.002	0.002	0.002	0.002
		2	7.386	8.278	8.526	8.511	8.374	8.167

† see Eq. (3.6);
* in atomic units.

Table III

Values of r_0 [Eq. (4.5)] and of the $^2\Pi$ Resonance Parameters

The multipole expansion (2.11) of the static potential of CO molecule	r_0 (a.u.)	δ_0 (rad.)	E_r (eV)	Γ_0 (eV)
Contains the original dipole term	1.605	-0.082	1.753	0.278
Contains the dipole term renormalized by ζ_d [Eqs. (4.9) and (4.10)]	1.541	-0.067	1.740	0.242

Table IV

Convergence of $\sigma^{J}_{0\to j'}$, ($\mathring{A}^2$), Calculated from the Frame-Transformation Theory using the Pseudo-Potential, with the Number of Rotational States Coupled in Eq. (2.12) in the Outer-Region: Incident Electron Energy = 1.75 eV, r_t = 11.774 (a.u.), Even Parity[§]

J	j'^{*}_{max}	N_t[†]	0→0	0→1	0→2	0→3	0→4	0→5	0→6	0→7
0	2	3	10.860	0.691	0.339					
	3	4	10.861	0.699	0.338	0.001				
	4	5	10.861	0.699	0.338	0.001	0.000			
	5	6	10.861	0.699	0.338	0.001	0.000	0.000		
1	2	5	0.647	5.103	1.416					
	3	7	0.959	4.547	0.678	2.142				
	4	9	0.959	4.546	0.679	2.141	0.000			
	5	11	0.959	4.547	0.679	2.141	0.000	0.000		
2	2	6	26.872	4.209	7.471					
	3	9	24.914	4.107	6.868	3.142				
	4	12	17.551	3.852	6.445	2.122	18.651			
	5	15	17.547	3.850	6.441	2.138	18.636	0.001		
	6	18	17.548	3.850	6.442	2.138	18.634	0.001	0.001	
	7	21	17.548	3.850	6.442	2.138	18.634	0.001	0.001	0.000
3	2	6	0.059	0.018	0.029					
	3	10	0.059	0.016	0.030	0.003				
	4	14	0.059	0.015	0.030	0.003	0.000			
	5	18	0.059	0.011	0.033	0.003	0.000	0.001		
	6	22	0.059	0.011	0.033	0.003	0.000	0.001	0.000	
4	2	6	0.015	0.008	0.010					
	3	10	0.015	0.008	0.010	0.000				
	4	15	0.015	0.008	0.010	0.000	0.000			
	5	20	0.015	0.008	0.010	0.000	0.000	0.000		
	6	25	0.015	0.008	0.011	0.001	0.000	0.000	0.001	
	7	30	0.015	0.008	0.011	0.001	0.000	0.000	0.001	0.000
5	2	6	0.005	0.007	0.007					
	3	10	0.005	0.007	0.007	0.000				
	4	15	0.005	0.007	0.007	0.000				
	5	21	0.005	0.007	0.007	0.000	0.000	0.000		
6	2	6	0.002	0.006	0.004					
	3	10	0.002	0.006	0.004	0.000				
	4	15	0.002	0.006	0.004	0.000	0.000			
7	2	6	0.001	0.005	0.003					
	3	10	0.001	0.005	0.003	0.000				
	4	15	0.001	0.005	0.003	0.000	0.000			
8	2	6	0.001	0.004	0.002					
	3	10	0.001	0.004	0.002	0.000				
	4	15	0.001	0.004	0.002	0.000	0.000			
9	2	6	0.000	0.004	0.001					
	3	10	0.000	0.004	0.001	0.000				
	4	15	0.000	0.004	0.001	0.000	0.000			
10	2	6	0.000	0.003	0.001					
	3	10	0.000	0.003	0.001	0.000				
	4	15	0.000	0.003	0.001	0.000	0.000			

[§]
*See text for the description of these quantities.
[†]Highest rotational state (starting from j' = 0) coupled in Eq. (2.12).
[†]Total number of coupled channels $(j\ell)$ in Eq. (2.12).

Table V

Convergence of $\sigma^{J}_{1\to j'}$, ($\mathring{A}^2$), Calculated from the Frame-Transformation Theory using the Pseudo-Potential, with the Number of Rotational States Coupled in Eq. (2.12) in the Outer-Region: Incident Electron Energy = 1.75 eV, r_t = 11.774 (a.u.), Even Parity[§]

J	j'^{*}_{max}	$N_t^{\dagger}$	1→0	1→1	1→2	1→3	1→4	1→5	1→6	1→7
0	2	3	0.230	0.238	0.005					
	3	4	0.233	0.245	0.005	0.002				
	4	5	0.233	0.245	0.005	0.002	0.000			
	5	6	0.233	0.245	0.005	0.002	0.000	0.000		
1	2	5	1.702	21.981	1.292					
	3	7	1.516	18.825	0.974	5.082				
	4	9	1.516	18.823	0.983	5.077	0.001			
	5	11	1.516	18.823	0.983	5.076	0.001	0.000		
2	2	6	1.403	0.168	1.074					
	3	9	1.369	0.285	1.019	0.867				
	4	12	1.284	0.547	0.959	0.404	1.225			
	5	15	1.284	0.547	0.959	0.404	1.224	0.000		
	6	18	1.284	0.547	0.959	0.404	1.224	0.000	0.000	
	7	21	1.284	0.547	0.959	0.404	1.224	0.000	0.000	0.000
3	2	6	0.006	15.695	2.234					
	3	10	0.005	15.457	2.078	2.081				
	4	14	0.005	14.323	2.037	1.894	1.750			
	5	18	0.004	10.576	1.971	1.754	1.211	10.367		
	6	22	0.004	10.573	1.970	1.753	1.220	10.358	0.001	
4	2	6	0.003	0.020	0.007					
	3	10	0.003	0.019	0.008	0.012				
	4	15	0.003	0.019	0.007	0.012	0.001			
	5	20	0.003	0.019	0.007	0.012	0.001	0.000		
	6	25	0.003	0.019	0.004	0.014	0.002	0.000	0.001	
	7	30	0.003	0.019	0.004	0.014	0.002	0.000	0.001	0.000
5	2	6	0.002	0.004	0.003					
	3	10	0.002	0.004	0.003	0.003				
	4	15	0.002	0.004	0.003	0.003	0.000			
	5	21	0.002	0.004	0.003	0.003	0.000	0.000		
6	2	6	0.002	0.001	0.003					
	3	10	0.002	0.001	0.003	0.002				
	4	15	0.002	0.001	0.003	0.002	0.000			
7	2	6	0.002	0.001	0.002					
	3	10	0.002	0.001	0.002	0.001				
	4	15	0.002	0.001	0.002	0.001	0.000			
8	2	6	0.001	0.000	0.002					
	3	10	0.001	0.000	0.002	0.001				
	4	15	0.001	0.000	0.002	0.001	0.000			
9	2	6	0.001	0.000	0.002					
	3	10	0.001	0.000	0.002	0.001				
	4	15	0.001	0.000	0.002	0.001	0.000			
10	2	6	0.001	0.000	0.002					
	3	10	0.001	0.000	0.002	0.000				
	4	15	0.001	0.000	0.002	0.000	0.000			

[§]See text for the definition of these quantities.

*Highest rotational state (starting from j' = 0) coupled in Eq. (2.12).

†Total number of coupled channels ($j\ell$) in Eq. (2.12).

Table VI

Convergence of $\sigma^{J}_{1\to j}$, ($\mathring{A}^2$), Calculated from the Frame-Transformation Theory using the Pseudo-Potential, with the Number of Rotational States Coupled in Eq. (2.12) in the Outer-Region: Incident Electron Energy = 1.7 eV, r_t = 11.774 (a.u.), Odd Parity§

J	j'^{*}_{max}	$N_t^{\dagger}$	1→1	1→2	1→3	1→4	1→5	1→6
1	2	2	0.440	2.972				
	3	3	0.444	2.987	0.003			
	4	4	0.444	2.987	0.003	0.000		
	5	5	0.444	2.987	0.003	0.000	0.000	
2	2	3	2.596	0.802				
	3	5	1.727	0.993	5.529			
	4	7	1.730	0.998	5.525	0.001		
	5	9	1.730	0.998	5.525	0.001	0.000	
	6	11	1.730	0.998	5.525	0.001	0.000	0.000
3	2	3	0.045	0.004				
	3	6	0.045	0.004	0.005			
	4	9	0.045	0.003	0.005	0.000		
	5	12	0.045	0.003	0.005	0.000	0.000	
	6	15	0.045	0.003	0.005	0.000	0.000	0.000
4	2	3	0.014	0.002				
	3	6	0.014	0.002	0.002			
	4	10	0.014	0.002	0.002	0.000		
	5	14	0.014	0.002	0.002	0.000	0.000	
5	2	3	0.006	0.002				
	3	6	0.006	0.002	0.001			
	4	10	0.006	0.002	0.001	0.000		
	5	15	0.006	0.002	0.001	0.000	0.000	
	6	20	0.006	0.002	0.001	0.000	0.000	0.000
6	2	3	0.003	0.001				
	3	6	0.003	0.001	0.001			
	4	10	0.003	0.001	0.001	0.000		
	5	15	0.003	0.001	0.001	0.000	0.000	
7	2	3	0.002	0.001				
	3	6	0.002	0.001	0.001			
	4	10	0.002	0.001	0.001	0.000		
	5	15	0.002	0.001	0.001	0.000	0.000	
8	2	3	0.001	0.001				
	3	6	0.001	0.001	0.000			
	4	10	0.001	0.001	0.000	0.000		
9	2	3	0.001	0.001				
	3	6	0.001	0.001	0.000			
	4	10	0.001	0.001	0.000	0.000		
10	2	3	0.001	0.001				
	3	6	0.001	0.001	0.000			
	4	10	0.001	0.001	0.000	0.000		

§ See text for the description of these quantities

* Highest rotational state (starting from j' = 1) coupled in Eq. (2.12). The ground rotational state (j' = 0) will not be present in odd parity channels.

† Total number of coupled channels ($l+1$) in Eq. (2.12).

Table VII

Elastic and Excitation Cross-Sections† for (0→j') Transitions

Incident Electron Energy E_0 (eV)	$\sigma_{0\to0}$	$\sigma_{0\to1}$	$\sigma_{0\to2}$	$\sigma_{0\to3}$	$\sigma_{0\to4}$	$\sigma(0)$
0.005	3.17	44.38	0.68	0.00	0.00	48.23
0.008	3.70	31.14	0.72	0.00	0.00	35.56
0.01	3.97	26.15	0.73	0.00	0.00	30.85
0.02	5.02	14.83	0.74	0.00	0.00	20.59
0.03	5.77	10.47	0.75	0.00	0.00	16.99
0.05	6.88	6.67	0.76	0.00	0.00	14.31
0.08	8.04	4.37	0.78	0.00	0.00	13.19
0.10	8.64	3.58	0.79	0.00	0.00	13.01
0.20	10.56	2.06	0.85	0.01	0.00	13.48
0.40	12.15	1.53	0.96	0.02	0.00	14.66
0.60	12.66	1.52	1.07	0.03	0.00	15.28
0.80	12.79	1.60	1.16	0.06	0.02	15.63
1.00	12.79	1.72	1.27	0.12	0.07	15.97
1.10	12.82	1.80	1.33	0.16	0.13	16.24
1.20	12.94	1.90	1.39	0.23	0.24	16.70
1.30	13.21	2.06	1.49	0.34	0.46	17.56
1.40	13.84	2.36	1.65	0.53	0.95	19.33
1.50	15.37	3.00	2.02	0.94	2.19	23.52
1.55	16.88	3.62	2.41	1.33	3.50	27.74
1.60	19.37	4.65	3.11	1.94	5.80	34.87
1.65	23.28	6.31	4.35	2.87	9.76	46.57
1.70	27.93	8.41	6.18	3.96	15.24	61.72
1.75	29.45	9.38	7.52	4.28	18.64	69.27
1.80	25.69	8.12	7.15	3.38	16.59	60.93
1.85	20.82	6.22	5.98	2.24	12.40	47.66
1.90	17.35	4.80	4.96	1.45	9.01	37.57
1.95	15.18	3.90	4.25	0.96	6.74	31.03
2.00	13.82	3.33	3.78	0.67	5.25	26.85
2.20	11.51	2.38	2.99	0.22	2.65	19.75
2.40	10.67	2.07	2.78	0.11	1.79	17.42
2.60	10.19	1.93	2.73	0.07	1.41	16.33
2.80	9.84	1.84	2.75	0.06	1.20	15.69
3.00	9.57	1.78	2.79	0.05	1.08	15.27
3.50	9.01	1.65	2.96	0.06	0.94	14.62
4.00	8.59	1.54	3.14	0.08	0.90	14.25
4.50	8.27	1.45	3.33	0.10	0.89	14.04
5.00	8.02	1.36	3.50	0.11	0.90	13.89
6.00	7.71	1.21	3.82	0.14	0.95	13.83
7.00	7.58	1.07	4.08	0.17	1.01	13.91
8.00	7.59	0.97	4.27	0.18	1.07	14.08
9.00	7.71	0.87	4.39	0.20	1.12	14.29
10.00	7.86	0.80	4.43	0.21	1.17	14.47

Table VIII

Momentum Transfer Cross-Sections† for (0→j') Transitions

Incident Electron Energy E_0 (eV)	$\sigma^m_{0\to0}$	$\sigma^m_{0\to1}$	$\sigma^m_{0\to2}$	$\sigma^m_{0\to3}$	$\sigma^m_{0\to4}$	$\sigma^m(0)$
0.005	3.50	11.04	0.68	0.00	0.00	15.22
0.008	4.14	6.55	0.71	0.00	0.00	11.40
0.01	4.48	5.06	0.72	0.00	0.00	10.26
0.02	5.78	2.12	0.74	0.00	0.00	8.64
0.03	6.73	1.18	0.75	0.00	0.00	8.66
0.05	8.13	0.50	0.77	0.00	0.00	9.40
0.08	9.62	0.21	0.79	0.00	0.00	10.62
0.10	10.37	0.16	0.81	0.00	0.00	11.34
0.20	12.66	0.28	0.89	0.01	0.00	13.84
0.40	14.15	0.77	1.06	0.02	0.00	16.00
0.60	14.17	1.19	1.23	0.05	0.01	16.65
0.80	13.71	1.53	1.40	0.09	0.02	16.75
1.00	13.16	1.83	1.59	0.16	0.07	16.81
1.10	12.93	1.99	1.70	0.22	0.13	16.97
1.20	12.79	2.17	1.84	0.32	0.25	17.37
1.30	12.80	2.40	2.02	0.47	0.47	18.16
1.40	13.11	2.75	2.31	0.74	0.97	19.88
1.50	14.12	3.41	2.87	1.31	2.22	23.93
1.55	15.17	3.97	3.39	1.84	3.53	27.90
1.60	16.88	4.83	4.22	2.69	5.84	34.46
1.65	19.44	6.07	5.55	3.99	9.80	44.85
1.70	22.12	7.35	7.21	5.50	15.27	57.45
1.75	22.14	7.44	7.99	5.94	18.63	62.14
1.80	18.67	5.95	7.03	4.69	16.55	52.89
1.85	14.96	4.36	5.58	3.11	12.35	40.36
1.90	12.51	3.33	4.51	2.01	8.96	31.32
1.95	11.04	2.74	3.84	1.34	6.70	25.66
2.00	10.13	2.40	3.43	0.93	5.21	22.10
2.20	8.54	1.92	2.83	0.31	2.62	16.22
2.40	7.85	1.81	2.74	0.16	1.77	14.33
2.60	7.38	1.76	2.78	0.10	1.39	13.41
2.80	7.00	1.73	2.85	0.08	1.19	12.85
3.00	6.68	1.70	2.94	0.08	1.07	12.47
3.50	6.03	1.61	3.20	0.09	0.94	11.87
4.00	5.56	1.52	3.45	0.12	0.90	11.55
4.50	5.20	1.42	3.69	0.15	0.91	11.37
5.00	4.94	1.33	3.92	0.17	0.93	11.29
6.00	4.58	1.16	4.34	0.22	1.00	11.30
7.00	4.37	1.03	4.70	0.25	1.08	11.43
8.00	4.22	0.92	5.00	0.28	1.18	11.60
9.00	4.09	0.83	5.23	0.30	1.26	11.71
10.00	3.97	0.77	5.38	0.32	1.33	11.77

Table IX

Elastic and Inelastic Cross-Sections† for (1→j') Transitions

Incident Electron Energy§ E_0 (eV)	$\sigma_{1\to0}$	$\sigma_{1\to1}$	$\sigma_{1\to2}$	$\sigma_{1\to3}$	$\sigma_{1\to4}$	$\sigma_{1\to5}$	$\sigma(1)$
0.005	16.35	3.33	24.94	0.32	0.00	0.00	44.94
0.008	11.04	3.87	17.79	0.39	0.00	0.00	33.09
0.01	9.15	4.14	15.01	0.41	0.00	0.00	28.71
0.02	5.06	5.19	8.59	0.43	0.00	0.00	19.27
0.03	3.55	5.94	6.10	0.44	0.00	0.00	16.03
0.05	2.24	7.06	3.90	0.45	0.00	0.00	13.65
0.08	1.47	8.24	2.57	0.46	0.00	0.00	12.74
0.10	1.20	8.84	2.11	0.47	0.00	0.00	12.62
0.20	0.69	10.80	1.23	0.51	0.00	0.00	13.23
0.40	0.51	12.47	0.95	0.58	0.01	0.00	14.52
0.60	0.51	13.05	0.98	0.64	0.02	0.00	15.20
0.80	0.53	13.31	1.06	0.72	0.04	0.01	15.67
1.00	0.57	13.28	1.17	0.79	0.07	0.04	15.92
1.10	0.60	13.34	1.24	0.85	0.09	0.07	16.19
1.20	0.63	13.49	1.34	0.94	0.13	0.13	16.66
1.30	0.69	13.80	1.50	1.10	0.19	0.26	17.54
1.40	0.79	14.51	1.78	1.41	0.30	0.53	19.32
1.50	1.00	16.19	2.38	2.18	0.54	1.22	23.51
1.55	1.21	17.86	2.96	3.00	0.76	1.95	27.74
1.60	1.55	20.63	3.91	4.44	1.11	3.23	34.87
1.65	2.10	25.05	5.42	6.95	1.64	5.43	46.59
1.70	2.80	30.43	7.29	10.48	2.26	8.48	61.74
1.75	3.13	32.46	8.07	12.80	2.45	10.36	69.27
1.80	2.71	28.54	6.85	11.67	1.92	9.23	60.92
1.85	2.07	23.18	5.09	9.10	1.27	6.90	47.61
1.90	1.60	19.30	3.81	6.98	0.82	5.01	37.52
1.95	1.30	16.84	3.00	5.55	0.53	3.75	30.97
2.00	1.11	15.32	2.49	4.59	0.42	2.91	26.84
2.20	0.79	12.68	1.67	2.97	0.13	1.47	19.71
2.40	0.69	11.77	1.42	2.47	0.06	1.00	17.41
2.60	0.64	11.27	1.31	2.27	0.04	0.78	16.31
2.80	0.61	10.93	1.24	2.18	0.03	0.67	15.66
3.00	0.59	10.67	1.20	2.16	0.03	0.60	15.25
3.50	0.55	10.19	1.12	2.19	0.03	0.52	14.60
4.00	0.51	9.84	1.06	2.29	0.05	0.50	14.25
4.50	0.48	9.60	1.00	2.40	0.06	0.49	14.03
5.00	0.45	9.42	0.95	2.51	0.06	0.50	13.89
6.00	0.40	9.24	0.86	2.72	0.08	0.53	13.83
7.00	0.36	9.21	0.79	2.91	0.09	0.55	13.91
8.00	0.32	9.30	0.72	3.05	0.11	0.59	14.09
9.00	0.29	9.46	0.67	3.14	0.11	0.62	14.29
10.00	0.27	9.64	0.62	3.17	0.12	0.64	14.46

†in $\mathring{A}^2$.

§This value (E_0) corresponds to the energy of the electron incident on the ground rotational state of CO. The appropriate energy of incidence for the first rotational state of the molecule can be obtained from the energy conservation law: $E_1 = E_0 - 2B$, $B = 2.38\times10^{-4}$ eV for CO molecule.

Table X

Momentum Transfer Cross-Sections† for (1→j') Transitions

Incident Electron Energy§ E_0 (eV)	$\sigma^m_{1\to0}$	$\sigma^m_{1\to1}$	$\sigma^m_{1\to2}$	$\sigma^m_{1\to3}$	$\sigma^m_{1\to4}$	$\sigma^m_{1\to5}$	$\sigma^m(1)$
0.005	4.07	3.64	8.10	0.32	0.00	0.00	16.13
0.008	2.32	4.29	4.66	0.39	0.00	0.00	11.66
0.01	1.77	4.63	3.56	0.40	0.00	0.00	10.36
0.02	0.72	5.94	1.46	0.43	0.00	0.00	8.55
0.03	0.40	6.89	0.81	0.44	0.00	0.00	8.54
0.05	0.17	8.31	0.34	0.45	0.00	0.00	9.27
0.08	0.07	9.81	0.14	0.47	0.00	0.00	10.49
0.10	0.05	10.58	0.11	0.48	0.00	0.00	11.22
0.20	0.09	12.93	0.19	0.53	0.00	0.00	13.74
0.40	0.26	14.53	0.53	0.64	0.01	0.00	15.97
0.60	0.40	14.65	0.82	0.74	0.03	0.00	16.64
0.80	0.51	14.27	1.06	0.89	0.05	0.01	16.79
1.00	0.61	13.80	1.29	0.99	0.09	0.04	16.82
1.10	0.66	13.62	1.42	1.08	0.13	0.07	16.98
1.20	0.72	13.53	1.58	1.21	0.18	0.13	17.35
1.30	0.80	13.61	1.80	1.42	0.27	0.26	18.16
1.40	0.92	14.05	2.15	1.82	0.42	0.54	19.90
1.50	1.14	15.28	2.83	2.71	0.75	1.23	23.94
1.55	1.32	16.54	3.44	3.60	1.05	1.96	27.91
1.60	1.61	18.59	4.38	5.13	1.54	3.24	34.49
1.65	2.02	21.68	5.76	7.69	2.28	5.44	44.87
1.70	2.45	25.02	7.27	11.12	3.14	8.49	57.49
1.75	2.48	25.34	7.52	13.08	3.40	10.36	62.18
1.80	1.99	21.48	5.97	11.58	2.67	9.22	52.91
1.85	1.46	17.19	4.22	8.84	1.77	6.88	40.36
1.90	1.11	14.31	3.07	6.69	1.14	5.00	31.32
1.95	0.91	12.57	2.40	5.29	0.74	3.74	25.65
2.00	0.80	11.51	2.00	4.36	0.58	2.90	22.15
2.20	0.64	9.67	1.41	2.86	0.18	1.46	16.22
2.40	0.60	8.95	1.27	2.43	0.09	0.99	14.33
2.60	0.59	8.49	1.22	2.28	0.06	0.78	13.42
2.80	0.58	8.14	1.19	2.24	0.05	0.66	12.86
3.00	0.57	7.86	1.17	2.24	0.05	0.59	12.48
3.50	0.54	7.31	1.11	2.34	0.05	0.52	11.87
4.00	0.51	6.94	1.06	2.46	0.07	0.50	11.54
4.50	0.47	6.68	1.01	2.61	0.09	0.50	11.36
5.00	0.44	6.51	0.96	2.76	0.10	0.51	11.28
6.00	0.39	6.32	0.87	3.05	0.13	0.54	11.30
7.00	0.34	6.24	0.80	3.32	0.14	0.57	11.41
8.00	0.31	6.21	0.73	3.53	0.17	0.62	11.57
9.00	0.28	6.18	0.69	3.72	0.18	0.65	11.70
10.00	0.26	6.12	0.65	3.80	0.18	0.69	11.70

†in $\mathring{A}^2$.

§see foot note to Table IX.